HIGH-QUALITY SCREENING OF PHARMACOLOGICAL CHAPERONES FOR ENZYME ENHANCEMENT THERAPY

HIGH-QUALITY SCREENING OF PHARMACOLOGICAL CHAPERONES FOR ENZYME ENHANCEMENT THERAPY

By MEERA SHANMUGANATHAN, B.Sc

A Thesis Submitted to the School of Graduate Studies in Partial Fulfilment of the Requirements for the Degree

Doctor of Philosophy

February 2015

Doctor of Philosophy — McMaster University

(Chemistry and Chemical Biology) — Hamilton, Ontario

TITLE: High-quality screening of pharmacological chaperones for enzyme enhancement therapy

AUTHOR: Meera Shanmuganathan, B.Sc. (Simon Fraser University)

SUPERVISOR: Associate Professor Dr. Philip Britz-McKibbin

PAGES: xvii, 152

Abstract

Enzyme enhancement therapy based on pharmacological chaperones (PCs) represents a promising new therapeutic strategy for the treatment of rare genetic disorders associated with protein misfolding. PCs are small extrinsic molecules that activate, stabilize and promote folding as a way to rescue mutant enzymes from endoplasmic reticulum-associated protein degradation. To date, high throughput drug screening has relied on fluorescence-based inhibition and/or thermal stability assays for putative PC selection from large chemical libraries with confirmatory testing on patient-derived cell-based assays or animal models. However, conventional primary screening methods do not directly measure for chaperone activity that may contribute to high attrition rates in drug discovery. The major aim of this thesis is to develop and validate a high quality screening strategy for the discovery of novel PCs that restore the activity of denatured/mutant enzymes associated with Gaucher disease (GD) and phenylketonuria (PKU). Chapter II introduces a simple yet selective capillary electrophoresis (CE)-based inhibition assay for improved characterization of previously-approved FDA drugs that function as putative PCs for β-glucocerebrosidase (GCase), a lysosomal enzyme associated with GD. A novel *in-vitro* assay based on restoration of enzyme activity via denaturation (READ) was developed in Chapter III for unambiguous characterization of the chaperone activity of previously identified PCs for GCase when using CE with UV detection. Chapter IV subsequently adapted READ to a fluorescence-based high throughput screening platform to discover novel stilbene derivatives as PCs from a chemical library comprising structural unique compounds after *in silico* assessment of drug-like activity. Chapter V then used this two-tiered screening strategy to discover plant-derived natural products that enhance the activity of phenylalanine hydroxylase (PAH), the enzyme associated with PKU. In summary, an integrated two-tiered strategy for high quality screening of PCs has been developed in this thesis, which is anticipated to enhance drug discovery while reducing false discoveries for treatment of various human diseases associated with deleterious protein misfolding.

Acknowledgements

Firstly, I would like to express my deepest gratitude to my supervisor, Dr.Philip Britz-McKibbin, for his endless encouragement, excellence guidance and mentorship throughout the high and low tides of the entire graduate journey. Without his help it would not have been possible to overcome the many obstacles along the way. Additionally, I would like thank my committee members, Dr. Giuseppe Melacini and Dr. Kalai Saravanamuttu for their constructive feedbacks, critiques and supports during committee meetings. I would like to also thank Britz group members past (Jennilee Gavina, Richard Lee, Lisa D'Agostino, Naomi L. Kuehnbaum) and present (Karen Lam, Alicia DiBattista, Nadine Wellington, Adriana De Macedo, Michelle Saoi, Mai Yamamoto) for making the lab environment friendly and enjoyable.

This work would not have been possible without the following collaborators: Dr. Michael Tropak and Dr. Don Mahuran from the Hospital for Sick Children in Toronto, Canada for their generous donation of Cerezyme/Imiglucerase. Dr. Aurora Martinez group at the University of Bergen, Norway their generous donation of human recombinant WT-PAH and clinically relevant two PKU-mutants. Dr. J. McNulty and his group members, Alex Nielsen and Dave McLeod from McMaster University, for their support with synthesizing chemically unique small molecules for a small chemical library. In addition, I would like to thank Dr. John Brennan for letting me use Tecan Infinite® 200 PRO NanoQuant Microplate Reader in his laboratory.

A special gratitude goes to all my family members and friends who supported me in many ways to strive towards my goal. Last but not least, I would like express appreciation to my husband, for his continuous encouragement and full support.

Table of Contents

List of Figures

Supplemental Figures

List of Tables

Supplemental Tables

List of Abbreviations and Symbols

HEPES	(4-(2-hydroxyethyl)-1-piperazineethanesulfonic acid
DPPL	(E)-2,3-diphenylprop-2-en-1-ol
MMP	1,2,3-Trimethoxy-5-[2-(4-methoxyphenyl) ethenyl]benzene
DGJ	1-deoxynorjirimycin
AdDNJ	2-acetamido-1,2-dideoxynoijirimycin
ADNJ	2-aceto-2-deoxynojirimycin
Compound III	3-Amino-2-benzyl-7-nitro-4-(2-quinolyl)-1,2-dihydroisoquinolin-1-one
DHQ	3-Dehydroquinate
DSA	3-Dehydroshikimic acid
DAHP	3-Deoxy-D-arabino-heptulosonic acid-7-phosphate
Me-Tyr	*3-O*-methyl-*L*-tyrosine
MSMT	4-(4-Methoxystyryl)-2-methylthiazole
F-Phe	4-Fluoro-*L*-phenylalanine hydrocholride
MU	4-Methylumbelliferone
MUG	4-Methylumbelliferyl-β-D-glucopyranoside
Compound IV	5,6-Dimethyl-3-(4-methyl-2-pyridinyl)-2-thioxo-2,3-dihydrothieno [2,3-d] pyrimidin-4(1H)-one
5-EPS-3-P	5-Enolpyruvylshikimate-3-phosphate
ACAS	6-acetamido-6-deoxycastanospermine
ABX	Ambroxol
Fe^{2+}	Ammonium iron (II) sulfatehexahydrate
Å	Angstrom
ANS	Anilino-naphthalene sulfonic acid
BGE	Background electrolyte
GCase	Beta-glucocerebrosidase
BHX	Bromhexine

CE	Capillary electrophoresis
Δ	Change
CS	Chorismate
CV	Coefficient of variance
CBE	Conduritol-β-epoxide
m	Cooperativity for inactivation
R^2	Correlation for determination of linerity
CF	Cystic Fibrosis
CFTR	Cystic firbrosis transmembrane conductance regulator
CYP	Cytochrome P450
E4P	D-erythrose-4-phosphate
DSC	Differential scanning calorimetry
DSF	Differential scanning fluorimetry
BH2	Dihydrobiopterin
DTZ	Diltiazem
DMSO	Dimethyl sulfoxide
DTT	*DL*-dithiothreitol
QA	*D*-quinic acid
EOF	Electroosmotic flow
ESI	Electrospray ionization
ER	Endoplasmic reticulum
E	Enzyme
ES	Enzyme and the substrate complex
ERT	Enzyme replacement therapy
ESA	Ethoxyshikimate
FLZ	Fluphenazine
F	Folded
FDA	Food and drug administrator

GA	Gallic acid
GD	Gaucher disease
GlcCer	Glucosylceramide
Gly	Glycine
GuHCl or GndCl	Guandium hydrochloride
AC_{50}	Half-maximal activity constant
IC_{50}	Half-maximal inhibition constant
HSCT	Heamatopoietic stem cell transplantation
HPLC	High-performance liquid chromatography
HTS	High-throughput screening
HBAs	Hydrogen bond acceptors
HBDs	Hydrogen bond donors
HDX	Hydrogen-deuterium exchange
HPA	Hyperphenylalaninaemia
IRT	Immunoreactive trypsiongen
IEM	In-born error of metabolism
K_i	Inhibition and/or dissociationg constant
I	Inibitors
V_0	Initial velocity
IS	Internal standard
IFG	Isofagomine
LIF	Laser-induced fluorescence
Holo	Ligand associated enzyme complex
apo	Ligand free enzyme
LOD	Limit of detection
LOQ	Limit of quantification
Phe	*L*-phenylalanine
Tyr	*L*-Tyrosine

LSDs	Lysosomal storage disorders
MNT	Mannitol
MALDI	Matrix-assisted laser desorption inonization
V_{max}	Maximum velocity
K_m	Michaelis-Menten constant
C_M	Mid-point for urea inactivation
T_m	Mid-point temperuature for denaturation
α	Modifying factor
MW	Molecular weight
ISL	Myo-inositol
NO-DNJ	N-(7-oxdecyl) deoxynojirimycin
NGT	N-acetyl-glucosamine-thiazoline
LABNAc	N-benzyl-2-acetamido-1,4-imino-1,2,4-trideoxy-L-arabinitol
NB-DGJ	N-butyl-1-deoxynojirimycin
NBS	Newborn screening
NDJ	N-Nonyldeoxynojirimycin
NOEV	N-octyl4-epi-β-valienamine
NMR	Nuclear magnetic resonance
Log P	Octanol-water partition coefficient
PCT	Pharmacological chaperone therapy
PCs	Pharmacological chaperones
PAH	Phenylalanine hydroxylase
PKU	Phenylketonuria
PEP	Phosphoenolpyruvate
PDA	Photodiode array
PYR	Pyrimethamine
READ	Restoration of enzyme activity upon denaturation
RBs	Rotational bonds

S3P	Shikimate-3-phosphate
SA	Shikimic acid
NaCl	Sodium chloride
SDS	Sodium dodecyl sulfate
SUPREX	Stability of unpurified proteins from rates of hydrogen-deuterium exchange
SRT	Substrate reduction therapy
SPR	Surface plasmon resonance
MS/MS	Tandem mass spectrometry
TC	Taurocholic acid
BH4	Tetrahydrobiopterin
TRESI	Time-resolved electrospray ionization
TPSA	Total polar surface area
Trp	Tryptophan
Tyr	Tyrosine
UV	Ultraviolet
U	Unfolded
WT	Wild type

Declaration of Academic Achievement

The following materials has been previously published and is reprinted with written permission:

Chapter I. Reprinted and adapted from *Shanmuganathan. M., Britz-McKibbin. P. High-quality drug screening by capillary electrophoresis: a review. Anal.Chim.Acta. 773, 24-36.* Copyright (2013) Elsevier.

Chapter II. Reprinted and adapted from *Shanmuganathan. M., Britz-McKibbin. P. Inhibitor screening of pharmacological chaperones for lysosomal β-glucocerebrosidase by capillary electrophoresis*. 399 (8), 2843 - 2853. Copyright (2011) Springer

Chapter III. Reprinted and adapted from *Shanmuganathan. M, Britz-McKibbin. P. Functional screening of pharmacological chaperones via restoration of enzyme activity upon denaturation. 51 (2), 7651-7653.* Copyright (2013) American Chemical Society.

Chapter I: Introduction

1.1 Enzyme Associated Disorders and Biomolecular Interactions with Small Molecules

Enzymes catalyze metabolic reactions that regulate cellular activity while maintaining homeostasis under physiological conditions. Thus, enzymes are a major class of protein target when developing treatment strategies for human diseases.[1,2] For instance, cancer is associated with aberrant enzyme activity that contributes to common phenotypic behaviour, including cell self-sufficiency, proliferation and insensitivity to growth inhibition or apoptosis.[3] In this context, small molecules that function as selective protein kinase inhibitors represent a therapeutic approach for cancer treatment.[3,4] The discovery of enzyme inhibitors with antimicrobial activity is relevant to the treatment of acute infections involving pathogenic bacteria or parasites.[5] Inhibition of deleterious protein aggregation and plaque formation also represents a promising approach for treatment and/or prevention of neurodegenerative disorders, such as Alzheimer's disease.[6,7] Many genetic diseases are associated with mutant enzymes with deficient catalytic activity resulting in toxic substrate accumulation that may be salvaged by pharmacological chaperones (PCs), small molecules that enhance folding and stabilization of misfolded protein.[8] Indeed, both endogenous metabolites and xenobiotics modulate the expression and activity of enzymes in vivo, such as human cytochrome P450 (CYP) monooxygenases that play critical roles in primary metabolism and drug detoxification.[9] Hence, selective inhibition, stabilization and/or activation of disease-related enzymes by small molecules enable modulation of cellular activity relevant to human health.

1.2 Expanded Newborn Screening: New Therapies for Treatment of Genetic Diseases

Universal newborn screening (NBS) programs were first introduced over fifty years ago for the early detection and treatment of in-born error of metabolism (IEM) as a way to reduce morbidity and mortality rates of infants with rare genetic diseases.[10,11] Most IEMs result in partial or complete loss in protein function/enzyme activity that can severely impact normal human metabolism leading to acute trauma and/or death if not diagnosed and treated promptly.[12,13] The advent of multiplexed tandem mass spectrometry (MS/MS) technology has led to expanded NBS for pre-symptomatic diagnosis of rare yet treatable genetic disorders.[14] The overall selection criteria for justifying inclusion of an IEM within NBS programs were first described by Wilson and Jungner in 1968, which is summarized in **Table 1.1.** Although the diagnostic performance of MS/MS-based assays is important for inclusion of fatal or debilitating diseases within provincial neonatal screening panels,[15] effective treatment options remain crucial for reducing mortality and clinically significant morbidity among children.[16] For instance, early detection of phenylketonuria (PKU) by MS/MS associated with hyperphenylalaninemia allows for timely intervention based on a *L*-phenylalanine (Phe)-restricted diet and/or tetrahydrobiopterin (BH_4) supplementation to prevent irreversible neurological impairment.[11] However, the lack of dietary and/or pharmaceutical strategies for treatment of other inherited disorders represents major barriers to NBS due to ethical issues regarding screening without tangible benefits to patient care or healthcare savings. Lysosomal storage disorders (LSDs) are a class of in-born errors of metabolism that result in protein deficiency, where mutant enzymes have low residual catalytic activity for glycolipid substrates in the lysosome.

Table 1.1. Criteria for inclusion of metabolic disorders in NBS.[22]
Adapted from *Pediatr. Clin. North Am.*, 2009, **56**, 505–13

• Significant morbidity and/or mortality
• *Available and effective treatment*
• Clinical validity and clinical utility of screen
• Economically "reasonable" and cost-effective
• Known and significant incidence in population to be screened

Gaucher disease (GD) represents the most common form of LSD that is associated with clinically relevant mutations of β-glucocerebrosidase (GCase).[17,18] Currently, enzyme replacement therapy using a recombinant enzyme is the main therapy for treatment of GD and related LSDs; however limitations include high costs, biweekly intra-venous injections, adverse allergic reactions and/or poor efficacy when treating severe disease phenotypes associated with neurological symptoms in the case of type 2/3 GD patients.[19] Alternatively, enzyme enhancement therapy based on small molecules that can restore the function of mutant enzymes represents a promising therapeutic option for treatment of human diseases associated with protein misfolding.[20,21] Due to stringent dietary management practices that may lead to poor adherence, nutritional deficiencies and/or variable clinical outcomes, there is growing interest in oral-based therapies that address the underlying causes of protein deficiency, such as PCs.

1.3 Treatment Options for Lysosomal Storage Disorders

Lysosomes are membrane bound acidic organelles that contain over 50 different hydrolytic enzymes that are responsible for cellular digestion of macromolecules including glycoproteins, glycosphingolipids, glycogens, cholesterol, peptides, oligosaccharides, and polysaccharides.[23,24] Lysosomal enzymes can be divided into four basic categories: (I) glycolipid metabolizing enzymes (β-glucosidase,), (II) glycogen metabolizing enzymes (α-glucosidase) (III) oligosaccharide metabolizing enzymes (mucopolysaccharidoses), and (IV) glycoprotein metabolizing enzymes (P-glycoprotein).[23] Over 50 different LSDs have been characterized to date with a collective

incidence rate ranging from 1:1500 to 1:700 that is dependent on ethnicity and regions with high rate of consanguinity.[23,24] Although the clinical phenotype is highly variable and weakly associated with genotype, the more severe form of LSDs are early-onset (infancy through early childhood) and are characterized by little-to-no enzyme residual activity (< 10%) with severe clinical neurological manifestations. On the other hand, milder forms of LSDs are late-onset (adolescence through adulthood) and are associated with appreciable enzyme residual activity (~10-25%) with no symptoms involving the central nervous system.[23] During the past two decades, different treatment options have been introduced to treat LSD, however limitations are associated with each option as summarized in **Table 1.2.**[25] Heamatopoietic stem cell transplantation (HSCT) was first introduced as a therapeutic approach for LSDs in 1990 based on the use of healthy heamatopoietic stem cells. However, HSCT therapy involves high risk and complicated procedures that require compatible donors while being ineffective for some LSDs. Alternatively, enzyme replacement therapy (ERT) is based on intravenous administration of a recombinant form of deficient enzyme, which compensates for the underlying enzyme defect by increasing cellular enzyme activity as first introduced in 1991 for GD. ERT was subsequently expanded in early 2000s to other LSDs as shown in **Table 1.3**, such as Fabry and Pompe diseases. In addition, substrate reduction (SRT) therapy was introduced in 2000 for GD patients with mild to moderate form without neurological symptoms based on an oral drug, *N*-butyl-deoxynorijimycin (Zavesca), which was then expanded to Niemann-pick C in 2004.[25] Zavesca lowers the rates of synthesis of all glucosylceramide (GlcCer)-based glycolipids, thus reducing glycolipid accumulation that is needed for treatment of clinical symptoms of GD. However, several factors limit the effectiveness of these treatments which impose a burden on patients.[26] For example, ERT, requires bi-weekly administration that has poor delivery to bones and lungs, while being unable to cross the blood-brain barrier. In addition, treatment of GD by ERT is expensive with annual cost estimated at above $250,000 per patient due to complicated expression, purification and quality control measures requires in the biopharmaceutical industry.[27]

Table 1.2. Advantages and limitations of different therapeutic interventions for LSDs.[25] Adapted from *EMBO Mol. Med.*, 2009, **1**, 268–279

Therapies	***Advantages***	***Limitations***
HSCT	o Sustained corrective after a single procedure o Cross-correction of host's cells by secreted enzymes	o Procedure-related risks and mortality o Not effective in some diseases o Time required to identify compatible donors o Poor engraftment in tissues like bone/heart
ERT	o Long-term experience and documented efficacy in thousands of patients treated o Registries available to document natural disease history and efficacy	o Poor distribution of recombinant enzymes in specific tissues o Inability to cross the blood brain barrier o Frequent infusions required/quality of life o Extremely high costs
SRT	o Oral administration o Little impact on quality of life	o Limited clinical experience (only GD) o Long-term adverse effects unknown
PCT	o Better bio-distribution o Can target neurodegeneration o Oral administration/lower costs o Little impact on quality of life	o Limited clinical experience o Long-term adverse effects unknown o Only patients with specific "responsive" mutations amenable to treatments
Gene Therapy	o Sustained correction after a single procedure o Cross-correction by enzymes secreted by factory organs	o Very limited clinical experience, still under development o Long-term safety concerns

HSCT, heamatopoietic stem cell transplantation; ERT, enzyme replacement therapy; SRT, substrate reduction therapy; PCT, pharmacological chaperone therapy

By contrast, SRT with Zavesca is given orally three times a day to patients with mild to moderate type 1 GD, who are unable or unwilling to receive ERT. However, treatment of GD by SRT has adverse side effects such as, diarrhoea, abdominal pains and tremor. Moreover, long-term reduction in glycolipid levels could affect a variety of cell functions due to its essential roles in normal cell physiology.[28] Furthermore, both SRT and ERT treatments focus on substrate accumulation but do not on attenuate lysosomal proteolysis of mutant enzyme. Alternatively, there has been considerable progress in the development

Table 1.3 Approved enzyme replacement therapy and preclinical study of pharmacological chaperone therapy for lysosomal storage disorders.[24]
Please note that further details GD as the most common form of LSD is summarized in **Table 1.4**. Adapted from *Assay Drug Dev. Technol.*, 2011, **9**, 213–235

LSDs, affected enzymes, (approved drugs), PCT

- **Fabry disease,** α-Galactosidase A, (Fabrayzyme (agalsidase beta) & Replagal (agalsidase alpha)), Galactose (preclinical) & 1-deoxynorjirimycin (DGJ) (phase 3)[31–33]
- **GM1 Gangliosidosis,** Acid β-Galactosidase, (none), N-octyl4-epi-β-valienamine (NOEV), 1-deoxynorjiimycin (DGJ), DGJ derivatives, N-butyl-1-deoxynojirimycin (NB-DGJ), Galactose, Fluorous iminoalditols (preclinical) [34–38]
- **GM2 Gangliosidosis (Tay-Sachs/Sandhoff)**, Acid-β-Hexosaminidase, (none), N-acetyl-glucosamine-thiazoline (NGT), 2-acetamido-1,2-dideoxynoijirimycin (AdDNJ), 2-aceto-2-deoxynojirimycin (ADNJ), 6-acetamido-6-deoxycastanospermine (ACAS), M-2297 (nitro-indan-1-one), M45373 (pyrrole[3,4-d]pyridazin-1-one), M-31850 (bisnaphthalimide), N-benzyl-2-acetamido-1,4-imino-1,2,4-trideoxy-L-arabinitol (LABNAc) (preclinical), Pyrimethamine (phase 2)[39–43]
- **Pompe disease**, Acid α-Glucosidase, ((Myzozyme (alaglusidase alfa) & Lumizyme (alglucosidase alfa)), 1-deoxynojirimycin (DNJ), N-butyl-1-deoxygalactonojirimycin (NB-DNJ), N-(7-oxdecyl) deoxynojirimycin (NO-DNJ) (preclinical)[44,45]
- **Krabbe**, Galactocerebrosidase, (none), α-Lobeline (preclinical)[46]
- **Batten**, Palmitoyl & protein thioesterase, (none), CS38 (preclinical)[47]
- **MPS I Hurlder / Hurler-Scheie**, α-L-iduronidase, (Aldurazyme (Iaronidase)), none[24]
- **MPS II Hunter**, Iduronate sulphate sulphatase, (Elaprase (idursulfase)), none[24]
- **MPS III Sanfilippo Syndrome type C**, Heparan sulfate acetyl-CoA, α-glucosaminnidine, N-acetyltransferase, (none), Glucosamine (preclinical)[48]
- **MPS VI (Maroteaux-Lamy)**, N-acetylgalactosamine-4-sulfatase, (Naglazyme (galsulfase)), none[24]

and evaluation of pharmacological chaperone therapy (PCT) as a potential treatment for many genetic diseases that result from misfolded and/or unstable proteins, including LSDs as shown in **Table 1.3**.[29,30] PCT was introduced as a promising approach for Fabry disease in 2001 and then it was expanded to other LSDs, including Gaucher, Tay-Sachs, Sandhoff, Pompe, Krabbe, Battern and Morquio B Moreover, combination therapies may provide better overall efficacy for treatment of LSDs that overcome limitations associated with each therapeutic approach. For instance, the combination of ERT and SRT can be used for GD patients to obtain therapeutic effects across tissues and organs unresponsive to ERT alone.[29] For instance, gene therapy based on restoring defective enzyme activity by inserting new wild type gene into recipient's cell was introduced in 2008, however the therapy development is still under investigation.[25] Thus, a synergistic effect of this strategy may be useful in patients who poorly respond to a specific therapy alone, such as ERT with PCT.

1.4 Pharmacological Chaperone Therapy

Molecular chaperones are proteins that assist in proper folding of macromolecules into functional three-dimension structures while preventing aggregation into non-functional structural forms.[49] Similarly, chemical chaperones are small molecules that bind to mutant or misfolded proteins and facilitate their folding, such as organic osmolytes (e.g., *N*-methylamine oxide). However, osmolytes require high concentration for effective stabilization of protein to counter-act various perturbants, including elevated temperatures, hypertonic environments and chemical denaturants.[50,51] In contrast, PCs are small molecules that bind specifically to mutant enzyme with high affinity in order to stabilize and promote folding of mutant protein thereby evading endoplasmic reticulum (ER)-associated degradation as shown in **Figure 1.1**.[17] Similar to endogenous molecular chaperones that assist in the folding of native protein, PCs are extrinsic low molecular weight compounds that offer a low-cost yet effective therapeutic option for treatment of genetic disorders associated with protein misfolding. Substrate mimics remain the predominant type of PC for treatment of LSDs since they act as competitive inhibitors

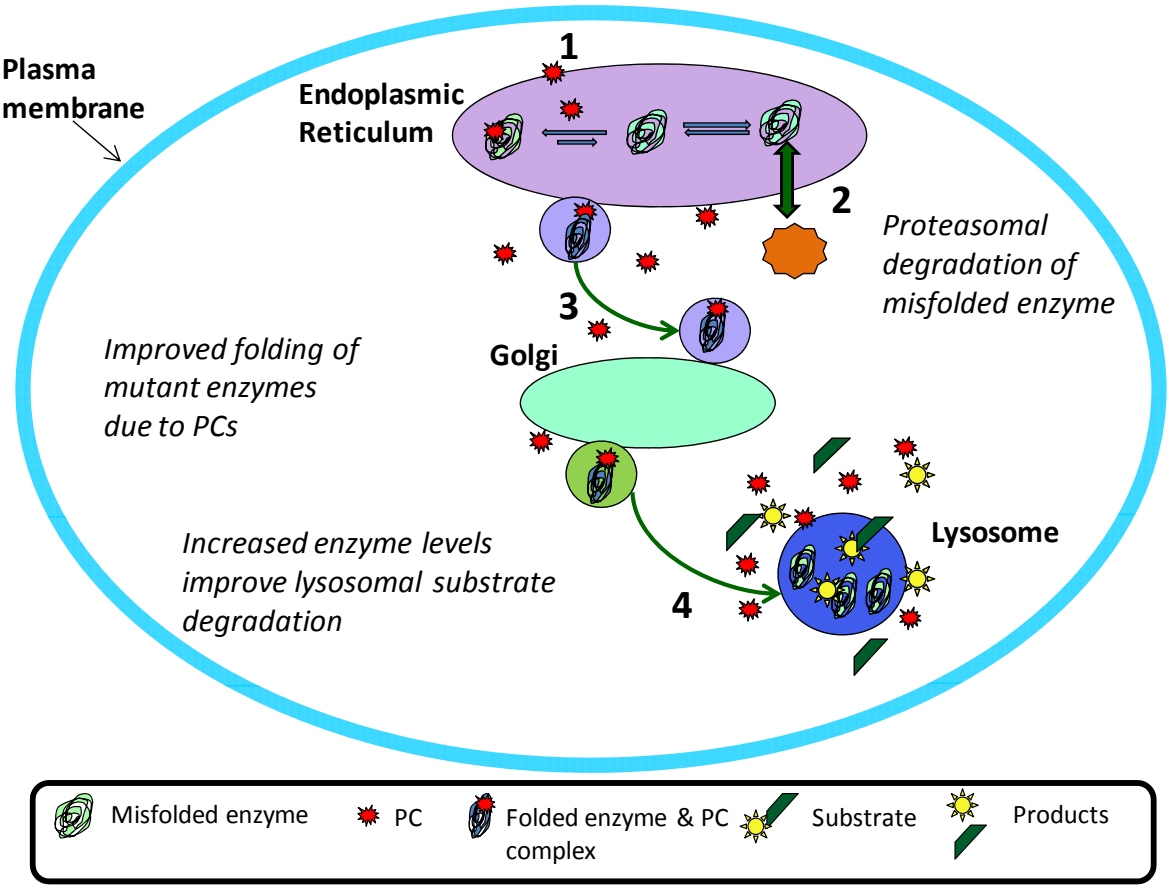

Figure 1.1. Mechanism of action of Pharmacological chaperones (PC). PCs bind selectively to mutant protein and enhance the folding of mutant proteins (1) and prevent the degradation process in ER (2), thereby increasing the traffic of mutant proteins out of the ER to their final destination, such as the lysosome (3 & 4).

with specific yet high affinity binding to the active site of a target enzyme that often results in increased stabilization for the *holo*-enzyme comples.[8,52] The reversible exchange of competitive inhibitor with substrate is dependent on the relative concentration and affinity of each species. For instance, competitive inhibitors with an inhibition constant (K_i) close to the Michaelis-Menten constant (K_m) of the substrate bind with an equal affinity the active site of the enzyme. Although inhibition of enzyme would otherwise prevent substrate conversion, dissociation of inhibitors is favoured under high concentration of substrate as in the case of massive accumulation of glucosylceramide in the lysosome of GD patients.[53] Moreover, PCs that exhibit a pH-dependent binding to an active site with high affinity at neutral pH in the ER, but with lower affinity under acidic

conditions of the lysosome would salvage the mutant protein from proteolysis while preventing adverse effects caused by enzyme inhibition.[54,23] Similarly, an allosteric or remote binder would confer stability to the mutant enzyme to ensure proper trafficking while not competing with the substrate for the active site once in the lysosome.[55,56] Therefore, the development of high quality screening assays for selection of PC candidates for genetic disorders associated with protein misfolding is a crucial element in drug development.[57,58]

1.4.1 Inhibition Assays for Primary Screening of Pharmaceutical Agents

In-vitro kinetic assays are frequently used in early stages of drug discovery to identify lead compounds derived from a natural product extract or chemical library that can reach over one million compounds.[1] Inhibitors, such as natural and synthetic substrate mimics, bind selectively yet with high affinity (K_i = nM-μM) to the active site of an enzyme thereby attenuating product formation. In this case, enzyme inhibitors act towards the suppression of activated and/or over-expressed enzymes associated with human diseases. Enzyme inhibition studies also provide deeper insight into the molecular mechanisms of enzyme action, protein function, cell signalling pathways and disease pathogenesis.[59] Inhibition can involve either irreversible or reversible interactions; an irreversible inhibitor reacts covalently with specific amino acid residues of an enzyme. In contrast, a reversible inhibitor dissociates rapidly upon forming a stable yet non-covalent enzyme-ligand complex due to favourable changes in entropy and/or enthalpy upon drug binding.[60] An inhibitor with high potency and specificity for a target enzyme is required to minimize drug toxicity, which can then be subsequently evaluated using appropriate *in-vitro*, cell-based assays and/or animal models. Overall, reversible inhibitors are categorized as competitive, uncompetitive, non-competitive or mixed-type depending on the site(s) of drug interaction with enzyme as reflected by orthosteric (*i.e.,* active site) and/or allosteric (*i.e.,* non-active site) binding as shown in **Figure 1.2**.

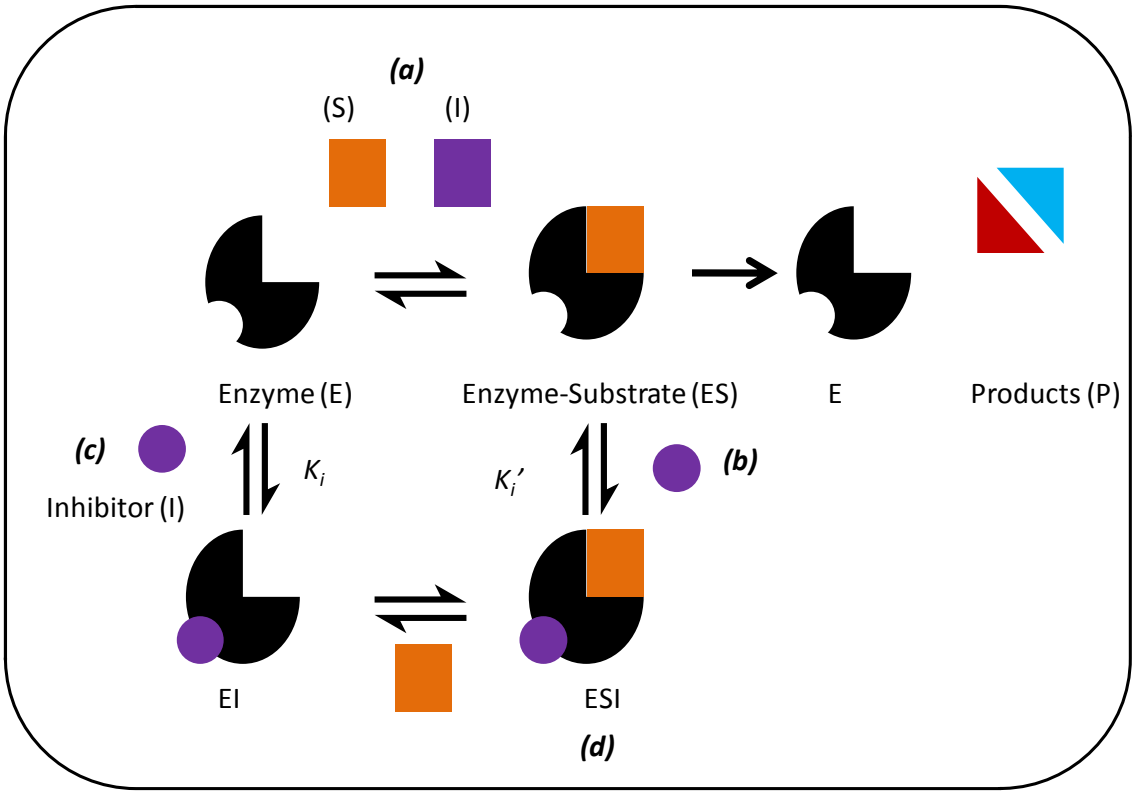

Figure 1.2. Four different types of interactions of reversible inhibitors, competitive, uncompetitive, mixed-type and non-competitive. (a) A competitive inhibitor competes with the substrate for access to the active site of *E* as binding of the substrate and inhibitor cannot take place simultaneously. (b) Uncompetitive inhibition takes place when an inhibitor binds only to the complex formed between the enzyme and the substrate (ES complex). (c) A mixed-type inhibitor binds to free enzyme or the enzyme-substrate complex and the inhibitor binds different site than substrate binds. (d) In non-competitive inhibition both substrate and inhibitor bind simultaneously and thus the complex doesn't proceed to form product.[53]

Drugs that interact allosterically with enzymes offer advantages in terms of higher specificity since non-active sites are less conserved among different classes of protein.[61] Also, since allosteric ligands do not directly compete with substrate binding in the active site, better control of enzyme activity can be realized. The potency and mode of binding of an inhibitor are evaluated by enzyme kinetic parameters, such as K_I and half-maximal inhibition constant (IC_{50}).[62] Similar properties and kinetic parameters are also used to describe the potency of enzyme activators, including half-maximal activity constant (AC_{50}); however, more complicated assay formats are often required when screening molecules that bind to a membrane-bound receptor involved in modulating enzyme activity via a signalling pathway.[63] Inhibitor binding to cytosolic enzymes not only

attenuates substrate conversion, but can also modulate protein function in unanticipated ways, including conformational stability, folding dynamics, protein-protein interactions and catalytic coupling efficiency. For instance, unproductive substrate binding to various cytochrome P450 (CYP) isoforms can induce redox uncoupling resulting in elevated hydrogen peroxide production and enzyme deactivation.[64] Similarly, ligand binding can induce stabilization of folded protein conformers that is not always directly related to inhibitor potency.[65] Thus, there is urgent need for improved assays that accurately measure the potency of enzyme inhibition while also revealing global impacts on protein structure and function.

1.4.2 High-throughput Screening Requirements for Small Molecule Drug Discovery

Enzyme assays used for high-throughput screening (HTS) must satisfy several criteria in drug discovery, including adequate sensitivity, selectivity, sample throughput and automation using a miniaturized assay format.[66] However, a large fraction of screening hits are spurious due to non-specific interactions or aggregate formation under *in-vitro* conditions that contribute to a high false discovery rate.[67] Careful selection of appropriate positive/negative controls during optimization and validation of HTS is critical to ensure a large signal response window (*i.e., Z* factor) above a defined threshold when using a biologically relevant assay.[68] Nonetheless, many lead candidates (*i.e.,* hits) have unfavourable therapeutic potential due to their low bioavailability, high toxicity and poor pharmacokinetic properties that excludes their clinical translation.[69] Indeed, there is growing recognition that drug discovery is prone to high attrition in clinical trials when screening small molecules on the basis of protein structural homology instead of functionally relating enzymes by their ligand binding behaviour.[70] Recent HTS strategies that utilize cell-based assays (*e.g.,* patient tissue) and bioinformatics to filter tentative hits with likely pharmacological properties have been introduced to improve lead candidate optimization.[71]

1.4.3 Analytical Platforms for Primary Screening of Small Molecules

To date, various analytical platforms have been used for primary screening of drug-like activity using enzyme targets. However, many methods suffer from poor selectivity that contributes to false-positives. Fluorescence and radiometric techniques are widely used in primary screening due to their inherent sensitivity and multiplexed capability when using a multi-well plate format. However, fluorescence microarrays are constrained by spectral interferences due to auto-fluorescence or fluorescence quenching when using synthetic fluorogenic substrates,[72] whereas radiometric methods require hazardous radiolabeled substrates in a certified facility.[73,74] Indeed, HTS assays that use different synthetic labeled substrates and/or detection modes can generate widely inconsistent hits when using the same chemical library and enzyme target.[75] Thus, alternative label-free methods are needed with greater selectivity in order to reduce false-positives. For instance, assays using surface plasmon resonance (SPR) and high-performance liquid chromatography-mass spectrometry (HPLC-MS) are increasingly applied for inhibitor screening of protein kinases. SPR is a label-free technique based on measuring dynamic changes in refractive index induced upon ligand binding to an immobilized enzyme target that allows for determination of the thermodynamics and kinetics of bio-molecular interactions.[76,77] However, SPR is not well suited for screening of small molecules that constitute the majority of pharmaceuticals. HPLC-MS is more applicable to inhibitor screening of small molecules that benefits from high selectivity while allowing for qualitative identification of drug candidates in a single run.[78] Separation optimization and long elution times limit sample throughput for complex library mixtures while consuming large amounts of organic solvents.[79] Alternatively, continuous flow immobilized enzyme-reactor columns offer a rapid screening format for compound mixtures by MS/MS.[80] In this case, sol-gel column preparation requires encapsulation and immobilization of a specific protein, which may not suitable for labile and membrane-bound enzyme systems. Recently, segmented flow electrospray ionization (ESI)-MS has been developed for high-throughput screening of inhibitors without chromatographic separation, where mixing of enzyme, substrate and quencher are automated using an array of phase separated

nanodroplets.[81] Nevertheless, the major limitation of all direct infusion MS-based screening methods is the wide disparity in solute ionization efficiency and matrix-induced ion suppression effects that compromises quantitative analyses notably for complex sample mixtures, such as natural product extracts.[14]

Capillary electrophoresis (CE) offers a versatile micro-separation format for drug screening due to its short analysis times, low reagent costs and minimal sample requirements. Miniaturization and/or multiplexing of electrophoretic separations in a microfluidic or capillary array format greatly increases sample throughput.[82–85] Separation of both charged and neutral analytes is achieved by optimization of background electrolyte (BGE) conditions. For instance, the high separation efficiency and tuneable selectivity in CE enables resolution of stereospecific enzyme-catalyzed reactions when using chiral additives in the BGE, such as cyclodextrins and bile salts.[86–88] Thus, CE plays an important role in drug discovery notably in applications involving chiral analysis (*e.g.,* enantiomeric excess), pharmacokinetic/bioavailability studies (*e.g., pK_a*, lipophilicity, brain unbound fraction), and increasingly characterization of biopharmaceuticals.[89,90] Various detection formats can be coupled directly to CE, including UV absorbance, laser-induced fluorescence (LIF), MS and electrochemical detection.[91] CE with UV absorbance detection is the most widely used detection format with moderate sensitivity when using native substrates or their chromogenic analogs, whereas LIF detection enables ultra-sensitive detection of fluorescent-labeled substrates when using an appropriate laser source for excitation. Further improvements in concentration sensitivity and sample processing can also be realized in CE when using on-line sample pre-concentration techniques in conjunction within-capillary chemical derivatization.[92] CE-MS represents a promising yet relatively unexplored format for drug screening that benefits from high resolution separations together with compound identification when using accurate mass, isotope ratio and MS/MS experiments.[78,79] For instance, CE-MS using a metabolomics approach allows for characterization of enzymes of unknown function by identifying specific metabolites transformed within complex mixtures.[93, 94] However, as electrospray ionization (ESI) is widely used in CE-MS,[95,96]

separations require volatile BGEs that limit selectivity while imposing compatibility issues with respect to buffer conditions required for optimum enzyme activity. Thus, alternative ion sources for CE-MS, such as atmospheric photoionization ionization, can expand the range of buffers and additives for improving separation performance without ion suppression, including phosphate and sodium dodecyl sulfate (SDS) micelles.[97] Recent advances towards developing more sensitive yet robust interfaces are critical for wider acceptance of CE-MS, such as porous sprayer and bevelled tip designs.[95,98] In all cases, extensive confirmatory testing of therapeutic efficacy and safety is needed to validate putative hits from primary *in-vitro* screens prior to human clinical trials.

1.4.4 Current Screening Strategy Used to Identify PCs for LSDs

HTS of large chemical libraries for identification of lead PC candidates is crucial for drug development because it reveals novel and structurally unique candidates that are not only competitive inhibitors or activators, but also allosteric site binders. **Figure 1.3** illustrates the overall work flow applied for identification, characterization and validation of PCs that target lysosomal enzymes.[24] To date, the majority of PCs for LSDs are competitive inhibitors that target the active site of an enzyme using biochemical assays based on enzymatic inhibition and/or thermodynamic stability assays. Inhibition assays are typically performed in HTS microarray format using a variety of fluorogenic or chromogenic synthetic substrates with either purified recombinant enzymes or lysates from cells due to challenges to express and purify large quantity of mutant enzymes.[99] The binding of lead PC candidates are also examined with other lysosomal enzymes to confirm specificity. Furthermore, many *in-vitro* assays have been developed to monitor changes in the physical stability of lysosomal enzymes as a function of temperature, pH and/or ligand binding.

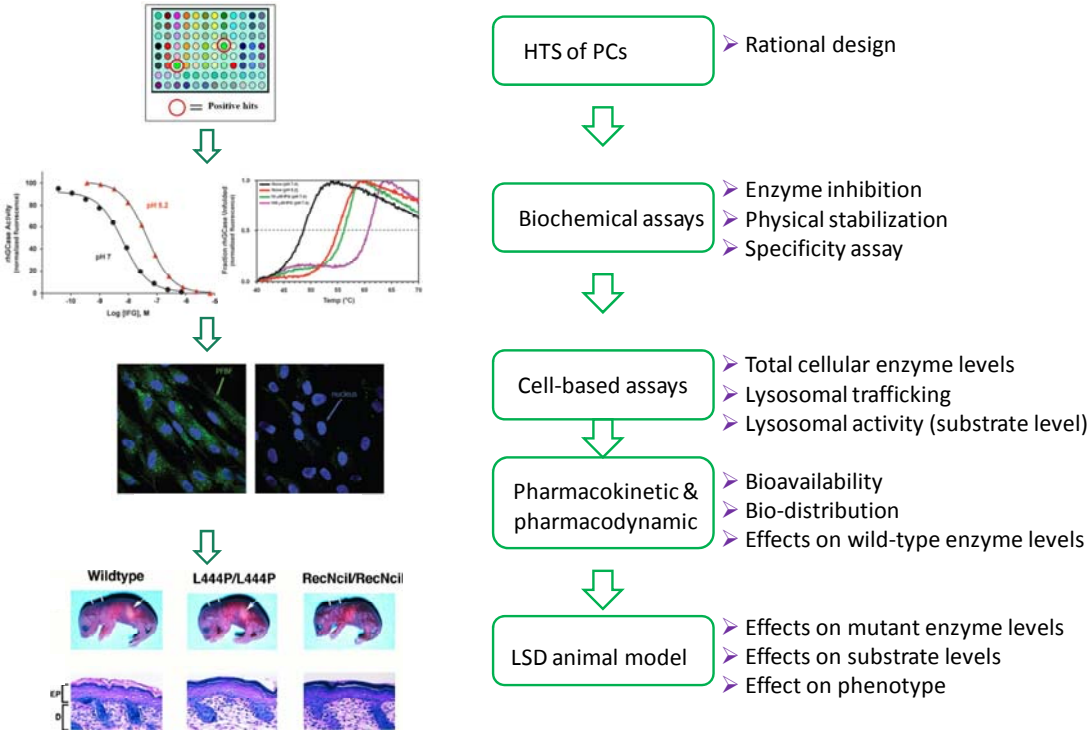

Figure 1.3. Schematic showing the overall drug screening strategy used to identify PC candidates for treatment of LSDs from large chemical libraries, complex natural product extracts or previously approved FDA drugs .[24] Adapted from *Assay Drug Dev. Technol.*, 2011, **9**, 213–235.

Thermal stabilization assays using various techniques such as circular dichroism and differential scanning calorimetry are used to demonstrate the binding and stabilization effects of PCs on lysososmal enzymes based on changes in melting temperature (T_m). A stronger interaction with increased protein stabilization upon PC binding results in apparent shifts towards higher T_m..[54,100] Recently, hydrogen-deuterium exchange (HDX)-MS has also been used to assess the stability of enzyme upon PC binding as a function of chemical denaturant due to deuteron exchange when measuring mass-resolved peptide fragments after pepsin digestion.[101] While thermal stability assay measures global protein stability, HDX-MS can resolve local protein regions stabilized upon PC binding. Fibroblasts derived from patients diagnosed with a specific LSD are primarily used to develop cell-based assays for PCs. Cell-based assays are crucial to assess the effect of PCs at the cellular level, as well as evaluate their efficacy to treat different enzyme

mutations and clinically relevant patient genotypes. Cell-based assays are used to demonstrate increased levels of total cellular levels of the enzyme after incubation with a PC in a dose-dependent manner. This establishes drug efficacy for rescuing mutant enzyme from ER-degradation in affected patient cell lines while also demonstrating potential bioavailability in terms of cell uptake since the PC has penetrated the plasma and ER membranes.[24] However, cell-based assays do not provide information whether mutant enzymes has trafficked to the lysosome and is able to hydrolyse endogenous substrate. Thus, two analytical methods based on Western blotting and fluorescence-based inhibition are used to assess increases in both local protein abundance and enzyme activity, respectively after PC incubation in cells relative to controls, such as a DMSO blank and wild-type enzyme in cells derived from unaffected subjects.

1.4.5 Recent Progress in the Clinical Translation of PCs for Treatment of LSDs

Since the efficacy of PCT is based on enzyme enhancement in order to alleviate deleterious substrate accumulation in the lysosome, kinetic assays are needed to quantify enzyme activity in cell lysates. Since all PCs for LSDs to date have been competitive or mixed-type inhibitors, a washout procedure of drug from cells is necessary prior to cell lysis as carryover of residual PC may lead to bias with a lower apparent enzyme activity. At the same time, performing a washout may also decrease the apparent activity of non-inhibiting PCs, such as allosteric activators. In this case, the simplest approach is to achieve a complete "PC-free" cell state after a washout period, this timeframe is limited by the half-life of the enzyme that has been chaperoned by the PC.[24] For instance, in many cases the half-life of the mutant enzyme is shorter than the wild-type enzyme. Also, the half-life of the wild-type enzyme may vary according to experimental conditions, such as cell type or cell growth conditions. In addition to characterizing the efficacy and safety (*i.e.,* toxicity) of lead PCs using cell-based assays, the ability of a PC to restore enzymatic activity in the lysosomes of disease relevant tissues also needs to be evaluated *in-vivo* using appropriate animal models. For instance, several mouse models express common missense mutant forms for LSDs, which can be used for testing and optimizing

dosage and oral administration for PCs.[24] Although mouse models serve as a way to evaluate the effects of the PC on enzyme and/or substrate levels in disease-relevant tissues, phenotypic similarity to human clinical presentation is lacking. Also, multiple and frequent dose response regimes of PCs using animal models are often not feasible due to its small size and longevity. Nonetheless, the knowledge gained through mouse models of Pompe and Fabry diseases could be applied to other LSDs, as well as larger animal species to evaluate the long-term effects of PCs on clinically relevant endpoints. For instance, successful translation of PCs need to establish whether there is a significant reduction in morbidity or mortality upon early intervention of LSDs that also reduces overall healthcare expenditures, such as reduction in seizures and improved cognitive development for affected children with severe neuronopathic forms of GD (type 2/3). Over the past decade, PCT has been established using cellular and animal models, as well as early stage clinical trials in affected patients with GD as shown in **Table 1.4**.[24] Iminosugars or iminosaccharide, are common components of plants and may exhibit medicinal properties, such as anti-diabetic and anti-viral activity. However, they have also been the primary focus in drug development for LSDs due to their potential use of both glucosylceramide synthase inhibitors (Zavesca, SRT for GD).[102] For instance, 1-deoxynorijimycin (DNJ), a natural iminosugar isolated from mulberry leaves, was identified as one of the first promising PCs used in a phase I clinical trial since it acts as a potent inhibitor and stabilizer to treat for α-glucosidase deficiency in Pompe disease. However, DNJ failed in a subsequent phase II clinical trial due to adverse effects observed in several patients at high dose administration.[24,103,104] In contrast, 1-deoxygalactonojirimycin (DGJ, Migalastat) is an iminosugar currently in phase III clinical trial as a PC candidate for treatment of Fabry disease.

Table 1.4. Lead pharmacological chaperone compounds that target wild-type, modified recombinant and/or mutant GCase for the treatment of GD.[24] Adapted from *Assay Drug Dev. Technol.*, 2011, **9**, 213–235

Pharmacological Chaperones (Status, assay and activity)

- **N-nonyl-deoxynojirimycin (NN-DNJ) and N-hexanoic adamantyl amide deoxynojirimycin (Preclinical)**, in-vitro thermal stability assay using wild-type and N370S, cell-based assay using fibroblast of N370S, L444P and G202R. Moderate increased in activity of N370S and G202R mutations but not L444P [123–126]
- **N-(7-oxadecyl)deoxynojirimycin (Preclinical)**, cell-based assay using N370S fibroblasts, increased activity 1.5 fold[125]
- **N-(n-dodecyl)deoxynojirimycin (Preclinical)**, cell based assay using N370S fibroblasts, decreased activity[125,127]
- **α-1-C-octyl-deoxynojirimycin (CO-DNJ) and α-1-C-nonyl-deoxynojirimycin (CN-DNJ) (Preclinical)**, in-vitro inhibition assay, cell-based assay using N370S fibroblasts, (increased activity by 1.7-fold at 20 μM and by 1.7-fold at 2.5 μM, respectively [127]
- **1,5-dideoxy-1,5-iminoxylitol (DIX) and derivatives (Preclinical)**, in-vitro inhibition assay, cell-based assay using N370S fibroblasts[118]
- **Isofagomine (IFG), (Phase 2 but recently failed)**, in-vitro inhibition and thermal stability assays, cell-assay using N370S and L444P fibroblasts, increased activity 3-fold and 1.3-fold, respectively[128,129]
- **5-N-,6-O-(N'-octyliminomethylidene-nojirimycin (NOI-NJ) and derivatives (Preclinical)**, cell-based assay using N370S, N188S, G202R and F213I and moderate enhancement in activity[130]
- **Diltiazem (DTZ) (Preclinical)**, in-vitro and thermal stability assays, cell-based assay using N370S, L444P fibroblasts, moderately increased activity in N370S but not in L444P[131]
- **Ambroxol (ABX) (Pilot study)**, in-vitro and thermal stability assays, cell-based assay using N370S and L444P fibroblasts[111]
- **5-((4-methylphenyl)thio)quinazoline-2,4-diamine and 5-(3,5-dichlorophenoxy)-N-(4-pyridinyl)-2-furamide (Preclinical)**, in-vitro and thermal stability assay, cell-based assay using N370S fibroblasts and specificity assay using hexosaminidase, increased activity of N370S at 12.5 μM 1.5-fold and 2.5-fold, respectively[101]
- **6-thio-(5N,6S)-[4-(N'-dansylamino)butyliminomethylidene] nojirimycin (Preclinical)**, in-vitro inhibition assay and cell-based assay using N370S and L444P fibroblast[132]
- **O-alkyl iminoxylitol derivatives (Preclinical)**, in-vitro inhibition assay, cell-based assay using N370S fibroblasts[133]

DGJ has showed promising clinical outcomes during phase II clinical trial with decreased accumulation of globotriaosylceramide in multiple tissues with a 50% enhancement in α-galactosidase activity in blood, skin and kidney in the majority of patients under investigation.[105,104] Pyrimethamine, a commonly used as an anti-malarial drug, was also identified as a potent inhibitor of β-hexosaminidase A that is relevant to Tay-Sachs and Sandhoff diseases However, further characterization was recently terminated due to adverse health effects and poor tolerance during phase II clinical trials, such as tremors, ataxia, blurred vision and weakness at high dosage regimes.[104,42] Nevertheless, PC development to date has been mainly focused on GD since it is the most common LSD with β-GCase serving as a model lysosomsal enzyme for characterization of new classes of PCs.

1.5 Motivation and Specific Aims: Better Characterization of PCs for Gaucher Disease

GD is the most common LSD caused by mutations in GCase that has an estimated incidence of 1 in 60,000 in the general population, but with a higher incidence rate among Ashkenazi Jews of 1 in 850.[106] Of the 200 mutations related with GD, two single-point mutations, N370S and L444P are largely associated with non-neuronopathic (type 1) and neuronopathic (type 2/3) forms of the disease in the population, respectively**.** The N370S allele is the most prevalent allele in the Ashkenazi Jewish population (75%) and in the general population (30%), whereas the L444P allele occurs at higher frequency among general population (38%) and in the Jewish population (3%).[107] In contrast, F213I and G202R are less common mutations located in the active site domain as depicted in an X-ray crystal structure for GCase in **Figure 1.4a**. These clinically important variants are largely degraded in the ER by the proteasome, instead of being properly folded and trafficked to the lysosome. ERT was approved by the Food and Drug Administration (FDA) in 1994 for treatment of GD (type I). ERT is based on using a human modified recombinant GCase expressed in the Chinese hamster ovary cell (Imiglucerase or

Cerezyme by Genzyme Corporation) to compensate for underlying protein deficiency in GD type 1 patients. However, Cerezyme suffers from high costs, requires bi-weekly intravenous administration and is not effective for treatment of neurological symptoms (*i.e.,* type 2/3GD) since it does not cross the blood-brain barrier (BBB).[28,108] Until recently, Cerezyme was the only available ERT that treated more than 5000 patients worldwide for more than fifteen years. However, a short supply of Cerezyme arose due to a viral contamination at Genzyme Corporation manufacturing site in 2009, which led to the entry of two additional recombinant enzymes in the market for the treatment of GD in 2010.[28] Shire Human Genetics Therapies (USA) received FDA approval in February 2010 for marketing gene-activated human GCase, Velaglucerase. Velaglucerase alfa has potential advantages due to production in human cell line with the WT human sequence whereas Imiglucerase has a single-point mutation. Furthermore, Protalix Bio Therapeutics (Israel), received FDA approval in May 2012 for marketing plant-cell-derived GCase, Taliglucerase alfa, which derived from a high-yield plant cell system that can be easily up-scalable in disposable bioreactors and free from any exposure to mammalian tissues.[28] Glycosylation modifications of recombinant enzymes are critical for bioavailability, uptake and delivery to different cell types; however, these recombinant GCase likely have more analogous protein glycosylation patterns since they have shown similar activity during clinical trials. Although introduction of new ERTs promise lower cost due to easier manufacturing and purification processes without viral infection, ERT still has limitations of lifetime dependency on intravenous infusions and not effective for treatment of neurological symptoms due to incapability to cross the BBB.[109] Alternatively, PCT represents a promising new yet cost effective therapeutic strategy for genetic disorders based on promotion of protein folding with increased trafficking of native protein to the lysosome.[110] The discovery of PC activity among previously approved drugs with an established safety record offers a convenient approach for "fast-tracking" the translation of new treatments for rare genetic disorders associated with protein misfolding and enzyme deficiency.

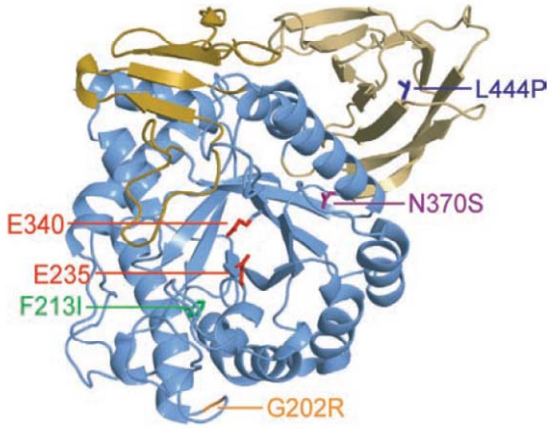

GCase	*Residual activity per total protein (%)*
Wild type	100
N370S	32 ± 7
L444P	12 ± 7
G202R	10 ± 5

Figure 1.4 X-ray structure of GCase mutations and residual activity associated with those mutants. Location of GCase mutations that are amenable to PCT, the two common mutations, N370S and L444P are located in domain I and domain II, respectively. L444P mutation is located in Ig-like domain (II) remote from active site and not amenable to chaperoning by active-site directed or competitive molecules. In contrast, mutations on active-site domain (I), N370S, F213I and G202R, can be corrected or influenced by active-site directed PCs. The catalytic nucleophiles, E 235 and E340 are shown in red.[113] The residual activity of GCase variants in patient derived cells, residual activity of N370S, L444P and G202R are expressed as percentage of WT activity.[114]

Indeed, there is growing interest in exploring new molecular targets for "off-patent" pharmaceuticals in order to reduce costs in orphan drug development and late-stage attrition due to adverse health effects.[111] Indeed, this premise implies that most drugs developed to date are rarely selective in their biomolecular interactions with protein in living organisms. Protein deficiency in GD is associated with increased ER-associated degradation pathways, where aberrant/mutant GCase is tagged for proteolysis by the ubiquitin-proteasome system as a way to prevent misfolding-induced toxicity, such as protein aggregation.[51,112] Even with adequate trafficking of mutant GCase to the lysosome, residual catalytic activity levels lower than 25-30% represents a critical threshold value when GD symptoms likely manifest due to substrate accumulation. However, even modest enhancement in protein trafficking and enzymatic activity with the aid of PCT may be sufficient to attenuate early onset and severe clinical phenotypes, such as neuronopathic forms of type 2/3 GD. Despite the early use of oral tetrahydrobiopterin (BH4) supplementation for treatment of mild phenylketonuria (PKU) since it serves as an intrinsic cofactor that also stabilizes the conformation of some mutant forms of

phenylalanine hydrolyase (PAH),[115–117] the first report of PCs as novel therapeutic agents for genetic disorders consisted of competitive drug inhibitors to lysosomal enzymes (GD and Fabry) that increased *holo*-protein conformational stability upon reversible binding.[118–121] However, substrate-based mimics represent paradoxical therapeutic agents for EET since inhibitors attenuate catalytic activity that is ultimately needed for relief of deleterious substrate accumulation.[62,118,120,122] To date, HTS for PCs has relied on fluorescence-based inhibition assays for lead candidate selection from large chemical libraries with confirmatory testing based on thermal stability and/or patient-derived cell-based assays.[24,68,121] For these reasons, major drug patents of PCs for treatment of GD have largely consisted of potent reversible inhibitors of GCase[17] as summarized in **Table 1.4**. For instance, isofagomine (IFG) is an iminosugar and a competitive inhibitor of GCase with low nanomolar potency *in-vitro*, however due to high polarity has poor distribution and cellular uptake that lowers its overall efficacy *in vivo*.[134] Indeed, recent phase II clinical results for IFG (Plicera) for adults with type 1 GD have demonstrated no adverse health effects with a significant increase in GCase activity measured in white blood cells.[135] However, for most patients no significant improvements in clinical outcomes were observed under two dose regimes during a six month trial period and subsequent clinical investigations have been terminated. The lack of efficacy reported in preliminary clinical trials of IFG for treatment of adult type 1 GD patients has dampened enthusiasm of PCs for EET. Although the poor bioavailability and cell uptake of IFG has been implicated in its lower biological activity *in-vivo*, the high attrition rate of PCs likely stem from the inherent bias of primary screens based on enzyme inhibition. For instance, ambroxol (ABX) is widely used mucolytic agent that was first discovered as a mixed-type inhibitor of GCase using thermal stability assay as a primary screen despite its weak inhibitory potency.[24] A recent pilot study was conducted to assess the tolerability and efficacy of ABX as a PC for adult GD (type 1) patients have demonstrated no adverse health effects with notable decrease in liver and spleen volume. However, no significant improvement in clinical outcomes for most patients were observed under the dose regime examined.[136,137] Thus, there is on-going interest in developing novel PCs with improved

therapeutic efficacy for oral treatment of LSD without adverse health effects. The major goal of this thesis is to better characterize PC candidates for target enzymes of clinical relevance by developing novel screening assays that directly assess chaperone activity of small molecules lacking undesirable inhibitory properties.

1.6 Expansion of PCT to Phenylketonuria (PKU)

Phenylalanine hydroxylase (PAH) is a homo-tetramer enzyme that catalyzes the hydroxylation of *L*-phenylalanine (Phe) to *L*-tyrosine (Tyr) in the presence of iron and a redox-active cofactor, tetrahydrobiopterin (BH4) supplying two electrons needed for the reaction.[138] Indeed, phenylketonuria (PKU) is related to a functional deficiency in PAH and represents one of the most prevalent genetic diseases causing irreversible mental retardation and impaired growth in affected children if left untreated. PKU is an inherited autosomal recessive inborn error of amino acid metabolism associated with more than 500 mutations, where classic PKU patients have plasma level of Phe levels greater than 1200 μM.[139] Currently, dietary (Phe) restriction and BH4 supplementation are the only two available treatment options for PKU where dietary restriction, which imposes a major burden on patients often leading to malnutrition and psychosocial complications. Moreover, BH4 therapy is only effective for certain phenotypes associated with mild PKU.[140] Alternatively, PCT offers a safe yet cost-effective therapy to correct folding of endogenous PAH mutants related to severe mutations that do not respond or comply to dietary management alone.[141] However, primary screening of PC candidates for PAH based on *in-vitro* inhibition assay is not ideal for up-scaling to HTS due to weak native fluorescence properties Tyr with deep UV excitation.[142,143] However, unlike GCase is membrane-bound monomeric protein (**Figure 1.4**) needs a bile salt surfactant for catalytic function, PAH is an oxireductase cytosolic protein (**Figure 1.5**) that requires a cofactor, molecular oxygen and iron for catalytic function, while forming a homotetramer in solution upon substrate binding. Furthermore, urea unfolding may cause PAH to dissociate from tetramer to irreversible trimer, dimer and monomer forms. In addition, no reference PCs are commercially available to validate *in-vitro* assays for PAH due to

recent exploration of PCs for PAH, whereas its catalytic mechanism and oligomerization processes remain poorly understood.

1.7 Thesis Overview and Motivation

The advent of MS/MS technology has led to expanded NBS for pre-symptomatic diagnosis of rare yet treatable genetic disorders. Although the diagnostic performance of MS/MS-based assays is important for inclusion of fatal or debilitating diseases within provincial neonatal screening panels, effective treatment options remains crucial for reducing mortality and clinically significant morbidity among children . Currently, there is no ideal therapeutic treatment available for some genetic disorders caused by protein misfolding, such as GD and PKU. However, PCT represents a promising yet cost effective therapeutic strategy for genetic disorders. However, to date high throughput drug screening has relied on fluorescence-based *in-vitro* inhibition assays for lead PC

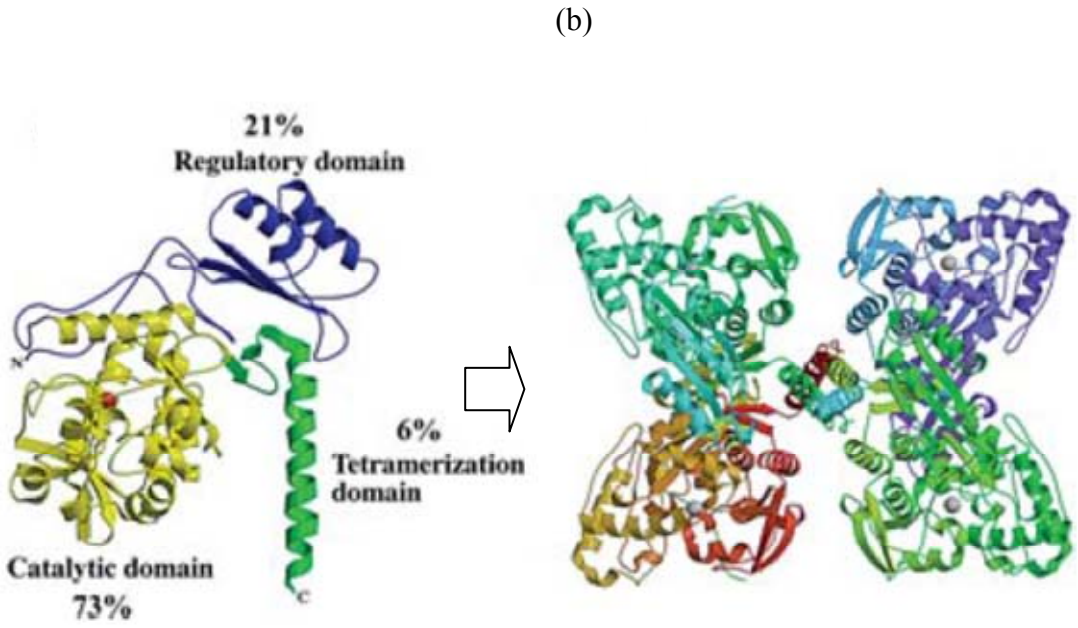

Figure 1.5. The X-ray crystal structure of the human PAH. (a) PAH is a homotetrameric protein with 452 amino acids residues per subunit and each subunit consists of three domains: catalytic domain, regulatory domain and tetramerization domain. Iron atom (shown in red) binds to O_2 in the catalytic domain whereas BH4 binds to the regulatory domain. Percentage of mutations found in BH4 responsive PKU patients is indicated for each domain. (b) The native tetramer form of the enzyme.[116]

candidate selection from large chemical libraries with confirmatory testing based on thermal stability and/or patient-derived cell-based assays. Inhibition assay only focuses on the selection of potent active site competitive inhibitor but exclusion of allosteric or distal site inhibitors. In fact, potent active-site inhibitors that stabilize mutant/misfolded enzymes are not ideal PC candidates since they ultimately attenuate product turn-over rates by competing with substrate binding to active site. This approach does not accurately reflect chaperone activity while leading to high rates of false positives and false negatives, which often require secondary assays and repeated testing to confirm activity. Therefore, there is an urgent need for an improved functional assay that allows for characterization of ligand interactions that enhances protein conformational stability while restoring sufficient activity upon refolding. In this thesis, restoration of enzyme activity upon denaturation (READ) was introduced as a new approach for functional screening of PCs based on direct evaluation of the potency of ligands to stabilize yet enhance the catalytic activity of GCase under denturing conditions when using CE. This approach was later adapted to a fluorescence-based HTS format for the identification of new classes of PC for GCase. Additionally, a complimentary refolding assay was developed for direct characterization of chaperone activity based on the potency of PCs to properly refold yet enhance the catalytic activity of an enzyme under denaturing conditions. This "two-tiered" strategy was then applied to screen a chemical library consisting of structurally unique small molecules after *in silico* assessment for drug-like properties. Compounds that activate, stabilize and refold wild type (WT) GCase activity in a dose-response manner under denaturating conditions were selected as lead candidates for subsequent testing, such as cell-based assays. A similar approach was also developed for identification of novel PCs for PAH, including mutant forms of PAH associated with mild to severe PKU phenotypes. This integrative screening approach has identified several novel PCs that possess greater chaperone activity than conventional inhibitors for GCase and PAH, including structurally unique stilbene derivatives and plant-derived natural products (e.g. shikimic acid, D-quinic acid), respectively. We anticipate that this

work will lead to the translation of safe, efficacious yet low cost treatment of genetic diseases in support of expanded NBS initiatives.

1.8 Major Objectives and Key Research Contributions

To date, fluorescence-based HTS *in-vitro* assays based on enzyme inhibition and/or thermal stability are typically used for primary/secondary screening of potential PC candidates from chemical libraries, including FDA-approved off-patent drugs.[144,99] Several of these PCs exhibit pH-dependent binding with higher binding affinity under neutral pH (reflective of ER) and lower affinity under acidic pH (reflective of lysosome); however, their mode of interactions with GCase are not well understood. In *chapter II* of this thesis, we developed a simple, sensitive yet selective inhibition assay based on CE for better understanding pH-dependent binding phenomena of some of the previously FDA-approved drugs for GCase. CE offers a versatile micro-separation format for inhibitor screening due to its short analysis times, low reagent costs and minimal sample requirements that can be coupled to various on-line detectors.[26] Enzyme kinetic studies were performed at relevant physiological conditions of the lysosome (pH 5.2) and ER (pH 7.2). The CE based inhibition assay was first validated using well characterized PCs of GCase, IFG, which is a potent active site inhibitor with favorable pH-dependent of recombinant GCase. Additionally, four other previously FDA-approved drugs recently identified as putative PCs for GCase were included for further characterization. Moreover, pK_a determination was also performed in order to better understand the pH-dependent phenomena of PC binding to GCase under acidic and neutral pH environments reflective of lysosomes and ER, respectively. However, within our study, the previously FDA-approved drugs were found to have low micromolar activity with undesirable pH-dependent binding in contrast to the ten-fold higher activity of IFG under acidic conditions. To the best of our knowledge, this is the first CE-based screening method rigorously characterized mode of biding and pH-dependent activity of PCs for GCase when using non-linear regression of enzyme inhibition curves.[62] However, the following

questions regarding molecular mechanisms significant to identification of a promising PC remain unanswered:

a) Do all inhibitors induce stabilization to a mutant or partially unfolded native enzyme?
b) Can a stabilizer also enhance refolding and reversibly restore enzyme catalytic activity?

PCs are small molecules have the similar function as molecular chaperones assisting in proper folding of proteins into functional three dimensional structures. However, the current *in-vitro* inhibition assays examine activity or inhibition of PCs under native/folded conditions. Therefore, it would be ideal to examine drug binding under denaturing conditions where the protein is largely unfolded with low residual catalytic activity. To note, mutant GCase are largely unavailable to include in primary inhibition assays due to their rapid degradation in the ER. Thus, an unfolded WT enzyme may represent a better model for PC screening with similar residual activity (5-10%) as common disease causing mutants. *Chapter III* of this thesis, a CE based assay was introduced as a new approach for direct screening of PCs, which evaluates the potency of ligands to stabilize yet enhance the catalytic activity of WT-GCase under denaturing conditions. READ was validated with a series of recently discovered PCs with variable potency and binding modes for GCase as a model system. In addition, dynamic protein unfolding experiments were conducted to investigate the rate, extent and reversibility of GCase denaturation in urea using CE as a unique screening platform.[65] Although READ was initially developed for high-quality screening of PCs for GCase using CE, it can be also applied to other enzymes and be adapted to high-throughput format.

Chapter IV of the thesis, a fluorescence based stabilization assay was first adapted from the original CE based READ for identification of PC candidates for GCase using a chemical library consisting of structurally unique small molecules after *in silico* assessment for drug-like properties. First the assay conditions were optimized to enable shorter incubation times under two different urea conditions as a function of PC dosage

whereas negative and positive PC controls were also incorporated to validate the assay and evaluate data quality. In addition, a complimentary refolding assay was developed for confirmatory testing of chaperone activity. Two unique stilbene derivatives and six structural analogs demonstrated over 2.5-fold activity enhancement for refolding WT GCase relative to recent PCs (ABX and DTZ) for treatment of GD.

In *chapter V* of the thesis, a similar functional "two-tiered" primary screening approach was also expanded for selection of PCs to other class of cytosolic/non-lysosomal enzymes, such as PAH that is relevant to PKU.[142] Primary screening strategies for selection of PCs for PAH rely on thermal stabilization assay due to the lack of inhibition assays suitable for HTS.[145,146] However, thermal stabilization assays are limited by irreversible protein aggregation involving multimeric protein, such as PAH. Therefore, a label-free CE kinetic assay was developed as a functional screening approach for the identification of novel PCs from a chemical library that assist in the refolding of PAH under denaturing conditions, including two relevant PAH mutants associated with mild to severe PKU. Shikimic acid (SA) was found to function as a novel PC for PAH that restored the activity of a severe PAH mutant over 5-fold at 20 μM. SA is a safe and widely used natural product that is ironically used as a key precursor for aromatic amino acid biosynthesis by plants and microbes. This is the first time we have shown that "two-tiered" functional assay using WT enzymes under chemical denaturing conditions can lead to the discovery of PC candidates with activity towards clinically relevant mutant enzymes.

1.9 References

1. Z. M. Tang, T. D. Wang, and J. W. Kang, *Electrophoresis*, 2007, **28**, 2981–2987.

2. Z. M. Tang and J. W. Kang, *Anal. Chem.*, 2006, **78**, 2514–2520.

3. D. Hanahan and R. A. Weinberg, *Cell*, 2000, **100**, 57–70.

4. J. M. Zhang, P. L. Yang, and N. S. Gray, *Nat. Rev. Cancer*, 2009, **9**, 28–39.

5. L. L. Silver, *Clin. Microbiol. Rev.*, 2011, **24**, 71–109.

6. R. Weaver, K. E. N. S. Graham, I. G. Beattie, and R. O. B. J. Riley, *Drug Metab. Dispos.*, 2003, **31**, 955–966.

7. R. Scatena, G. E. Martorana, P. Bottoni, G. Botta, P. Pastore, and B. Giardina, *Expert Opin. Investig. Drugs*, 2007, **16**, 59–72.

8. J. Q. Fan, *Biol. Chem.*, 2008, **389**, 1–11.

9. I. G. Denisov, T. M. Makris, S. G. Sligar, and I. Schlichting, *Chem. Rev.*, 2005, **105**, 2253–2277.

10. D. M. Frazier, D. S. Millington, S. E. McCandless, D. D. Koeberl, S. D. Weavil, S. H. Chaing, and J. Muenzer, *J. Inherit. Metab. Dis.*, 2006, **29**, 76–85.

11. S. a Berry, C. Brown, M. Grant, C. L. Greene, E. Jurecki, J. Koch, K. Moseley, R. Suter, S. C. van Calcar, J. Wiles, and S. Cederbaum, *Genet. Med.*, 2013, **15**, 591–9.

12. D. H. Chace, *Clin. Chem.*, 2003, **49**, 1797–1817.

13. D. Marsden and H. Levy, *Clin. Chem.*, **56**, 1071–1079.

14. K. R. Chalcraft and P. Britz-McKibbin, *Anal. Chem.*, 2009, **81**, 307–314.

15. A. Dajnoki, A. Mühl, G. Fekete, J. Keutzer, J. Orsini, V. Dejesus, X. K. Zhang, and O. a Bodamer, *Clin. Chem.*, 2008, **54**, 1624–9.

16. B. Wilcken, M. Haas, P. Joy, V. Wiley, F. Bowling, K. Carpenter, J. Christodoulou, D. Cowley, C. Ellaway, J. Fletcher, E. P. Kirk, B. Lewis, J. McGill, H. Peters, J. Pitt, E. Ranieri, J. Yaplito-Lee, and A. Boneh, *Pediatrics*, 2009, **124**, e241–8.

17. J. M. Benito, J. M. García Fernández, and C. Ortiz Mellet, *Expert Opin. Ther. Pat.*, 2011, **21**, 885–903.

18. K. F. Lutsky and N. C. Tejwani, *Bull. NYU Hosp. Jt. Dis.*, 2007, **65**, 37–42.

19. T. M. Deegan, Patrick B. cox, *Drug Des. Dev. Ther.*, 2012, 81–106.

20. R. J. Desnick, *J. Inherit. Metab. Dis.*, 2004, **27**, 385–410.

21. J. Inherit, H. Genetics, and N. York, *J. Inherit. Metab. Dis.*, 2004, **27**, 385–410.

22. P. M. Fernhoff, *Pediatr. Clin. North Am.*, 2009, **56**, 505–13, Table of Contents.

23. R. E. Boyd, G. Lee, P. Rybczynski, E. R. Benjamin, R. Khanna, B. a Wustman, and K. J. Valenzano, *J. Med. Chem.*, 2013, **56**, 2705–25.

24. K. J. Valenzano, R. Khanna, A. C. Powe, R. Boyd, G. Lee, J. J. Flanagan, and E. R. Benjamin, *Assay Drug Dev. Technol.*, 2011, **9**, 213–235.

25. G. Parenti, *EMBO Mol. Med.*, 2009, **1**, 268–279.

26. A. H. Futerman, J. L. Sussman, M. Horowitz, I. Silman, and A. Zimran, *Trends Pharmacol. Sci.*, 2004, **25**, 147–151.

27. E. Beutler, *PLoS Med.*, 2004, **1**, 118–121.

28. D. Elstein, *Curr. Pharm. Biotechnol.*, 2011, **12**, 854–860.

29. J. Shayman, S. Larsen, *Journal of Lipid Research*, 2014, **55**, 1215-1225.

30. S. H. Shin, G. J. Murray, S. Kluepfel-Stahl, A. M. Cooney, J. M. Quirk, R. Schiffmann, R. O. Brady, and C. R. Kaneski, *Biochem. Biophys. Res. Commun.*, 2007, **359**, 168–173.

31. T. Okumiya, S. Ishii, T. Takenaka, R. Kase, S. Kamei, H. Sakuraba, and Y. Suzuki, *Biochem. Biophys. Res. Commun.*, 1995, **214**, 1219–1224.

32. J. Frustaci, A, Chimenti, C, Ricci, R, Natale, L, Russo, M.A, Pieroni, M, Desnick, R, *N. Engl. J. Med.*, 2001, **345**, 25–32.

33. A. Kato, Y. Yamashita, S. Nakagawa, Y. Koike, I. Adachi, J. Hollinshead, R. J. Nash, K. Ikeda, and N. Asano, *Bioorg. Med. Chem.*, 2010, **18**, 3790–3794.

34. H. Iwasaki, H. Watanabe, M. Iida, S. Ogawa, M. Tabe, K. Higaki, E. Nanba, and Y. Suzuki, *Brain Dev.*, 2006, **28**, 482–6.

35. L. Tominaga, Y. Ogawa, M. Taniguchi, K. Ohno, and J. Matsuda, *Brain Dev.*, 2001, **23**, 284–287.

36. A. Caciotti, M. A. Donati, A. d'Azzo, R. Salvioli, R. Guerrini, E. Zammarchi, and A. Morrone, *Eur. J. Paediatr. Neurol.*, 2009, **13**, 160–4.

37. K. Fantur, D. Hofer, G. Schitter, A. J. Steiner, B. M. Pabst, T. M. Wrodnigg, A. E. Stütz, and E. Paschke, *Mol. Genet. Metab.*, 2010, **100**, 262–8.

38. G. Schitter, A. J. Steiner, G. Pototschnig, E. Scheucher, M. Thonhofer, C. a Tarling, S. G. Withers, K. Fantur, E. Paschke, D. J. Mahuran, B. a Rigat, M. B. Tropak, C. Illaszewicz, R. Saf, A. E. Stütz, and T. M. Wrodnigg, *Chembiochem*, 2010, **11**, 2026–33.

39. G. H. B. Maegawa, M. Tropak, J. Buttner, T. Stockley, F. Kok, J. T. R. Clarke, and D. J. Mahuran, *J. Biol. Chem.*, 2007, **282**, 9150–9161.

40. M. B. Tropak, J. E. Blanchard, S. G. Withers, E. D. Brown, and D. Mahuran, *Chem. Biol.*, 2007, **14**, 153–64.

41. M. B. Tropak, S. P. Reid, M. Guiral, S. G. Withers, and D. Mahuran, *J. Biol. Chem.*, 2004, **279**, 13478–87.

42. J. T. R. Clarke, D. J. Mahuran, S. Sathe, E. H. Kolodny, B. a Rigat, J. a Raiman, and M. B. Tropak, *Mol. Genet. Metab.*, 2011, **102**, 6–12.

43. J. S. S. Rountree, T. D. Butters, M. R. Wormald, S. D. Boomkamp, R. a Dwek, N. Asano, K. Ikeda, E. L. Evinson, R. J. Nash, and G. W. J. Fleet, *ChemMedChem*, 2009, **4**, 378–92.

44. T. Okumiya, M. a Kroos, L. Van Vliet, H. Takeuchi, A. T. Van der Ploeg, and A. J. J. Reuser, *Mol. Genet. Metab.*, 2007, **90**, 49–57.

45. G. Parenti, A. Zuppaldi, M. Gabriela Pittis, M. Rosaria Tuzzi, I. Annunziata, G. Meroni, C. Porto, F. Donaudy, B. Rossi, M. Rossi, M. Filocamo, A. Donati, B. Bembi, A. Ballabio, and G. Andria, *Mol. Ther.*, 2007, **15**, 508–14.

46. W. C. Lee, D. Kang, E. Causevic, A. R. Herdt, E. a Eckman, and C. B. Eckman, *J. Neurosci.*, 2010, **30**, 5489–97.

47. G. Dawson, C. Schroeder, and P. E. Dawson, *Biochem. Biophys. Res. Commun.*, 2010, **395**, 66–9.

48. M. Feldhammer, S. Durand, and A. V Pshezhetsky, *PLoS One*, 2009, **4**, e7434.

49. A. J. L. Macario and E. Conway de Macario, *N. Engl. J. Med.*, 2005, **353**, 1489–1501.

50. P. Leandro and C. M. Gomes, *Mini-Reviews Med. Chem.*, 2008, **8**, 901–911.

51. T. Arakawa, D. Ejima, Y. Kita, and K. Tsumoto, *Biochim. Biophys. Acta - Proteins Proteomics*, 2006, **1764**, 1677–1687.

52. D. P. Germain and J.-Q. Fan, *Int. J. Clin. Pharmacol. Ther.*, 2009, **47 Suppl 1**, S111–S117.

53. A. Cornish-Bowden, *Biochemistry*, 1974, **137**, 143.

54. R. L. Lieberman, J. A. D'Aquino, D. Ringe, and G. A. Petsko, *Biochemistry*, 2009, **48**, 4816–4827.

55. C. Porto, M. C. Ferrara, M. Meli, E. Acampora, V. Avolio, M. Rosa, B. Cobucci-Ponzano, G. Colombo, M. Moracci, G. Andria, and G. Parenti, *Mol. Ther.*, 2012, **20**, 2201–11.

56. M. R. Landon, R. L. Lieberman, Q. Q. Hoang, S. L. Ju, J. M. M. Caaveiro, S. D. Orwig, D. Kozakov, R. Brenke, G. Y. Chuang, D. Beglov, S. Vajda, G. A. Petsko, and D. Ringe, *J. Comput. Aided. Mol. Des.*, 2009, **23**, 491–500.

57. T. J. Carlson and M. B. Fisher, *Comb. Chem. High Throughput Screen.*, 2008, **11**, 258–264.

58. R. Zang, D. Li, I. Tang, J. Wang, and S. Yang, *Int. J. Biotechnol. Wellness Ind.*, 2012, 31–51.

59. W. Zheng, J. Padia, D. J. Urban, A. Jadhav, O. Goker-Alpan, A. Simeonov, E. Goldin, D. Auld, M. E. LaMarca, J. Inglese, C. P. Austin, and E. Sidransky, *Proc. Natl. Acad. Sci. U. S. A.*, 2007, **104**, 13192–7.

60. E. Freire, *Chem. Biol. Drug Des.*, 2009, **74**, 468–472.

61. R. Nussinov, C. J. Tsai, and P. Csermely, *Trends Pharmacol. Sci.*, 2011, **32**, 686–693.

62. M. Shanmuganathan and P. Britz-McKibbin, *Anal. Bioanal. Chem.*, 2011, **399**, 2843–2853.

63. J. M. Cunliffe, M. R. Whorton, R. K. Sunahara, and R. T. Kennedy, *Electrophoresis*, 2007, **28**, 1913–1920.

64. J. Harskamp, P. Britz-McKibbin, and J. Y. Wilson, *Anal. Chem.*, 2012, **84**, 862–866.

65. M. Shanmuganathan and P. Britz-Mckibbin, *Biochemistry*, 2012, **51**, 7651–7653.

66. L. M. Mayr and D. Bojanic, *Curr. Opin. Pharmacol.*, 2009, **9**, 580–588.

67. S. L. McGovern, E. Caselli, N. Grigorieff, and B. K. Shoichet, *Biochemistry*, 2002, **41**, 8967.

68. W. Zheng, J. Padia, D. J. Urban, A. Jadhav, O. Goker-Alpan, A. Simeonov, E. Goldin, D. Auld, M. E. LaMarca, J. Inglese, C. P. Austin, and E. Sidransky, *Proc. Natl. Acad. Sci. U. S. A.*, 2007, **104**, 13192–7.

69. A. P. Beresford, H. E. Selick, and M. H. Tarbit, *Drug Discov. Today*, 2002, **7**, 109–116.

70. M. J. Keiser, J. J. Irwin, and B. K. Shoichet, *Biochemistry*, 2010, **49**, 10267–10276.

71. E. Goldin, W. Zheng, O. Motabar, N. Southall, J. H. Choi, J. Marugan, C. P. Austin, and E. Sidransky, *PLoS One*, 2012, **7**.

72. Z. M. Tang, Z. Y. Wang, and J. W. Kang, *Electrophoresis*, 2007, **28**, 360–365.

73. J. Iqbal and C. E. Müller, *J. Chromatogr. A*, 2011, **1218**, 4764–71.

74. J. Iqbal and C. E. Muller, *J. Chromatogr. A*, 2012, **1218**, 4764–4771.

75. M. A. Sills, D. Weiss, Q. Pham, R. Schweitzer, X. Wu, and J. Z. J. Wu, *J. Biomol. Screen.*, 2002, **7**, 191–214.

76. H. S. Kwon, K. C. Han, K. S. Hwang, J. H. Lee, T. S. Kim, D. S. Yoon, and E. G. Yang, *Anal. Chim. Acta*, 2007, **585**, 344–349.

77. Z. Liu, A. P. Drabovich, S. N. Krylov, and J. Pawliszyn, *Anal. Chem.*, 2007, **79**, 1097–100.

78. J. M. Halket, D. Waterman, A. M. Przyborowska, R. K. P. Patel, P. D. Fraser, and P. M. Bramley, *J. Exp. Bot.*, 2005, **56**, 219–43.

79. C. Petucci, T. Lloyd, H. a Harris, X. Zhang, V. M. Chennathukuzhi, B. Mekonnen, and Y. Cai, *J. Mass Spectrom.*, 2010, **45**, 65–71.

80. E. M. Forsberg, J. R. A. Green, and J. D. Brennan, *Anal. Chem.*, 2011, **83**, 5230–5236.

81. S. W. Sun, T. R. Slaney, and R. T. Kennedy, *Anal. Chem.*, 2012, **84**, 5794–5800.

82. H. M. Pang, J. Kenseth, and S. Coldiron, *Drug Discov. Today*, 2004, **9**, 1072–1080.

83. S. Jambovane, E. C. Duin, S. K. Kirn, and J. W. Hong, *Anal. Chem.*, 2009, **81**, 3239–3245.

84. Y. I. Yagi, K. Abe, K. Ikebukuro, and K. Sode, *Biochemistry*, 2009, **48**, 10255–10266.

85. L. J. Ma, X. Y. Gong, and E. S. Yeung, *Anal. Chem.*, 2000, **72**, 3383–3387.

86. D. Koval, J. Jiraskova, K. Strisovsky, J. Konvalinka, and V. Kasicka, *Electrophoresis*, 2006, **27**, 2558–2566.

87. D. Koval, V. Kasicka, J. Jiracek, and M. Collinsova, *Electrophoresis*, 2006, **27**, 4648–4657.

88. J. M. A. Gavina, C. E. White, T. M. Finan, and P. Britz-McKibbin, *Electrophoresis*, 2010, **31**, 2831–2837.

89. A. Espada and M. Molina-Martin, *Drug Discov. Today*, 2012, **17**, 396–404.

90. Y. Liu, O. Salas-Solano, and L. A. Gennaro, *Anal. Chem.*, 2009, **81**, 6823–6829.

91. J. Zhang, Y. J. Lou, J. Hoogmartens, and A. Van Schepdael, *Electrophoresis*, 2006, **27**, 4827–4835.

92. A. S. Ptolemy and P. Britz-McKibbin, *J. Chromatogr. A*, 2006, **1106**, 7–18.

93. N. Saito, M. Robert, S. Kitamura, R. Baran, T. Soga, H. Mori, T. Nishioka, and M. Tomita, *J. Proteome Res.*, 2006, **5**, 1979–1987.

94. N. Saito, M. Robert, H. Kochi, G. Matsuo, Y. Kakazu, T. Soga, and M. Tomita, *J. Biol. Chem.*, 2009, **284**, 16442–16451.

95. E. J. Maxwell, X. F. Zhong, H. Zhang, N. van Zeijl, and D. D. Y. Chen, *Electrophoresis*, 2010, **31**, 1130–1137.

96. E. J. Maxwell and D. D. Y. Chen, *Anal. Chim. Acta*, 2008, **627**, 25–33.

97. R. Mol, G. J. de Jong, and G. W. Somsen, *Anal. Chem.*, 2005, **77**, 5277–5282.

98. R. Ramautar, J. M. Busnel, A. M. Deelder, and O. A. Mayboroda, *Anal. Chem.*, 2012, **84**, 885–892.

99. D. J. Urban, W. Zheng, O. Goker-Alpan, A. Jadhav, M. E. LaMarca, J. Inglese, E. Sidransky, and C. P. Austin, *Comb. Chem. High Throughput Screen.*, 2008, **11**, 817–824.

100. M. Aguilar-Moncayo, M. I. García-Moreno, A. Trapero, M. Egido-Gabás, A. Llebaria, J. M. G. Fernández, and C. O. Mellet, *Org. Biomol. Chem.*, 2011, **9**, 3698–3713.

101. M. B. Tropak, G. J. Kornhaber, B. A. Rigat, G. H. Maegawa, J. D. Buttner, J. E. Blanchard, C. Murphy, S. J. Tuske, S. J. Coales, Y. Hamuro, E. D. Brown, and D. J. Mahuran, *Chembiochem*, 2008, **9**, 2650–2662.

102. G. Horne, F. X. Wilson, J. Tinsley, D. H. Williams, and R. Storer, *Drug Discov. Today*, 2011, **16**, 107–18.

103. T. K. Chaudhuri and S. Paul, *Febs J.*, 2006, **273**, 1331–49.

104. J. A Shayman and S. D. Larsen, *J. Lipid Res.*, 2014, **55**, 1215–1225.

105. E. R. Benjamin, J. J. Flanagan, a Schilling, H. H. Chang, L. Agarwal, E. Katz, X. Wu, C. Pine, B. Wustman, R. J. Desnick, D. J. Lockhart, and K. J. Valenzano, *J. Inherit. Metab. Dis.*, 2009, **32**, 424–40.

106. B. Meusser, C. Hirsch, E. Jarosch, and T. Sommer, *Nat. Cell Biol.*, 2005, **7**, 766–772.

107. A R. Sawkar, W. D'Haeze, and J. W. Kelly, *Cell. Mol. Life Sci.*, 2006, **63**, 1179–92.

108. J. Goldblatt, J. M. Fletcher, J. McGill, J. Szer, and M. Wilson, *Blood Cells Mol. Dis.*, **46**, 107–110.

109. A. Zimran, *Blood*, 2011, **118**, 1463–1471.

110. B. Brumshtein, H. M. Greenblatt, T. D. Butters, Y. Shaaltiel, D. Aviezer, I. Silman, A. H. Futerman, and J. L. Sussman, *J. Biol. Chem.*, 2007, **282**, 29052–8.

111. G. H. B. Maegawa, M. B. Tropak, J. D. Buttner, B. a Rigat, M. Fuller, D. Pandit, L. Tang, G. J. Kornhaber, Y. Hamuro, J. T. R. Clarke, and D. J. Mahuran, *J. Biol. Chem.*, 2009, **284**, 23502–16.

112. D. B. Craig, T. T. Morris, and C. M. Q. Ong-Justiniano, *Anal. Chem.*, 2012, **84**, 4598–4602.

113. A. R. Sawkar, W. D'Haeze, and J. W. Kelly, *Cell. Mol. Life Sci.*, 2006, **63**, 1179–1192.

114. A. R. Sawkar, S. L. Adamski-Werner, W. C. Cheng, C. H. Wong, E. Beutler, K. P. Zimmer, and J. W. Kelly, *Chem. Biol.*, 2005, **12**, 1235–1244.

115. S. W. Gersting, F. B. Lagler, A. Eichinger, K. F. Kemter, M. K. Danecka, D. D. Messing, M. Staudigl, K. a Domdey, C. Zsifkovits, R. Fingerhut, H. Glossmann, A. a Roscher, and A. C. Muntau, *Hum. Mol. Genet.*, 2010, **19**, 2039–49.

116. C. Heintz, R. G. H. Cotton, and N. Blau, *Hum. Mutat.*, 2013, **34**, 927–36.

117. S. Kure, D. Hou, T. Ohura, H. Iwamoto, S. Suzuki, N. Sugiyama, O. Sakamoto, K. Fujii, Y. Matsubara, and K. Narisawa, *J. Pediatr.*, 1999, **135**, 375–378.

118. H. H. Chang, N. Asano, S. Ishii, Y. Ichikawa, and J. Q. Fan, *Febs J.*, 2006, **273**, 4082–4092.

119. H. H. Chang, N. Asano, S. Ishii, Y. Ichikawa, and J. Q. Fan, *Febs J.*, 2006, **273**, 4082–4092.

120. R. A. Steet, S. Chung, B. Wustman, A. Powe, H. Do, and S. A. Kornfeld, *Proc. Natl. Acad. Sci. U. S. A.*, 2006, **103**, 13813–13818.

121. K. Yu,Z, Sawkar, A.R, Whalen, L.J, Wong, C, *J. Med. Chem.*, 2008, **50**, 94–100.

122. T. D. Butters, *Curr. Opin. Chem. Biol.*, 2007, **11**, 412–418.

123. C. Chaperones and G. Variants, *Acs Chem. Biol.*, 2006, **1**, 235–251.

124. A. R. Sawkar, S. L. Adamski-Werner, W. C. Cheng, C. H. Wong, E. Beutler, K. P. Zimmer, and J. W. Kelly, *Chem. Biol.*, 2005, **12**, 1235–1244.

125. A. R. Sawkar, W. C. Cheng, E. Beutler, C. H. Wong, W. E. Balch, and J. W. Kelly, *Proc. Natl. Acad. Sci. U. S. A.*, 2002, **99**, 15428–15433.

126. G. Sanchez-Olle, J. Duque, M. Egido-Gabas, J. Casas, M. Lluch, A. Chabas, D. Grinberg, and L. Vilageliu, *Blood Cells Mol. Dis.*, 2009, **42**, 159–166.

127. L. Yu, K. Ikeda, A. Kato, I. Adachi, G. Godin, P. Compain, O. Martin, and N. Asano, *Bioorg. Med. Chem.*, 2006, **14**, 7736–7744.

128. G. J. Kornhaber, M. B. Tropak, G. H. Maegawa, S. J. Tuske, S. J. Coales, D. J. Mahuran, and Y. Hamuro, *Chembiochem*, 2008, **9**, 2643–9.

129. R. A Steet, S. Chung, B. Wustman, A. Powe, H. Do, and S. A Kornfeld, *Proc. Natl. Acad. Sci. U. S. A.*, 2006, **103**, 13813–8.

130. Z. Luan, K. Higaki, M. Aguilar-Moncayo, H. Ninomiya, K. Ohno, M. I. García-Moreno, C. O. Mellet, J. M. García Fernández, and Y. Suzuki, *ChemBioChem*, 2009, **10**, 2780–2792.

131. B. Rigat and D. Mahuran, *Mol. Genet. Metab.*, 2009, **96**, 225–232.

132. Z. Luan, K. Higaki, M. Aguilar-Moncayo, L. Li, H. Ninomiya, E. Nanba, K. Ohno, M. I. García-Moreno, C. Ortiz Mellet, J. M. García Fernández, and Y. Suzuki, *ChemBioChem*, 2010, **11**, 2453–2464.

133. F. Oulaïdi, S. Front-Deschamps, E. Gallienne, E. Lesellier, K. Ikeda, N. Asano, P. Compain, and O. R. Martin, *ChemMedChem*, 2011, **6**, 353–61.

134. G. A Grabowski, *Hematology Am. Soc. Hematol. Educ. Program*, 2012, **2012**, 13–8.

135. T. M. Cox, *Biologics*, 2010, **4**, 299–313.

136. G. H. B. Maegawa, M. B. Tropak, J. D. Buttner, B. A. Rigat, M. Fuller, D. Pandit, L. I. Tang, G. J. Kornhaber, Y. Hamuro, J. T. R. Clarke, and D. J. Mahuran, *J. Biol. Chem.*, 2009, **284**, 23502–23516.

137. A. Zimran, G. Altarescu, and D. Elstein, *Blood Cells, Mol. Dis.*, 2013, **50**, 134–137.

138. C. Degraw, J.I, Cory, M, Skinner, W.A, Theisen, M.C, Mitoma, *J. Med. Chem.*, 1967, **10**, 64–66.

139. R. A. Williams, C. D. S. Mamotte, and J. R. Burnett, *Clin. Biochem. Rev.*, 2008, **29**, 31–41.

140. P. Strisciuglio and D. Concolino, *Metabolites*, 2014, **4**, 1007–17.

141. A. L. Pey, M. Ying, N. Cremades, A. Velazquez-Campoy, T. Scherer, B. Thöny, J. Sancho, and A. Martinez, *J. Clin. Invest.*, 2008, **118**, 2858–2867.

142. J. Underhaug, O. Aubi, and A. Martinez, *Curr. Top. Med. Chem.*, 2012, **12**, 2534–45.

143. M. Thórólfsson, B. Ibarra-Molero, P. Fojan, S. B. Petersen, J. M. Sanchez-Ruiz, and A. Martínez, *Biochemistry*, 2002, **41**, 7573–85.

144. G. H. B. Maegawa, M. B. Tropak, J. D. Buttner, B. A. Rigat, M. Fuller, D. Pandit, L. I. Tang, G. J. Kornhaber, Y. Hamuro, J. T. R. Clarke, and D. J. Mahuran, *J. Biol. Chem.*, 2009, **284**, 23502–23516.

145. J. Underhaug, O. Aubi, and A. Martinez, *Curr. Top. Med. Chem.*, 2012, **12**, 2534–45.

146. M. I. Flydal and A. Martinez, *IUBMB Life*, 2013, **65**, 341–9.

147. T. W. Loo and D. M. Clarke, *Expert Rev. Mol. Med.*, 2007, **9**, 1–18.

Chapter II:
Inhibitor Screening of Pharmacological Chaperones for Lysosomal β-Glucocerebrosidase by Capillary Electrophoresis

2.1 Abstract

Pharmacological chaperones (PCs) represent a promising therapeutic strategy for treatment of lysosomal storage disorders (LSDs) based on enhanced stabilization and trafficking of mutant protein upon orthosteric and/or allosteric binding. Herein, we introduce a simple yet reliable enzyme assay based on capillary electrophoresis (CE) for inhibitor screening of PCs that target the lysosomal enzyme, β-glucocerebrosidase (GCase). The rate of GCase-catalyzed hydrolysis of the substrate, 4-methylumbelliferyl-β-*D*-glucopyranoside was performed by CE with UV detection using different classes of PCs as a model system. The pH and surfactant dependence of inhibitor binding on recombinant GCase activity was also examined. Enzyme inhibition studies were investigated for five putative PCs including, isofagomine (IFG), ambroxol (ABX), bromhexine (BHX), diltiazem (DTZ) and fluphenazine (FLZ). IFG was confirmed as a potent competitive inhibitor of recombinant GCase with half-maximal inhibitory concentration (IC_{50}) of (47.5 ± 0.1) nM and (4.6 ± 1.4) nM at pH 5.2 and pH 7.2, respectively. In contrast, four other PCs were demonstrated to function as mixed-type inhibitors with lower micromolar activity at neutral pH relative to acidic pH conditions reflective of the lysosome. CE offers a convenient platform for characterization of PCs as a way to accelerate the clinical translation of previously approved drugs for oral treatment of rare genetic disorders, such as Gaucher disease.

2.2 Introduction

Over the past two decades, there has been remarkable progress in the development of therapies for treatment of lysosomal storage disorders (LSDs).[1] LSDs are a diverse group of in-born errors of metabolism associated with partial or complete loss in lysosomal enzyme activity, causing substrate accumulation that can severely impact normal human metabolism. For example, Gaucher disease (GD) is the most prevalent LSD caused by mutations in β-glucocerebrosidase (GCase) or acid-β-glycosidase that has an estimated incidence of 1 in 60,000 in the general population, but with a higher incidence rate among Ashkenazi Jews of 1 in 800.[2,3] Acute GCase deficiency results in the progressive accumulation of glucosylceramide (GlcCer) primarily in the lysosome, which can lead to severe morbidity with symptoms ranging from anemia, bone lesions, spleen/liver enlargement in type I disease and neurological impairment in types II and III disease [4]. Of the 200 known variants associated with GD, two mutations, N370S and L444P are frequently associated with non-neuronopathic and neuronopathic disease, respectively.[5] Currently, enzyme-replacement therapy (ERT) using recombinant GCase (Cerezyme) and substrate-reduction therapy (SRT) using *N*-butyldeoxynorjirimycin (Zavesca) are two approved treatment options for GD.[3,6] ERT compensates for underlying enzyme deficiency by transiently increasing intra-cellular GCase activity, whereas SRT lowers the rates of biosynthesis of GlcCer-based glycosphingolipids, thereby reducing substrate concentration. However, several factors limit the clinical efficacy of both these therapies which impose a burden on patients.[3,6] Alternatively, pharmacological chaperones (PCs) offer a novel treatment approach based on small molecules that bind selectively to mutant enzymes as a way to promote folding and trafficking of native protein to the lysosome while avoiding proteolysis in the endoplastic recticulum (ER).[7-10] To date, most PCs for GD have functioned as competitive inhibitors for wild-type and/or mutant GCases with high affinity for the catalytic domain via orthosteric binding that stabilizes overall protein conformation, such as isofagomine (IFG).[7-14] However, an allosteric or remote binder that confers stability to a misfolded enzyme without directly competing with the substrate for the active site may offer an improved therapeutic strategy with fewer adverse effects.[15]

Similarly, PCs that exhibit a pH-dependent binding to an active site with high affinity at neutral pH in the ER, but with lower affinity under acidic conditions of the lysosome would promote enzyme transport while minimizing competitive inhibition of the natural substrate.[16,17] Given recent advances in the treatment of LSDs, there is growing consideration for their inclusion within expanded newborn screening initiatives[18] for early detection and intervention of pre-symptomatic infants with improved long-term health outcomes, notably for early onset type II/III GD.[19,20]

Several types of enzyme assays have been reported to measure GCase enzyme activity, including fluorescence and calorimetric methods.[14,17,21-24] Recently, high-throughput inhibitor screening using fluorescence microarrays have been used to identify PCs with putative therapeutic activity for wild-type GCase.[14,24] However, a large fraction of primary ligand "hits" often fail at later stages of clinical trials[25] when rigorous characterization is not performed using relevant in vitro and/or in cellulo assays. In this work, capillary electrophoresis (CE) is introduced as a quantitative approach for characterization of PCs with activity for recombinant modified human GCase. CE offers a versatile micro-separation format for inhibitor screening due to its short analysis times, low reagent costs and minimal sample requirements that can be coupled to various on-line detectors.[26] CE is particularly useful in enzyme kinetic studies for resolution of complex mixtures of substrate, product and inhibitor stereoisomers,[27,28] whereas high-throughput drug screening can be realized when using multiplexed capillary array instrumentation[29,30] or microchip formats.[31] To date, several different formats have been reported for measuring enzyme kinetics in CE, where assays can be performed either off-line or on-line via electrophoretically-mediated microanalysis.[32-35] In general, off-line assays are easier to perform in CE since separation and enzyme incubation conditions are effectively decoupled, whereas enzyme quenching can be independently optimized to ensure robust assay performance To date, there have been few reports that have examined the kinetics of membrane-bound enzyme systems by CE, such as glycosidases, acetylcholinesterase, ecto-5'-nucelotidase and cytochrome P450.[26,36-41] Indeed, only a handful of these studies

have performed inhibitor screening often using conventional linearly transformed enzyme kinetic models.[39,41] Herein, we develop an inhibitor screening assay using CE with UV detection that is used for determination of the pH-dependent activity and mode of inhibition of five recently identified PCs with activity for GCase. Enzyme kinetic studies were performed at relevant physiological conditions of the lysosome (pH 5.2) and ER (pH 7.2), whereas thermal denaturation was used to abolish enzyme activity. The CE assay was first validated using isofagomine (IFG) as a potent active site inhibitor of recombinant GCase. In addition, four other previously approved Food and Drug Administration (FDA) drugs recently identified as putative PCs for GCase were characterized by CE, including ambroxol (ABX), bromhexine (BHX), diltiazem (DTZ) and fluphenazine (FLZ). To the best of our knowledge, this is the first CE-based screening method for PCs when using non-linear regression of enzyme inhibition curves.

2.3 Materials and Methods

2.3.1 Chemicals and Reagents

Deionized water for buffer, kinetic/inhibition assays and stock solution and buffer preparations was obtained using a Barnstead EASYpure® II LF ultrapure water system (Dubuque, IA, USA). 4-methylumbelliferone (MU) and *m*-nitrophenol were purchased from Sigma-Aldrich (St. Louis, MO, USA. Boric acid, acetate and phosphate were purchased from Sigma-Aldrich and used to prepare buffer solutions. In addition, 4-methylumbelliferyl-β-D-glucopyranoside (MUG) was used as the substrate in all kinetic and inhibition enzyme assays. Ambroxol (ABX), bromhexine (BHX), diltiazem (DTZ), fluphenazine (FLZ) and taurocholic acid (TC) were purchased from Sigma-Aldrich, whereas isofagomine (IFG) was obtained from Toronto Research Chemicals Inc (North York, ON, Canada). Dimethyl sulfoxide (DMSO) was purchased from Caledon Laboratories Ltd. (Georgetown, ON, Canada), whereas Cerezyme (Genzyme Canada Inc., Mississauga, ON, Canada) was a kindly provided to us as a gift by Dr. Michael Tropak and Dr. Don Mahuran at the Hospital for Sick Children (Toronto, ON, Canada). Stock

solutions of reagent were prepared in DMSO and stored at 4°C. Stock solutions of wild-type recombinant GCase were prepared in de-ionized water, aliquoted as 25 µL portions into 0.5 mL sterilized centrifuge tubes and stored at -80°C prior to use. Cerezyme (Imiglucerase) is a recombinant modified human GCase (≈ 62 kDa) that is partially deglycosylated after expression from Chinese hamster ovary cells, which differs from wild-type GCase by a single amino acid substitution (H495R) as well as glycosylation modifications at several amino acid residues.[42] Indeed, the activity and bioavailability of recombinant GCase is dependent on post-translational glycosylation events that is influenced by cell culture conditions.[43]

2.3.2 Calibration Curve and pK_a Determination

A stock solution of MU was diluted to twelve different concentrations ranging from 50 to 4000 µM in McIlvaine buffer (0.1 M citrate, 0.2 M phosphate buffer, pH 5.2 or pH 7.2), whereas *m*-nitrophenol was used as internal standard (IS) at a final concentration of 500 µM. The calibration curve was generated using an average of nine replicates performed over three days ($n = 9$) with good precision as reflected by a coefficient of variance (CV) under 5%. Average responses were derived from the measured peak area for MU as normalized to the IS, which provided good linearity over a 80-fold concentration range with a R^2 of 0.9996. The limit of quantification (LOQ) and limit of detection (LOD) for MU when using CE with UV absorbance detection at 320 nm were found to be 5 µM and 15 µM, respectively. The BGE for CE separations was 150 mM borate, pH 9.5 unless otherwise stated. Equivalent ionic strength solutions (≈ 40 mM) of acetate buffer (pH 3-6), phosphate buffer (pH 6-8) and borate buffer (pH 8-10) were used as the BGE for pK_a determination of weakly basic PCs by CE.

3.2.3 Enzyme Kinetics and Inhibitor Screening

Enzyme incubations were performed in McIlvaine buffer (pH 5.2 or pH 7.2) with 10 mM taurocholate (TC) using 25 nM GCase. The initial substrate concentration of MUG ranged from 500-6000 µM. In all cases, 25 nM GCase and 10 mM TC in McIlvaine

buffer were equilibrated in a 37°C water bath for 15 min prior to initiation of the enzyme reaction by addition of MUG using a total volume of 500 µL. All enzyme assays were measured in triplicate by CE when performing three biological/inter-day replicates (n=9) unless otherwise stated. Aliquots (50 µL) were withdrawn from the bulk reaction mixture at 5 min intervals over 1 hr and placed in a centrifuge tube containing 50 µL of IS. All enzyme reactions were then quenched by thermal denaturation at 90°C for 10 min, followed by vortexing for 30 s and centrifugation for 6 s at 4 *g* prior to being stored frozen at -80ºC. Similar procedures were followed for the assay under neutral pH conditions, however enzyme reactions were monitored at 10 or 30 min intervals over 3 hrs. Competitive enzyme inhibition studies were performed by first preparing PC stock solutions in DMSO with serial dilution in McIlvaine buffer (pH 5.2 or 7.2) with 10 mM TC that contained varying concentrations of substrate, MUG (500–6000 µM). All inhibition studies were performed using three intra-day replicates (n=3) and initiated by addition of a pre-equilibrated mixture of inhibitor and MUG to a mixture of GCase (25 nM) and TC (10 mM) at 37ºC, where the total volume of the assay was 500 µL. All enzyme kinetic parameters, including K_m (Michaelis-Menten constant), V_{max} (maximum reaction velocity), IC_{50} (half-maximal inhibitory concentration), K_i (inhibition constant) and α (modifying factor) were processed by non-linear regression using Prism 5.0 software (Graphpad Software Inc., San Diego, USA) and Igor Pro 5.0 (Wavemetrics Inc., Lake Oswego, OR, USA).

3.3.4 Capillary Electrophoresis

Separations were performed on an Hewlett Packard 3D CE system (Agilent Technologies Inc., Waldbronn, Germany) equipped with UV photodiode array (PDA) detection using uncoated open tubular fused-silica capillaries (Polymicro Technologies Inc., Phoenix, AZ, USA) with dimensions of 50 µm inner diameter, 360 µm outer diameter and total capillary length of 35 cm. New capillaries were conditioned by rinsing with methanol for 10 min, de-ionized water for 10 min, 1 M NaOH for 15 min and background electrolyte (BGE) for 30 min. At the beginning of each day, the capillary was rinsed with 0.1 M

NaOH for 10 min and BGE for 15 min. Each separation started with a pre-rinsing of the capillary with 0.1 M NaOH for 2 min and BGE for 5 min followed by hydrodynamic injection of the sample at 50 mbar for 3 s. For kinetic/inhibition assays, separation of substrate (MUG), product (MU) and internal standard (*m*-nitrophenol) were performed under an applied voltage of 10 kV using a positive gradient pressure of 20 mbar over 5.0 min with UV absorbance monitored at 320 nm. At the end of the day, the capillary was flushed with 0.1 M NaOH for 15 min, BGE for 45 min and stored overnight in de-ionized water.

2.4 Theory

Various linearized graphical methods are widely used to determine inhibitory mechanisms and inhibition constants (K_i) of enzyme reactions.[44] Alternatively, non-linear least-square data fitting allows for quantitative assessment of various types of Michaelis-Menton, allosteric or inactivated enzyme systems without bias due to linear transformation of data and experimental error (*e.g.,* Lineweaver-Burk, Dixon plots *etc.*).[45-47] In general, there are four major classes of reversible inhibitors (*I*) as determined by the specific site of interaction (*i.e.,* catalytic or remote) and species of enzyme involved in binding (wild-type enzyme, *E* or enzyme-substrate complex, *ES*), including competitive, non-competitive, uncompetitive and mixed inhibition:[48]

$$\begin{array}{ccccc} & & \overset{+S}{\rightleftharpoons} & & \\ & E & & ES & \longrightarrow E + P \\ +I & \Big\updownarrow K_i & & +I & \Big\updownarrow K_i' \\ & EI & \underset{+S}{\rightleftharpoons} & EIS & \end{array} \qquad (1)$$

$$V_o = \frac{V_{\max} \cdot [S]}{\alpha K_m + \alpha'[S]} \qquad (2)$$

$$\alpha = 1 + \frac{[I]}{K_i} \text{ and } \alpha' = 1 + \frac{[I]}{K'_i}$$

where, V_0 is the initial velocity of the reaction, V_{max} is the maximum velocity, *[S]* is the substrate concentration, K_m is the Michaelis-Menten constant defined as the substrate concentration at half-maximum velocity, whereas α and α' are the modifying factors by the inhibitor concentration *[I]* and its two dissociation constants, K_i and K_i' associated with binding to *E* and/or *ES*, respectively. The potency of inhibition is often assessed in terms of the half-maximal inhibitory concentration (IC_{50}), which represents the concentration of an inhibitor that is required to reduce enzyme activity by 50%.[47] IC_{50} can be determined from non-linear regression of dose-dependent curves based on the following equation:

$$K_i = \frac{IC_{50}}{1 + ([S]/K_m)} \tag{3}$$

In competitive inhibition (K_i only; α' = 1 or $K'_i = \infty$), an inhibitor competes with the substrate for access to the active site of *E* as binding of the substrate and inhibitor cannot take place simultaneously, which can be described by simplification of eq. 2:

$$V_o = \frac{V_{\max} \cdot [S]}{\{K_m(1 + [I]/K_i) + [S]\}} \tag{4}$$

However, in uncompetitive inhibition (K'_i only; α = 1 or $K_i = \infty$), an inhibitor binds only to *ES* complex resulting in:

$$V_o = \frac{V_{\max} \cdot [S]}{\{K_m + [S](1 + [I]/K'_i)\}} \tag{5}$$

In contrast, during non-competitive inhibition ($K_i = K'_i$ and α = α'), both substrate and inhibitor can interact with the enzyme simultaneously (*EIS*) since binding occurs at

independent sites, however the affinity of the substrate (inhibitor) is unmodified by the inhibitor (substrate):

$$V_o = \frac{V_{\max} \cdot [S]}{(K_m + [S])(1 + [I]/K_i)\}} \quad (6)$$

In mixed-type inhibition ($K_i \neq K'_i$ and $\alpha \neq \alpha'$), the inhibitor binds differentially to *E* and/or *ES* complex while interacting with both active and remote sites, thus:

$$V_o = \frac{V_{\max} \cdot [S]}{\{K_m(1 + [I]/K_i) + [S](1 + [I]/K'_i)\}} \quad (7)$$

In this work, eqs. 4-7 were applied to identify the type of inhibition among different PCs for GCase, where R^2 was used to assess goodness of fit to a given inhibitor model. In addition, inhibition mechanisms were classified based on their apparent changes in K_m and V_{max} as a function of inhibitor concentration.[44,49]

2.5 Results and discussion

2.5.1 Impact of Buffer pH and Surfactant Concentration on GCase Activity

Cerezyme, an ERT supplement for treatment of type I GD for the past twenty years,[50] is a recombinant GCase that catalyzes the hydrolysis of the synthetic glycoside substrate, MUG to generate two products, namely MU and *D*-glucose. This reaction optimally occurs under acidic pH conditions with addition of TC (10 mM) as an anionic surfactant in order to mimic the localized environment of the lysosome.[51] TC also functions as a selective detergent for activating GCase while inhibiting β-glycosidase from human cell extracts which can interfere with the assay.[52] The time-dependent formation of MU by GCase was measured by CE with UV detection at 320 nm as shown in **Figure 2.1**. Resolution of MUG and MU was performed using 150 mM borate, pH 9.5 as the alkaline

BGE, where MUG is partially negatively charged due to reversible borate complexation[53] with the *D*-glucose moiety during separation, such that it migrates after the electroosmotic flow (EOF). In contrast, MU has a pK_a of 7.8 [51], thus it is fully ionized at pH 9.5 and migrates with a longer apparent migration time due to its larger negative mobility. In this study, the activity of GCase was determined under both acidic (pH 5.2) and neutral (pH 7.2) conditions reflective of local pH environment in the lysosome and ER, respectively. GCase enzyme activity is reduced about four-fold at neutral pH compared to acidic pH conditions as summarized in **Table 2.1**.

Several fluorescence-based kinetic assays have reported the use of alkaline quenching using 0.4M NaOH/0.4 M glycine, pH 10 as a way to terminate the enzyme reaction that allows for detection of natively fluorescent product.[14,15,22-24,51] However, this method was not observed to adequately quench GCase activity (data not shown), thus thermal denaturation was performed (90^{o}C for 10 min) to irreversibly unfold the protein prior to CE analysis. Optimal surfactant concentration for enhancing GCase activity was found with addition of 10 mM TC to the McIlvane buffer similar to previous fluorescence assays. Indeed, no significant activity of GCase was measured within a 2 hr timeframe without TC addition under acidic pH conditions when using 2 mM substrate concentration. Thus, *in-vitro* enzyme kinetic studies of GCase require an anionic bile surfactant under acidic pH conditions to ensure protein folding for optimal activity.

2.5.2 pK_a Determination of Model PCs

Given the importance of local pH conditions in modulating GCase activity which may impact substrate/inhibitor binding, the apparent pK_a of PCs were determined by CE. Unlike the basic anomeric nitrogen of the iminosugar IFG that has a pK_a of 8.6, [54] four previously approved FDA drugs recently identified as PCs for GCase [24,55] have more weakly basic amine moieties as a result of their chemical structure.

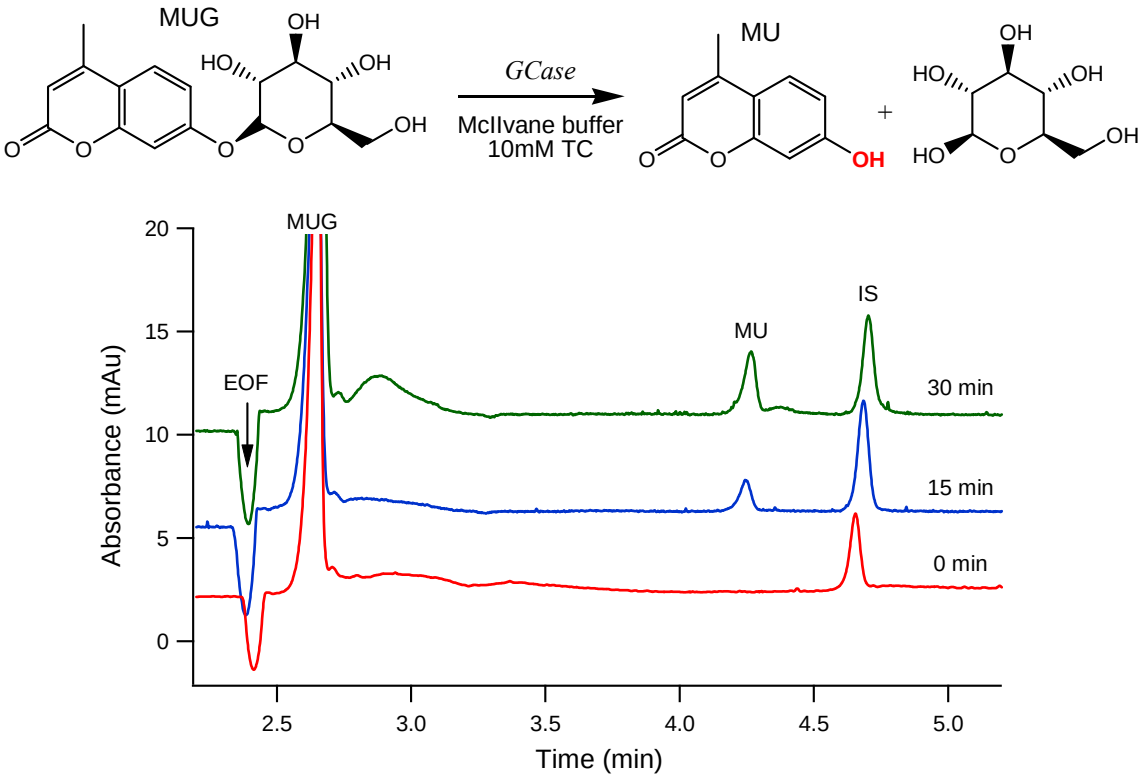

Figure 2.1 Optimization of GCase enzymatic conditions on CE. Enzyme-catalyzed hydrolysis of MUG by GCase (Cerezyme) in the presence of anionic surfactant (TC) to generate MU and *D*-glucose. Series of electropherograms depicting quantification of micromolar levels of MU as product from excess MUG as a function of enzyme incubation time. All separations were performed at 25°C, voltage of 10 kV with gradient pressure to 20 mbar within 5.0 min, total capillary length of 35 cm with UV detection at 320 nm using a BGE of 150 mM borate, pH 9.5.

Table 2.1. Summary of enzyme kinetic parameters for recombinant GCase.

Enzyme kinetics	***pH 5.2***	***pH 7.2***
K_m	1700 ± 280 μM	6095 ± 840 μM
V_{max}	19 ± 1 μM min^{-1}	5.1 ± 0.4 μM min^{-1}
k_{cat}	760 ± 40 min^{-1}	204 ± 16 min^{-1}

All parameters were determined by non-linear regression of Michaelis-Menten curves using eq. 2.

Thus, differences in the ionization state for these non-carbohydrate amines may impact their binding affinity with GCase that impacts overall activity. **Figure.2.2** summarizes the pH-dependent changes in apparent electrophoretic mobility (μ_{ep}) for the weakly basic

drugs by CE. BHX and its major metabolite ABX are widely used expectorants and mucolytic agents with anaesthetic properties for treatment of various bronchopulmonary disorders with a long clinical history of safety.[56] However, they possess significant differences in apparent pK_a with (6.49 ± 0.04) and (8.19 ± 0.02) for the tertiary amine (BHX) relative to the secondary amine (ABX), respectively. DTZ is a calcium channel blocker used in the treatment of hypertension, angina pectoris, and some types of arrhythmia [55] with a measured pK_a of (8.05 ± 0.02) that was similar to ABX. In contrast, FLZ is a neuroleptic agent used for the treatment of schizophrenia and various psychotic disorders[57] that was the least basic drug examined in this work with a pK_a of (6.12 ± 0.08). A recent study reported that ABX and DTZ displayed pH-dependent binding properties that enhance the conformational stability of recombinant GCase with non-inhibitory properties under strongly acidic relative to a neutral pH conditions.[24,55] However, these observations are not explained by their pK_a properties since ABX undergoes only a 3% relative change in ionization at pH 6.7 relative to 4.3.[24] This suggests that the pH-dependent activity for PCs is largely a result of changes in protein ionization (*e.g.,* organelle environment, glycosylation) that modulate conformation during translocation within the cell.[58] Indeed, BHX and FLZ appear to have favourable pK_a properties to modulate binding to GCase within the ER and lysosome as a result of their large relative changes in ionization within this pH range, however this is not supported by in vitro and in cellulo experiments.[24] Thus, the pH-dependent activity of PCs for GCase is not directly associated with changes in drug ionization properties. However, the distribution and bioavailability of PCs are still largely influenced by their physicochemical properties as reflected by the 10^3-fold lower potency of the hydrophilic iminosugar IFG in cell cultures as compared to in vitro assays.[59]

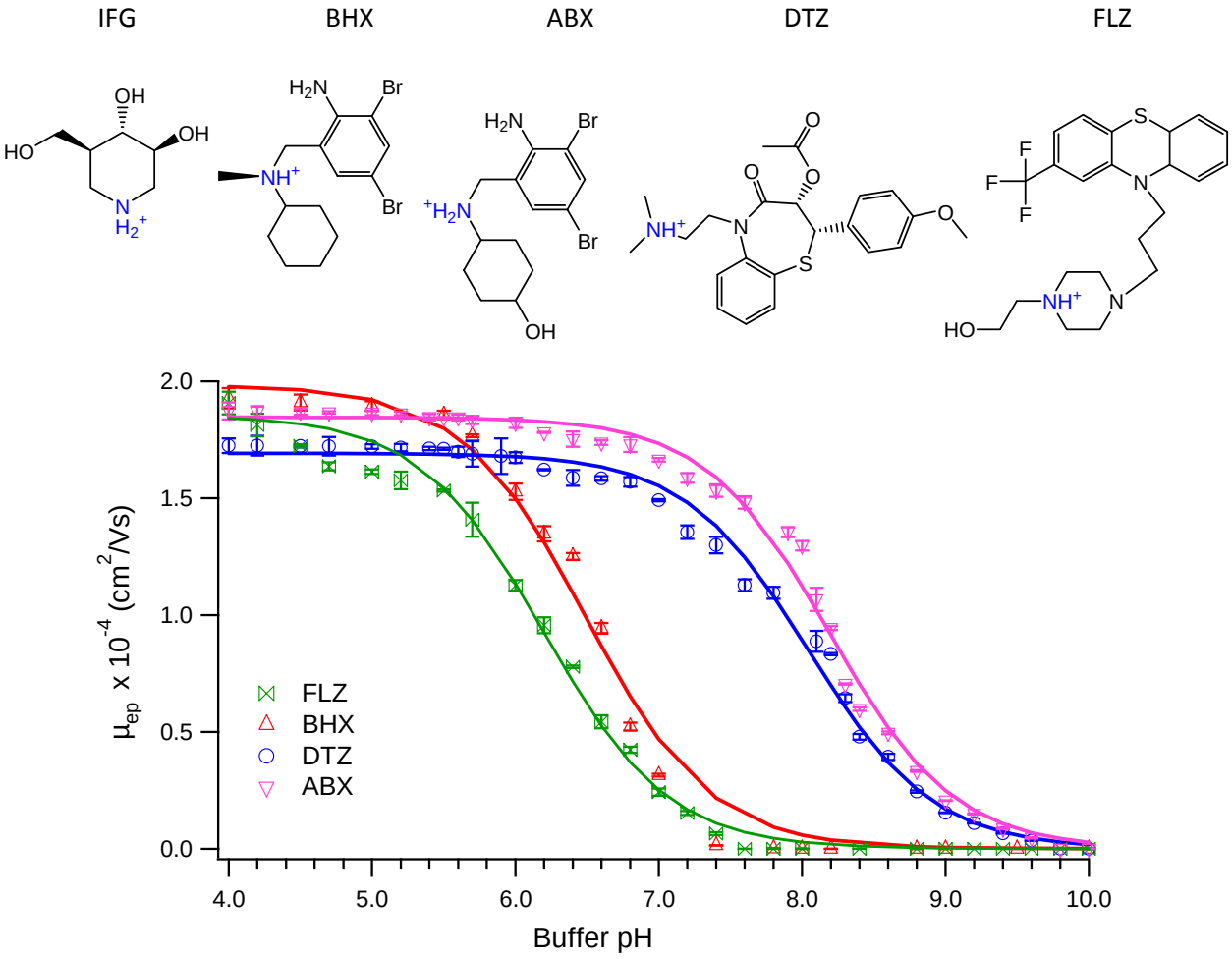

Figure 2.2 pKa determination of four previously FDA approved drugs. 2D chemical structures of putative PCs for recombinant GCase, including isofagomine (IFG), bromhexine (BHX), ambroxol (ABX), diltiazem (DTZ) and fluphenazine (FLZ). pK_a determination of four weakly basic non-carbohydrate PCs by CE based on apparent electrophoretic mobility (μ_{ep}) changes as a function of buffer pH. All separations were performed at 25°C, voltage of 25 kV, total capillary length of 35 cm with UV detection at 214 nm using an equimolar ionic strength (40 mM) buffers from pH 4-10. Error represents ± 1 σ with average precision for intra-day replicates (n=3) under 2%.

2.5.3 Competitive Inhibition of GCase

The optimized CE-based enzyme assay was next validated using the competitive inhibitor IFG, which has been demonstrated to promote folding of wild-type human GCase, as well as several clinically relevant mutants, including N370S, L444P, G202R and F213I.[11,59,60,61] Unlike its azasugar structural isomer 1-deoxy-nojirimycin, reversible binding of IFG to the active site of GCase is entropically-driven[54] that increases global

protein conformational stability[60] while enhancing lysosomal trafficking and cellular activity by 2 to 5-fold in various human tissue.[59, 61] **Figure.2.3a** depicts measured enzyme kinetic curves under acidic conditions (pH 5.2) as a function substrate (S) and IFG concentration when using CE. IFG was confirmed to function as a competitive inhibitor to recombinant GCase based on the excellent fit to the specific inhibition model (eq. 4, R^2= 0.9902), as well as the apparent changes to V_{max} (constant) and K_M measured at seven different IFG concentrations as shown in **Fig.2.3b.** The potency of the active site inhibitor was found to have a considerable pH-dependence based on an IC_{50} of (47.5 ± 0.1) nM and (4.6 ± 1.4 nM) at pH 5.2 and 7.2, respectively when using 3 mM MUG as substrate and 25 nM Cerezyme with 10 mM TC in all assays. These results are consistent with previous inhibition data for wild-type GCase when using a fluorescence microarray that were performed under similar reaction conditions with an IC_{50} of 59 nM and 5 nM at pH 5.2 and pH 7.2, respectively.[11,59] Since IFG does not undergo significant changes in ionization under these buffer pH conditions, this pH-dependent difference in activity is attributed to overall changes in protein structure. **Table 2.2** summarizes major parameters measured for IFG (and other PCs) in this study in terms of inhibitor potency, including IC_{50}, K_i and K_i' (*i.e.,* mixed-type inhibitors), as well as R^2 derived from non-linear regression fitting of the optimized inhibition model. Despite the apparent high potency of IFG in vitro, its poor distribution in vivo in conjunction with its lower affinity under acidic conditions (*i.e.,* ≈ 10-fold lower than neutral pH conditions) prevents adverse effects caused by acute build-up of glycosphingolipids due to substrate inhibition in the lysosome as a result of facile dissociation/displacement.[59] Indeed, recent phase II clinical results for IFG (Plicera) for adults with type I GD have demonstrated no adverse health effects with notable increase in GCase activity measured in white blood cells; however no significant improvement in clinical outcomes for most patients were observed under the dose regime examined.[50] Thus, there is on-going interest in the development of alternative PCs with improved therapeutic efficacy for oral treatment of GD without adverse health effects.

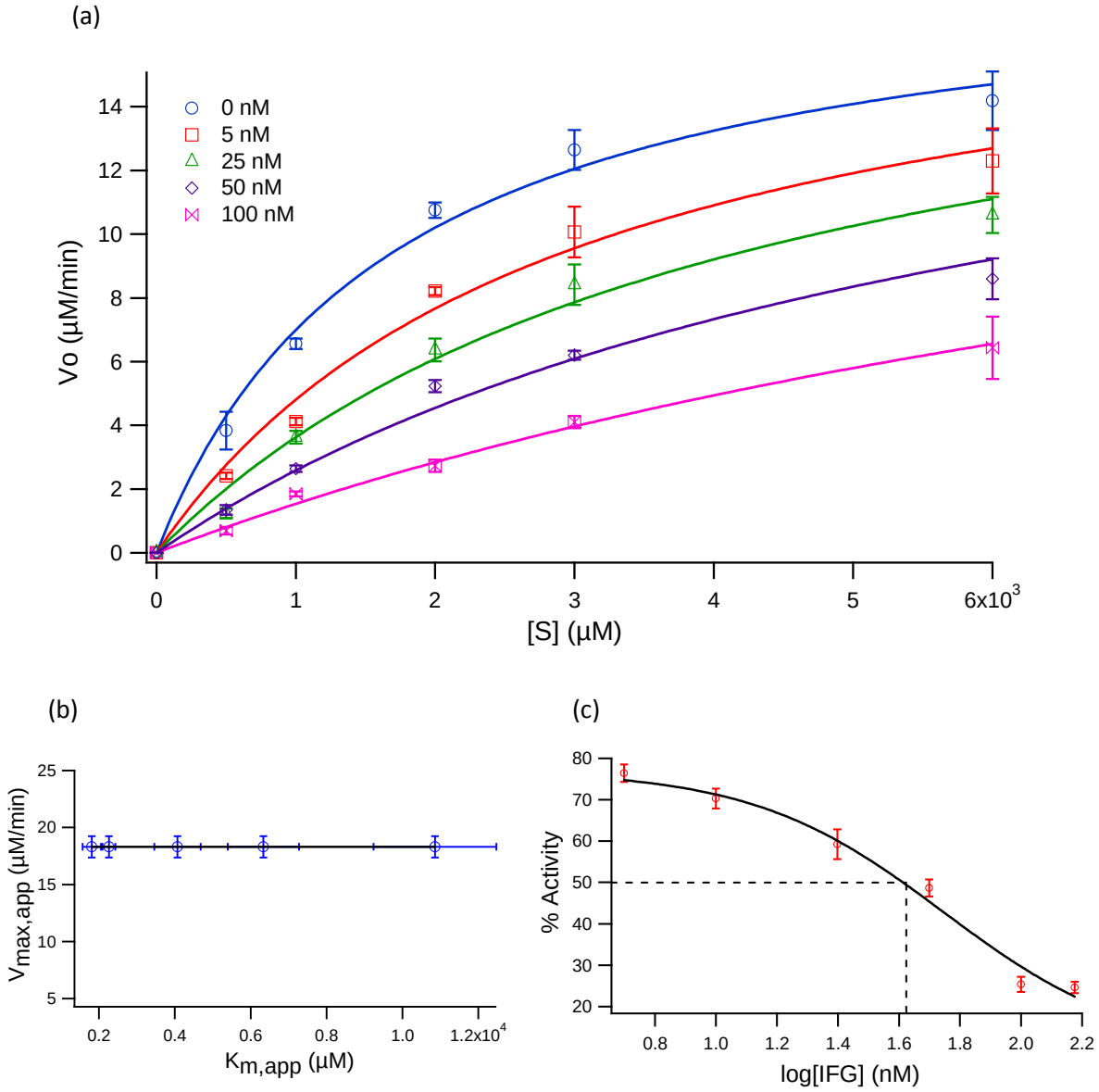

Figure 2.3 IFG binding inhibition curve of GCase (a) Inhibition curves for recombinant modified human GCase at pH 5.2 based on non-linear regression of modified Michaelis-Menten equation for active site inhibitor (eq. 4) as a function of IFG concentration. (b) correlation plot of changes to apparent V_{max} and K_m with increasing IFG concentration that confirms validity of a competitive inhibition model and (c) in vitro potency of IFG at seven different concentrations for determination of IC_{50} using 2 mM MUG at pH 5.2 via non-linear regression (eq. 3). All separation and enzyme assay conditions used are similar to Figure 1, where error represents ± 1 σ with intra-day precision (n=3) under 5%. **Table 2.2** summarizes major inhibitor parameters for PCs examined in this study.

2.5.4 Mixed-type Inhibition of GCase

Most PCs to date have served as active site inhibitors that enhance the stability and activity of native enzymes, however allosteric ligands[62] that specifically target distal sites on the protein offer several therapeutic advantages, such as greater selectivity and saturability.[63] Although rational-design synthesis of iminosugar analogs[17] or high-throughput screening of large-scale chemical libraries[64] have been reported for GCase, directed screening of FDA-approved drugs provides a cost-effective strategy for rapid translation of putative PCs for clinical treatment of rare genetic disorders.[24, 65] **Figure 2.4a** depicts CE-derived inhibition curves for GCase as a function of FLZ dosage, which is recognized to have several therapeutic applications with antipsychotic and antimutagenic activity, the latter property being investigated for cancer chemoprevention.[66] In this work, FLZ is demonstrated to function as a mixed-type inhibitor for recombinant GCase with an IC_{50} of (52.1 ± 0.2) μM and (140 ± 1) μM at pH 5.2 and 7.2, respectively as shown in **Figure 2.4b,c** and **Table 2.2**. FLZ was recently shown by secondary screening to function as a potent stabilizer of GCase against thermal denaturation; however it was subsequently found not to significantly enhance GCase levels or activity in Gaucher patient cells presumably as a result of poor bioavailability and/or metabolism in cellulo.[24] Similarly, ABX, BHX and DTZ were also determined to behave as mixed-type inhibitors of GCase with micromolar potency in vitro with IC_{50} ranging from 16 to 86 μM as summarized in **Table 2.2**. Unlike IFG, all non-carbohydrate PCs were found to have about 2-3-fold higher activity for GCase under acidic (pH 5.2) relative to neutral (pH 7.2) conditions in our study. Overall, consistent data was attained for PC activity for recombinant GCase in terms of in vitro potency and mode of inhibition although direct comparison with other reports is constrained as a result of enzyme reaction conditions. For instance, ABX[24] and DTZ[55] were reported to be non-inhibitory while acting as weak activators of GCase under strongly acidic conditions (≈ pH 4.3-4.5) unlike other pH conditions (pH > 5.6) whose underlying mechanism(s) are still poorly understood.

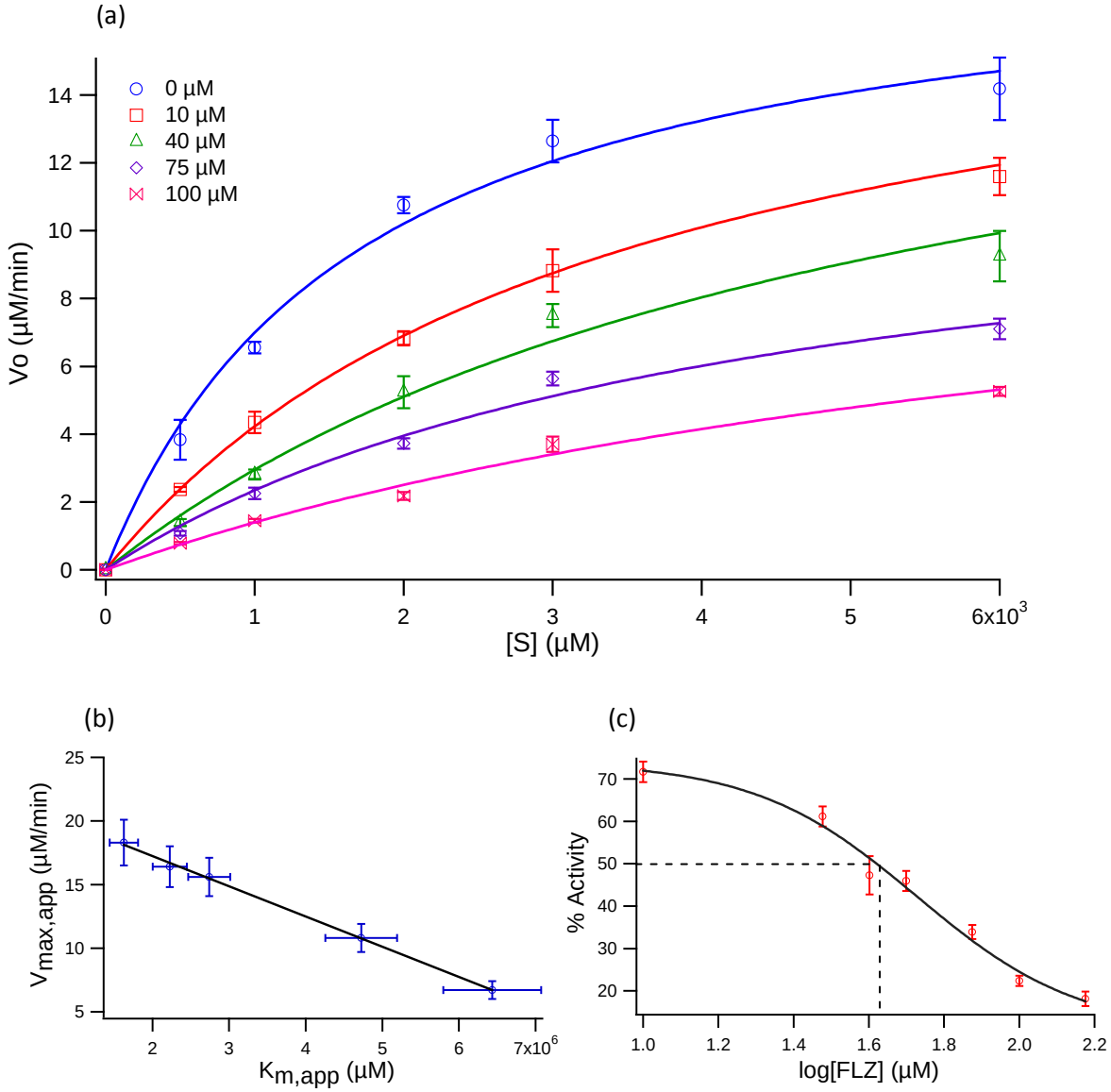

Figure 2.4 FLZ inhibition binding curve for GCase (a) Inhibition curves for recombinant modified human GCase at pH 5.2 based on non-linear regression of modified Michaelis-Menten equation for mixed type inhibitor (eq. 7) as a function of FLZ concentration. (b) linear correlation plot (R^2 = 0.9992) of changes to apparent V_{max} and K_m with increasing FLZ concentration that confirms validity of a mixed-type inhibition model and (c) in vitro potency of FLZ at seven different concentrations for determination of IC_{50} using 2 mM MUG at pH 5.2 via non-linear regression (eq. 3). All separation and enzyme assay conditions used are similar to Figure 3, where error represents ± 1 σ with intra-day precision (n=3) under 5%. **Table 2.2** summarizes major inhibitor parameters for PCs examined in this study.

Table 2.2. Summary of inhibition type and in-vitro potency of five different PCs that stabilize recombinant GCase as a function of buffer pH conditions by CE.

Name of PCs	***Mode of inhibition***	***IC_{50} (μM), pH 7.2***	***IC_{50} (μM), pH 5.2***	***IC_{50} (μM)[a]***	***K_i (μM)[a]***	***K'_i (μM)[a]***	***R^2***
Isofagomine (IFG)	Competitive	0.0046 ± 0.0014	0.0509 ± 0.0003	0.005[b], 0.059[c]	0.020 ± 0.002	*n/a*	0.9902
Ambroxol (ABX)	Mixed-type	50 ± 1	16.7 ± 0.6	31[d]	10 ± 2	60 ± 32	0.9906
Bromhexine (BHX)	Mixed-type	86 ± 1	30.5 ± 0.1	58[c]	26 ± 5	104 ± 56	0.9989
Diltiazem (DTZ)	Mixed-type	56 ± 3	34.5 ± 0.1	160[e]	28 ± 5	360 ± 290	0.9989
Fluphenazine (FLZ)	Mixed-type	140 ± 1	52.1 ± 0.2	*n/a*	20 ± 3	220 ± 140	0.9923

[a] *Inhibition constants and IC_{50} measured at pH 5.2 using 2 mM MUG and 25 nM GCase*
[b] *IC_{50} value was determined at pH 7.2 using 3 mM MUG*[59]
[c] *IC_{50} value was determined at pH 5.2 using 3 mM MUG*[11]
[d] *IC_{50} values were determined at pH 5.6 using GCase (8.8 nM) assayed with 2.5 mM MUG.*[24] *No error was reported for IC_{50}, however K_i and K'_i for ABX at pH 5.6 were (23 ± 3) μM and (160 ± 72) μM, respectively.*
[e] *IC_{50} values were estimated at pH 6.5 using GCase assayed with 3.2 mM MUG.*[55] *No error was reported for IC_{50}.*

Since both these basic drugs have $pK_a > 8$, this abrupt modulation in ligand affinity and function is associated with dynamic changes in GCase structure induced by the specific assay conditions examined. Future work is aimed at developing multivariate approaches for characterization of protein-ligand interactions[62] using wild-type and mutant strains of GCase as a way to improve the translation of functionally-active PCs for treatment of GD and related genetic disorders.[50]

2.6 Conclusion

In summary, the type and potency of inhibition were determined for five different PCs that induce stabilization of recombinant GCase upon orthosteric and/or allosteric binding. IFG was found to be a potent active site inhibitor ($K_i \approx 20$ nM) of GCase in vitro that displayed higher activity under neutral pH relative to acidic pH conditions reflective of the local ER and lysosome environment, respectively. In contrast, all other weakly basic non-carbohydrate PCs (*i.e.,* ABX, BHX, DTZ and FLZ) were found to function as mixed-type inhibitors with lower micromolar activity. Overall, the pH-dependence of PC activity was not found to be related to changes in their ionization state (*i.e.,* pK_a) suggesting that changes in protein conformation under strongly acidic conditions (pH < 5) impact inhibitor activity. Further research is needed to better understand the relationship between ligand binding and its impact on protein conformational stability and/or folding dynamics as a way to improve selection of lead drug candidates for clinical trials. The discovery of PC activity among previously approved drugs with an established safety record offers a novel approach for treatment of rare genetic disorders associated with protein misfolding and enzyme deficiency.

2.7 Acknowledgments

Financial support was provided by the Natural Science and Engineering Council of Canada (NSERC). The authors wish to thank Dr. Michael Tropak and Dr. Don Mahuran from the Hospital for Sick Children in Toronto, Canada for their generous donation of Cerezyme.

2.8 References

1. Platt, F. M; Lachmann, R.H. *Biochim. Biophys. Acta Molecul. Cell Res*.**2009**,1793,737-745.

2. Grabowski, G. A. *Adv. Human Genetics* **1993**, 21, 377-441.

3. Beutler, E; Nguyen, N. J; Henneberger, M. W; Smolec, J. M; McPherson, R. A; West, C; Gelbart, T. *Am. J. Human Genetics* **1993**, 52, 85-88.

4. Sawkar, A. R; Adamski-Werner, S. L; Cheng, W. C; Wong, C. H; Beutler, E; Zimmer, K. P; Kelly, J. W. *Chem. & Biol*. **2005**, 12, 1235-1244.

5. Chang, H. H; Asano, N; Ishii, S; Ichikawa, Y; Fan, J. Q. *FEBS J.* **2006**, 273, 4082-4092.

6. Futerman, A. H; Sussman, J. L; Horowitz, M; Silman, I; Zimran, A. *Trends Pharmacol.Sci.* **2004**, 25, 147-151.

7. Brooks, D. A. *Nature Chem. Biol.* **2007**, 3, 84-85.

8. Arakawa,T; Ejima, D; Kita, Y; Tsumoto, K. *Biochim. Biophys. Acta-Prot. & Proteomics*.**2006**, 1764, 1677-1687.

9. Bernier,V; Lagace, M; Bichet, D. G; Bouvier, M.*Trends Endocrinol. Metabol*. **2004**, 15, 222 - 228.

10. Fan, J. Q. *Trends Pharmacol. Sci.* **2003**, 24, 355-360.

11. Lieberman, R. L; Wustman, B. A; Huertas, P; Powe, A. C; Pine, C. W; Khanna, R; Schlossmacher, M. G; Ringe, D; Petsko, G. A. *Nature Chem. Biol*. **2007**, 3, 101-107.

12. Dvir, H; Harel, M; McCarthy, A. A; Toker, L; Silman, I; Futerman, A. H; Sussman, J. L. *EMBO Reports*. **2003**, 4, 704-709.

13. Walden, C. M; Sandhoff, R; Chuang, C. C; Yildiz, Y; Butters, T. D; Dwek, R. A; Platt, F. M; Van der Spoel, A. C. *J. Biol. Chem*. **2007**, 282, 32655-32664.

14. Zheng, W; Padia, J; Urban, D. J; Jadhav, A; Goker-Alpan, O; Simeonov, A; Goldin, E; Auld, D; LaMarca, M. E; Inglese, J; Austin, C. P; Sidransky, E. *Proc. Nat. Acad. Sci. U.S.A.* **2007**, 104, 13192-13197.

15. Lieberman, R. L; D'Aquino, J. A; Ringe, D; Petsko, G. A. Biochemistry, 2009, 48, 4816-4827.

16. Sawkar, A. R; D'Haeze, W; Kelly, J. W. *Cell. Molec. Life Sci*. **2006**, 63, 1179-1192.

17. Wang, G. N; Reinkensmeier, G; Zhang, S. W; Zhou, J; Zhang, L. R; Zhang, L. H; Butters, T. D, Ye, X. S. *J. Med. Chem*. **2009**, 52, 3146-3149.

18. Chalcraft, K. R; Britz-McKibbin, *P. Anal. Chem*. **2009**, 81, 307-314.

19. Marsden, D; Levy, H. *Clin. Chem*. **2009**, 56, 1071-1079.

20. Millington, D. S. *Clin. Chem*. **2005**, 51, 808-809.

21. Inglese, J; Auld, D. S; Jadhav, A; Johnson, R. L; Simeonov, A; Yasgar, A; Zheng W, Austin, C. P. *Proc. Nat. Acad. Sci. U.S.A*. **2006**, 103, 11473-11478.

22. Shen, J. S; Edwards, N. J; Bin-Hong, Y; Murray, G. J. *Biochem. Biophys. Res. Comm.* **2008**, 369, 1071-1075.

23. Sawkar, A. R; Cheng, W. C; Beutler, E; Wong, C, H; Balch, W. E; Kelly, J. W. *Proc. Nat. Acad. Sci. U.S.A.* **2002**, 99, 15428-15433.

24. Maegawa, G. H. B; Tropak, M. B; Buttner, J. D; Rigat, B. A; Fuller, M; Pandit, D; Tang, L. I; Kornhaber, G. J; Hamuro; Clarke, J. T. R; Mahuran, D. J. *J. Biol. Chem.* **2009**, 284, 23502-23516.

25. Bleicher, K. H; Bohm, H. J; Muller, K; Alanine, A. I. *Nature Reviews Drug Disc*. **2003**, 2, 369-378.

26. Zhang, J; Hoogmartens, J; Van Schepdael, A. *Electrophoresis*. **2008**, 29, 3694-3700.

27. Gavina, J. M. A; White, C. E; Finan, T. M; Britz-McKibbin, P. *Electrophoresis*, **2010**, 31, 2831-2837.

28. Koval, D; Kasicka, V; Jiracek, J; Collinsova, M. *Electrophoresis*, **2006**, 27, 4648 4657.

29. Ma, L. J; Gong, X. Y, Yeung E. S. *Anal. Chem*. **2000**, 72, 3383-3387.

30. Pang, H. M; Kenseth, J; Coldiron, S. *Drug Disc. Today*, **2004**, 9, 1072-1080.

31. Jambovane, S; Duin, E. C; Kirn, S. K; Hong, J. W. *Anal. Chem*. **2009**, 81, 3239-3245.

32. Fan, Y; Scriba, G. K. E. *J. Pharma. Biomed. Anal*. **2010**, 53, 1076-1090.

33. Zhang, J; Hoogmartens, J; Van Schepdael, A. *Electrophoresis*, **2006**, 27, 35-43.

34. Zhang, J; Hoogmartens, J; Van Schepdael, A. *Electrophoresis*, **2009**, 31, 65-73.

35. Telnarova, M; Vytiskova, S; Chaloupkova, R; Glatz, Z. *Electrophoresis*. **2004**, 25, 290-296.

36. Iqbal, J; Levesque, S. A; Sevigny, J; Muller, C. E. *Electrophoresis*. **2008**, 29, 3685-3693.

37. Kanie, Y; Kanie, O. *Electrophoresis*. 2003, 24, 1111-1118.

38. Iqbal, J; Jirovsky, D; Lee, S. Y; Zimmermann, H; Muller, C. E. *Anal. Biochem*. **2008**, 373, 129-140.

39. Van Dyck, S; Van Schepdael, A; Hoogmartens, J. *Electrophoresis*. **2002**, 23, 2854-2859.

40. Tang, Z. M; Wang, Z. Y; Kang, J. W. *Electrophoresis*, **2007**, 28, 360-365.

41. Martin-Biosca, Y; Asensi-Bernardi, L; Villanueva-Camanas, R. M; Sagrado, S; Medina-Hernandez, M. J. *J. Separation Sci*. **2009**, 32, 1748-1756.

42. Roeber, D; Achari, A; Manavalan, P; Edmunds, T; Scott, D. L. *Acta Cryst*. **2003**, D59, 343-344.

43. Brumshtein, B; Salinas, P; Peterson, B; Chan, V; Silman, I; Sussman, J. L; Savickas, P. J; Robinson, G. S; Futerman, A. H. *Glycobiology*, **2010**, 20, 24-32.

44. Yoshino, M; Murakami, K. *Med. Chem*. **2009**, 24, 1288-1290.

45. Kakkar, T; Boxenbaum, H; Mayersohn, M. *Drug Metabol. Dispos*. **1999**, 27, 756-762.

46. Maurer T; Fung, H. L. *AAPS PharmSci*. **2000**, 2, 8-18.

47. Kemmer, G; Keller, S. *Nature Protocol*. **2010**, 5, 267-281.

48. Chan, W. W. C. *Biochem. J.* **1995**, 311, 981-985.

49. Geng, W; Ke, J; Satoh, H; Bush, E. D. *AAPS PharmaSci*, **2001**, 3, W4464.

50. Smid, B. E; Aerts, J. M. F. G; Boot, R. G; Linthorst, F. E; Hollak, C. E. M. *Expert Opin. Invest. Drugs*, **2010**, 19, 1367-1379.

51. Urban, D. J; Zheng, W; Goker-Alpan, O; Jadhav, A; LaMarca, M. E; Inglese, J; Sidransky, E; Austin, C. P. *Combinat. Chem. High Throughput Screening*. **2008**, 11, 817-824.

52. Peters, S. P; Coyle, P; Glew, R. H. *Arch. Biochem. Biophys*. **1976**, 175, 569-582.

53. Kaiser, C; Segui-Lines, G; D'Amaral, J. C; Ptolemy, A. S; Britz-McKibbin, P. *Chem. Comm.* **2008**, 208, 338-340.

54. Bulow, A; Plesner, I. W; Bols, M. *J. Am. Chem. Soc*. **2000**, 122, 8567-8568.

55. Rigat, B; Mahuran, D. *Molecul. Genetics Metabol.* **2009**, 96, 225-232.

56. Malerba, M; Ragnoli, B. *Expert Opin. Drug Metab. Toxicol.* **2008**, 4, 1119-1129.

57. Gasiorowski, K; Brokos, B; Szyba, K; Leszek, J. *Mutagenesis*, **2001**, 16, 31-38.

58. Weely, S.V; Aerts, J. M. F. G; Leeuwen, M. B. V; Heikoop, J. C; Donker-Koopman, W. E; Barranger, J. A; Tager, J. M; Schram, A. W. *Eur. J. Biochem*. **1990**, 191, 669-677.

59. Steet, R. A; Chung, S; Wustman, B; Powe, A; Do, H; Kornfeld, S. A. *Proc. Nat. Acad. Sci. U.S.A.* **2006**, 103, 13813-13818.

60. Kornhaber, G. J; Tropak, B. B; Maegawa, G. H; Tuske, S. J; Coales, S. J; Mahuran, D. J; Hamuro, Y. *ChemBioChem*. **2008**, 9, 2643-2649.

61. Khanna, R; Benjamin, E. R; Pellegrino, L; Schilling, A; Rigat, B. A; Soska, R; Nafar, H; Ranes, B. E; Feng, J; Lun, Y; Powe, A. C; Palling, D. J; Wustman, B. A;

Schiffmann, R; Mahuran, D. J; Lockhart, D. J; Valenzano, K. J. *Febs Journal*, **2010**, 277, 1618-1638.

62. Gavina, J. M. A; Mazhab-Jafari, M. T; Melacini, G; Britz-McKibbin P. *Biochemistry*. **2009**, 48, 223-225.

63. Christopoulos, A. N*at. Rev. Drug Discovery*. **2002**, 1, 198-210.

64. Tropak, M. B; Kornhaber, G. J; Rigat, B. A; Maegawa, G. H; Buttner, J. D; Blanchard, J. E; Murphy, C; Tuske, S. J; Coales, S. J; Hamuro, Y; Brown, E. D; Mahuran, D. J. *ChemBioChem*. **2008**, 9, 2650-2662.

65. Maegawa, G. H; Tropak, M; Buttner, J; Stockley, T; Kok, F; Clarke, J. T; Mahuran, D. J. *J. Biol. Chem.* **2007**, 282, 9150-9161.

66. Cieslik-Boczula, K; Szwed, J; Jaszczyszyn, A; Gasiorowski, K; Koll, A. *J. Phys. Chem. B*. **2009**, 113, 15495-15502.

Chapter III:
Functional Screening of Pharmacological Chaperones via Restoration of Enzyme Activity upon Denaturation

3.1 Abstract

Pharmacological chaperones (PCs) are small molecules that stabilize and promote protein folding. Enzyme inhibition is widely used for PC selection, however it does not accurately reflect chaperone activity. We introduce a functional assay for characterization of PCs based on their capacity to restore enzyme activity that is abolished upon chemical denaturation. Dose-dependent activity curves were performed as a function of urea to assess the chaperone potency of various ligands to β-glucocerebrosidase as a model system. Restoration of enzyme activity upon denaturation enables direct screening of PCs for treatment of genetic disorders associated with protein deficiency, such as Gaucher disease.

3.2 Introduction

Gaucher disease (GD) is the most prevalent lysosomal storage disorder caused by a deficiency in β-glucocerebrosidase (GCase) that results in deleterious cellular accumulation of glucosylceramide (GlcCer). GCase catalyzes β-glycosidic bond cleavage of GlcCer to produce glucose and ceramide, a bioactive sphingolipid involved in heat stress response and apoptosis. Over 200 mutations in the GCase gene can lead to aberrant folding during protein assembly which triggers endoplasmic recticulum (ER)-associated degradation pathways.[1] Defective GCases form non-native conformers with lower thermal stability under neutral pH conditions of the ER that are susceptible to proteolysis with reduced trafficking.[2] However, most clinically relevant GCase mutants retain partial catalytic activity (< 30%) under acidic conditions of the lysosome.[3] To date, enzyme replacement therapy using recombinant enzyme is the most widely used treatment for

type I GD.[4] Alternatively, enzyme enhancement therapy based on small molecules that function as pharmacological chaperones (PCs)[5] offers a promising approach to salvage endogenous GCase via stabilization of the native conformer for treatment of neuronopathic forms of GD (type II/III). Since the first evidence of PCs as therapeutic agents for GD,[6] drug candidates have largely consisted of reversible active site inhibitors of GCase based on substrate mimics, such as natural and alkylated iminosugar analogs.[7] This has led to a counterintuitive principle that inhibitors enhance the activity of mutant enzymes by manipulating the ER folding environment. High-throughput screening of chemical libraries thus rely on enzyme inhibition,[8] where inhibitor potency for GCase is used as a major criterion for PC selection. However, primary screening by inhibition is biased towards the detection of ligands that influence the interaction of wild-type/folded GCase with a single fluorogenic substrate probe.[9] Indeed, not all inhibitors act as protein stabilizers as exemplified by false-positives that lack relevant chaperone activity.[10] For this reason, thermal stability assays are required as a secondary screen to confirm chaperone activity prior to testing with GD patient-derived cell cultures.[11]

3.3 Materials and Methods

3.3.1 Chemicals and Reagents

De-ionized water for buffer, stock solution and buffer preparations was obtained using a Barnstead EASYpure® II LF ultrapure water system (Dubuque, IA, USA). 4-methylumbelliferone (MU, product of GCase) and *m*-nitrophenol (internal standard) were purchased from Sigma-Aldrich (St. Louis, MO, USA). Boric acid, citrate and phosphate were purchased from Sigma-Aldrich and used to prepare buffer solutions. In addition, 4-methylumbelliferyl-β-D-glucopyranoside (MUG) was used as the substrate in all enzymatic assays. Ambroxol (ABX), bromhexine (BHX), diltiazem (DTZ), fluphenazine (FLZ), mannitol (MNT) and taurocholic acid (TC) were all purchased from Sigma-Aldrich, whereas isofagomine (IFG), conduritol-β-epoxide (CBE) and *N*-nonyldeoxynojirimycin (NDJ) were obtained from Toronto Research Chemicals Inc

(North York, ON, Canada). The natural substrate for glucucerebrosidase (GCase), β-glucosylceramide (GlcCer) or *D*-glucosyl-β1-1'-N-palmitoyl-*D*-erythro-sphingosine was obtained from Avanti Polar Lipids, Inc. (Alabaster, AB, USA). Dimethyl sulfoxide (DMSO) was purchased from Caledon Laboratories Ltd. (Georgetown, ON, Canada), whereas Cerezyme/Imiglucerase (Genzyme Canada Inc., Mississauga, ON, Canada) was kindly provided to us as a gift by Dr. Michael Tropak and Dr. Don Mahuran at the Hospital for Sick Children (Toronto, ON, Canada). Cerezyme (Imiglucerase) is a recombinant modified human GCase (≈ 62 kDa) clinically approved for enzyme replacement therapy to type I GD patients, which differs from wild-type GCase by a single amino acid substitution (H495R) as well as glycosylation modifications at several amino acid residues.[8] Stock solutions of reagent were prepared in DMSO and stored at 4^{o}C. Stock solutions of wild-type recombinant GCase were prepared in de-ionized water, aliquoted as 25 µL portions into 0.5 mL sterilized centrifuge tubes and stored at -80^{o}C prior to use. Note that PCs include both carbohydrate and non-carbohydrate analogs that largely function as active site or mixed-type inhibitors of GCase with widely different binding affinity, including the natural substrate (GlcCer), non-specific osmolyte (MNT) and non-specific covalent inhibitor (CBE).

3.3.2 Capillary Electrophoresis (CE)

All CE separations for measuring GCase activity and enzyme unfolding dynamics were performed on an Hewlett Packard 3D CE system (Agilent Technologies Inc., Waldbronn, Germany) equipped with UV photodiode array (PDA) detection using uncoated open tubular fused-silica capillaries (Polymicro Technologies Inc., Phoenix, AZ, USA) with dimensions of 50 µm inner diameter, 360 µm outer diameter and total capillary length of 35 cm. New capillaries were conditioned by rinsing with methanol for 10 min, de-ionized water for 10 min, 1 M NaOH for 15 min and background electrolyte (BGE) for 30 min. The BGE used in CE separations for enzyme kinetic and urea-induced protein unfolding studies was 150 mM borate, pH 9.5 and 100 mM HEPES, pH 7.2 with 20 mM taurocholate, respectively unless otherwise noted. At the beginning of each day, the

capillary was rinsed with 1.0 M NaOH for 10 min and BGE for 15 min. Each separation started with a pre-rinsing of the capillary with 1.0 M NaOH for 2 min and BGE for 5 min followed by hydrodynamic injection of the sample at 50 mbar for 3 s. For enzymatic assays, separation of fluorogenic substrate, 4-methylumbelliferyl-β-D-glucopyranoside (MUG), hydrolyzed product, 4-methylumbelliferone (MU) and internal standard (IS), *m*-nitrophenol were performed under an applied voltage of 10 kV using a positive gradient pressure of 20 mbar over 5.0 min with UV absorbance monitored at 320 nm. For protein unfolding studies, urea-induced denaturation was performed for GCase (15 μM) under an applied voltage of 25 kV with UV absorbance at 230 nm. Due to the use of high amounts of urea in sample/BGE, daily cleaning of electrode interface on the CE instrument are important to avoid build-up and carry-over of salts for reproducible separations. Our recent work determined the potency and mode of inhibition among several PCs for native/wild-type GCase using CE in both neutral and acidic buffer conditions without chemical denaturation (Chapter II).[12] This earlier study inspired us to develop a modified enzyme kinetic assay to can better characterize the chaperone activity of ligands based on their capacity to restore the functional activity of denatured GCase as a surrogate for misfolded/mutant enzyme. Although READ was developed using CE as a convenient format to measure enzyme kinetics and protein unfolding dynamics, other techniques can be used for high-throughput screening of PCs from chemical libraries, such as fluorescence microarrays, which will be the focus of future studies. In this case, improved detector sensitivity will enable shorter substrate incubation periods when evaluating a ligand at two urea conditions (0 and 4 M, instead of full activity curves) and three dosage levels (≈ nM-μM) for unambiguous assessment of binding mode and chaperone potency.

3.3.3 External Calibration Curve for Measurement of Enzyme Activity

A stock solution of MU was diluted to twelve different concentrations ranging from 50 to 4000 μM in McIlvaine buffer (0.1 M citrate, 0.2 M phosphate buffer, pH 5.2 or pH 7.2), whereas *m*-nitrophenol was used as internal standard (IS) at a final concentration of 500 μM. The calibration curve was generated using an average of nine replicates performed

over three days (n = 9) with good precision as reflected by a coefficient of variance (CV) under 5%. Average responses were derived from the measured peak area ratio for MU as normalized to the IS in triplicate (n = 3), which was used to assess GCase activity as a function of urea and PC type/dosage. Overall, good linearity over a 80-fold concentration range was realized for calibration as reflected by a R^2 of 0.9996. The limit of quantification (LOQ) and limit of detection (LOD) for MU when using CE with UV absorbance detection at 320 nm were found to be 15 μM and 5 μM, respectively.

3.3.4 READ-based Activity Curves for Assessment of Chaperone Potency

GCase activity as a function of urea was measured after 6 hrs of substrate incubation under neutral pH conditions based on the average peak area ratio of product, MU to IS, *m*-nitrophenol using CE with UV detection at 320 nm unless otherwise stated. Activity curves were normalized to 0 M urea for each aliquot of heat-quenched enzyme reaction to reduce long-term variations, which also enables direct comparison of the chaperone activity among PCs with widely different binding modes and inhibitory potency. Normalization of apparent enzyme activities also enabled isolation of stabilization effects induced by ligand binding that is confounded by variable inhibitory properties. Three key parameters associated with chaperone activity were derived from normalized GCase activity curves at a given dosage level, namely mid-point for urea inactivation (C_M), cooperativity for inactivation (m) and normalized activity at 4 M urea, where the ligand-free *apo*-GCase had a residual activity of only 1.5%. The latter urea concentration served as a useful transition point for GCase to assess the chaperone potency of a ligand that triggered a distinct enhancement in enzyme activity under denaturing conditions. Non-linear curve fitting (sigmoidal) was performed on normalized activity curves with Igor Pro 5.0 (Wavemetrics Inc., Lake Oswego, OR, USA) for determination of C_M, whereas linear regression using Excel (Microsoft Inc., Redmond, WA, USA) was performed for data in the active/inactive transition region for GCase for determination of m. PCs tested displayed a non-linear dose response in terms of GCase stabilization as reflected by an increase in apparent C_M. Linear regression of log-transformed data was used for

correlation of measured IC_{50} versus ligand-induced stabilization derived from READ experiments. Overall, a higher correlation for determination (R^2) was achieved when using the ratio of $\Delta C_M/\Delta m$ relative to ligand dosage as compared to the use of single parameters, such as ΔC_M *or* Δm.

3.3.5 Restoration of Enzyme Activity upon Denaturation

Enzyme kinetic studies were performed off-line in McIlvaine buffer (0.1 M citrate and 0.2 M phosphate, pH 7.2) with 10 mM taurocholate (TC) using recombinant GCase (25 nM). The use of a bile salt surfactant (10 mM TC) in the enzyme reaction is important for in vitro activation of the lysosomal enzyme while achieving selectivity since it denatures other cytosolic β-glycosidases derived from cell lysates. In most cases, enzyme kinetic studies were performed at pH 7.2 when characterizing PCs that target misfolded protein in the ER of the cell. First, GCase and TC in McIlvaine buffer were equilibrated in a 37^{o}C water bath for 15 min. Then, the mixture was incubated for 10 min with urea (0-7 M) in order to perturb the native conformational state of the enzyme that results in lower catalytic activity upon unfolding. The reaction mixture was subsequently incubated for 10 min with ligand/PC at two or more dosage levels. Finally, the enzyme reaction was initiated by addition of MUG as fluorogenic substrate using a total volume of 250 µL. The final concentrations of GCase, TC and MUG in the reaction solution were 25 nM, 10 mM and 2 mM, respectively. An aliquot (100 µL) was withdrawn from the bulk reaction mixture at 6 hrs and placed in a centrifuge tube containing 100 µL of IS. Due to the four-fold lower catalytic efficiency of GCase under neutral (pH 7.2) relative to acidic (pH 5.2) conditions that can be further attenuated by inhibitor binding and/or protein unfolding, a 6 hr incubation time prior to thermal quenching was required to attain adequate product turn-over for maximum sensitivity. All enzyme reactions were immediately quenched by thermal denaturation at 90^{o}C for 10 min, followed by vortexing for 30 s and centrifugation for 10 s at 4 *g* prior to being stored frozen at -80^{o}C. GCase activity was measured in triplicate by CE based on the average relative peak area ratio of MU to IS, where reproducibility of three biological replicates over three different days was good as

reflected by a coefficient of variance (CV) under 10 %. Note that READ offers several benefits for the screening of PCs that function as enzyme enhancers relative to thermal stability assays that measure protein conformational stabilization, since it allows for use of low protein concentrations (25 nM) due to the amplification effect of enzyme catalysis while revealing whether ligand binding induces refolding to a functionally-active conformer with full or partial catalytic activity without irreversible aggregation/precipitation. In comparison to other chemical denaturants (*e.g.,* guanidine hydrochloride), urea is also more compatible for solubilizing unfolded protein conformers in READ when using CE since it is does not contribute to Joule heating (*e.g.,* neutral additive) and is UV transparent above 214 nm.

3.3.6 Dynamic Protein Unfolding Studies and Reversibility in Urea

In order to correlate measured activity curves derived from READ experiments with urea-induced changes in GCase structure, protein unfolding studies were performed by CE with UV detection at 230 nm. To the best of our knowledge, GCase unfolding in urea has not been reported to date with the exception of guanidine hydrochloride as chemical denaturant when characterizing ligand-induced stabilization of *holo*-enzyme by H/D exchange and MALDI-MS.[8] Classical methods for protein characterization based on intrinsic fluorescence and circular dichroism are constrained by poor selectivity (*i.e.,* GCase has 12 Trp residues across three domains of enzyme) and limited sensitivity due to spectral interferences in the buffer, respectively. Given the complexity of the lysosomal enzyme system that comprises a poorly defined multidomain protein-anionic surfactant complex in solution, CE was used as a technique to characterize both the rate and reversibility of GCase unfolding in urea. First, dynamic protein unfolding studies were performed by measuring the rate of GCase denaturation as a function of urea and PC binding. GCase (15 μM) was pre-incubated with 0, 4 or 7 M urea with/without equimolar concentrations of IFG in McIlvaine buffer (pH 7.2) at increasing time intervals (5 min to 6 hrs) prior to sample injection. In order to maintain equilibrium conditions during protein electromigration, the BGE used for CE separations (100 mM HEPES, 20 mM TC, pH

7.2) also included urea, surfactant and IFG (in case of *holo*-GCase). Changes in the viscosity-corrected electrophoretic mobility, peak dispersion and absorbance response of GCase were parameters used to characterize the dynamics of urea-induced unfolding of the multimeric enzyme-surfactant complex in free solution. In addition, the reversibility of GCase folding was assessed by measuring its normalized catalytic activity when incubating in 4 M urea at increasing time intervals (10 min or 1 hr) relative to 0.5 M urea (folded/active state) after its dilution to 0.5 M urea (25 nM) to trigger refolding of enzyme. In this case, the relative peak area of MU to IS was measured by CE with UV detection at 320 nm in order to assess the extent of catalytic activity restored upon folding that is modulated by PC binding and denaturation time in urea. Under 4 M urea buffer conditions, GCase was found to undergo slow unfolding that generates a partially unfolded intermediate state after 10 min of denaturation, whereas it forms a largely unfolded protein state when the denaturation time was extended beyond 1 hr. Thus, the 6 hr substrate incubation time used in READ was adequate for achieving the required sensitivity for measuring product formation while allowing for sufficient time to reach steady-state conditions during urea-induced GCase unfolding.

3.4 Results and Discussion

Herein, we introduce a new assay for characterization of PCs based on their capacity to restore enzyme activity that is abolished in urea (**Fig 3.1**) in order to address the high attrition of conventional screens. Urea serves as a convenient perturbant to modulate the equilibrium distribution of protein conformers in solution without precipitation unlike thermal denaturation.[12] Seven model PCs were examined in this study, including competitive, mixed-type and covalent inhibitors of GCase together with GlcCer (natural substrate) and mannitol (MNT, non-specific osmolyte) as depicted in **Fig 3.2**. A fluorogenic substrate is then used to evaluate the residual activity of stabilized/refolded enzyme in urea relative to native *holo*-GCase (*i.e.,* 0 M urea with PC) by measuring the extent of product formation. Similar experiments are also performed for *apo*-GCase without ligand as a reference state to compare the dose response of PCs as a measure of

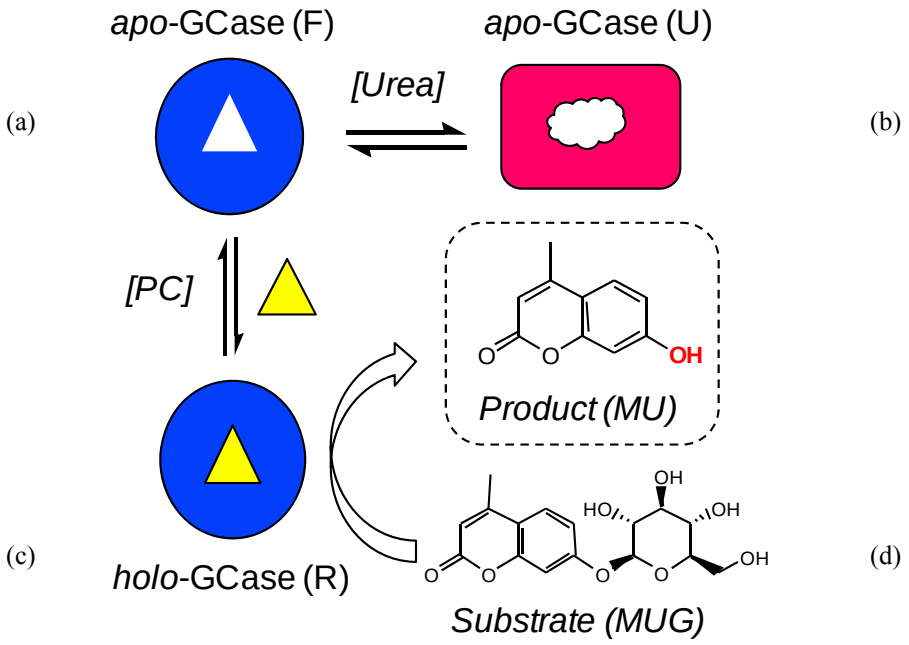

Figure 3.1 Restoration of enzyme activity upon denaturation (READ) for functional screening of PCs (a) Recombinant GCase (folded *apo*-enzyme, F) is first equilibrated under neutral pH conditions, (b) GCase is then partially/fully denatured (unfolded *apo*-enzyme, U) in urea, (c) PC is introduced in order to shift equilibrium distribution of native/active enzyme state (refolded *holo*-enzyme, R), and (d) normalized enzyme activity is measured by extent of fluorescent product formation after thermal quenching. PCs can function as enzyme enhancers via reversible orthosteric and/or allosteric binding.

their chaperone activity. Various methods can be used for READ, including fluorescence microarrays and multiplexed separation techniques, such as capillary electrophoresis (CE). CE with UV detection offers several advantages in terms of high selectivity, low sample requirements and short analysis times that avoids spectral interferences by resolving excess urea and free ligand, where both substrate and product are monitored simultaneously, including their stereoisomers.[13] **Fig 3.3a** depicts a series of electropherograms showing the impact of PC binding on modulating GCase activity under neutral pH conditions at 0 M (folded/active) and 4 M urea (unfolded /inactive). Under alkaline buffer conditions in CE, excess urea and ligand are neutral and co-migrate with the electroosmotic flow (EOF), which is then followed by substrate (MUG), product (MU) and internal standard (IS) that migrate as anions with increasing charge density.

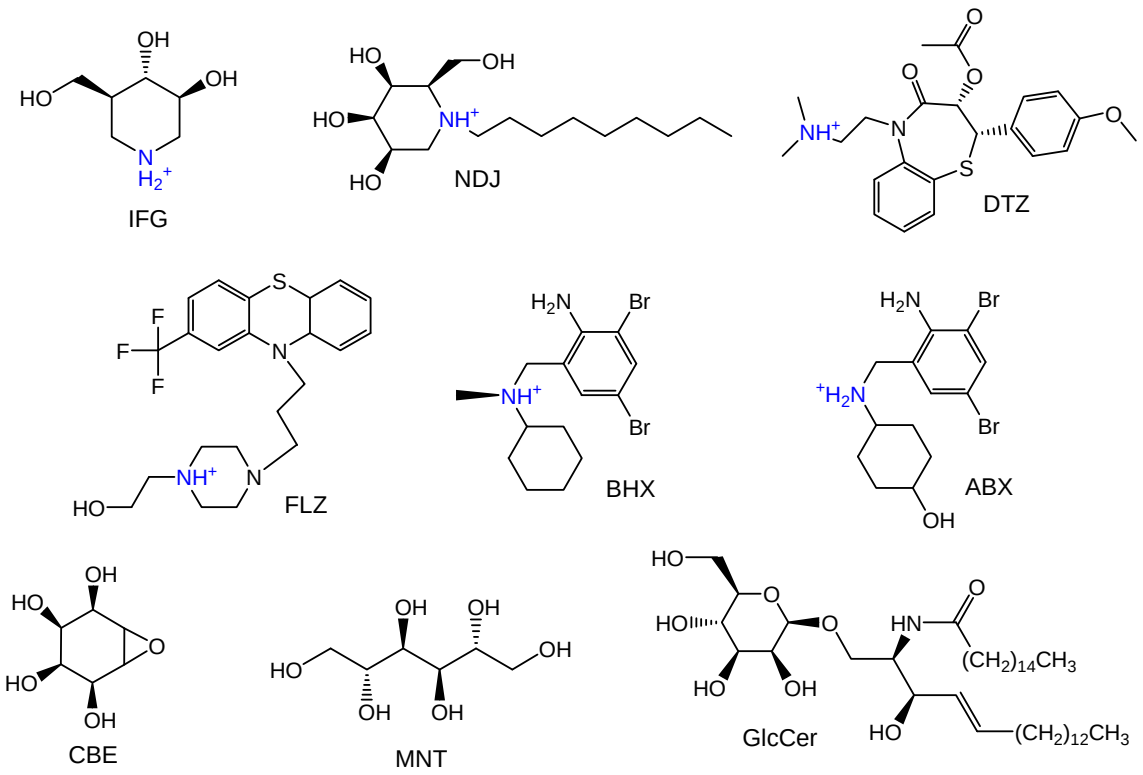

Figure 3.2 2D chemical structures of model PCs , including osmolyte and natural substrate for assessing the chaperone activity of small molecules that stabilize unfolded GCase and restore its activity upon urea denaturation. Note that some amine-based PCs are largely cationic at pH 7.2 due to their weaker acidity with $pK_a > 8$, including IFG, NDJ, DTZ and ABX. However, all UV-active ligands co-migrate with urea as neutral species under alkaline conditions (pH 9.5) of the background electrolyte used in CE.

The potent competitive inhibitor of GCase, isofagamine (IFG, IC_{50} = 4.6 nM, pH 7.2)[12] significantly attenuates product turn-over at 50 nM under native conditions, whereas it restores about 50% of normalized activity at 4 M urea that is nearly fully abolished (≈ 1.5%) for ligand-free *apo*-GCase. Thus, READ directly measures the chaperone capacity of a ligand to restore GCase activity while also revealing the potency of inhibition (or activation). Noteworthy, this approach avoids false-negatives when using classical inhibitor screens since ligand interactions that do not inhibit GCase can still facilitate folding to enhance enzyme activity under denaturing conditions. **Fig 3.3b** depicts normalized GCase activity curves for IFG as a function of urea at two dosage levels relative to *apo*-GCase.

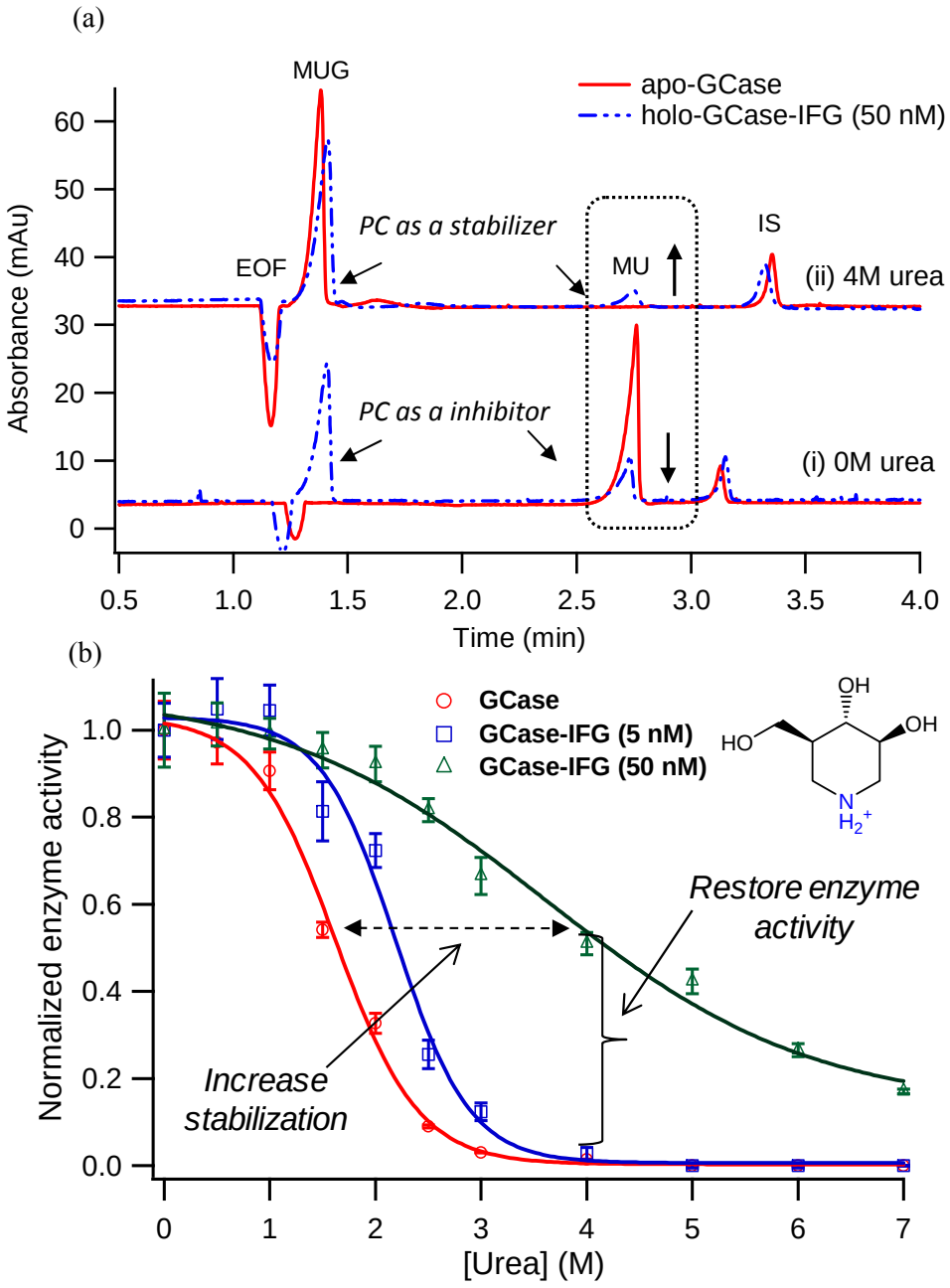

Figure 3.3 Dose-response curve of IFG for GCase based on READ (a) Electropherogram overlay depicting the contradictory properties of PCs, such as IFG that is a potent active site inhibitor of GCase that attenuates substrate turnover for the native enzyme at 0 M urea, whereas it enhances catalytic activity at 4 M urea, where *apo*-GCase is inactive (b) Dose-dependent activity curves for GCase for characterization of PCs as a function of ligand type/dosage when using READ, where error represents ± 1σ with precision (n=3) under 5%.

Each activity curve reflects the extent of ligand-induced stabilization of GCase that increases the population of refolded yet catalytically active enzyme in urea. Two parameters can be derived from these activity curves that are related to chaperone activity of a ligand similar to equilibrium protein unfolding,[14] namely the mid-point for urea inactivation (C_M) and cooperativity for inactivation (m). The former parameter reflects the intrinsic thermodynamic stability of *apo*-GCase and/or specific enzyme-ligand complex (*holo*-GCase), whereas the latter term indicates the sensitivity of enzyme conformers to urea denaturation. **Fig 3.3b** highlights that addition of only 5 nM of IFG (using 25 nM GCase) results in a shift in C_M relative to *apo*-GCase (ΔC_M) of 0.57 M that is further increased to about 2.0 M and 4.4 M (data not shown) with 50 nM and 500 nM IFG respectively, in a dose-responsive manner as shown in **Figure S3.1.** Similarly, a dose-dependent decrease in cooperativity relative to *apo*-GCase (Δm) was measured with IFG as indicated by a more shallow linear transition between active and inactive enzyme conformers. The lower cooperativity for *holo*-GCase is likely associated with independent unfolding of the three non-contiguous domains of GCase that is enhanced upon localized stabilization of the active site (in domain III) by competitive inhibitors, such as IFG.[15] This is in contrast to greater unfolding cooperativity upon ligand-induced stabilization of single domain proteins.[14] In general, the chaperone potency of a ligand for GCase is associated with greater *holo*-enzyme stabilization (ΔC_M), higher catalytic activity in urea and reduced cooperativity (Δm) that is achieved at low dosage levels. However, due to the10-fold weaker potency of IFG at pH 5.2,[12] ligand binding imparts a lower increase in *holo*-GCase stability under acidic conditions as shown in **Figure S3.2**. Dynamic protein unfolding studies were also performed in order to relate GCase activity curves with urea-induced structural changes to enzyme that are dependent on ligand type, dosage and/or buffer pH as shown in **Figure 3.4**. **Figure S3.3** compares activity curves of two distinct non-carbohydrate PCs derived from a FDA-approved drug library that function as mixed-type inhibitors of GCase. Ambroxol (ABX) is an anti-mucolytic agent recently shown to enhance the activity of mutant GCase in GD patient cells.[8]

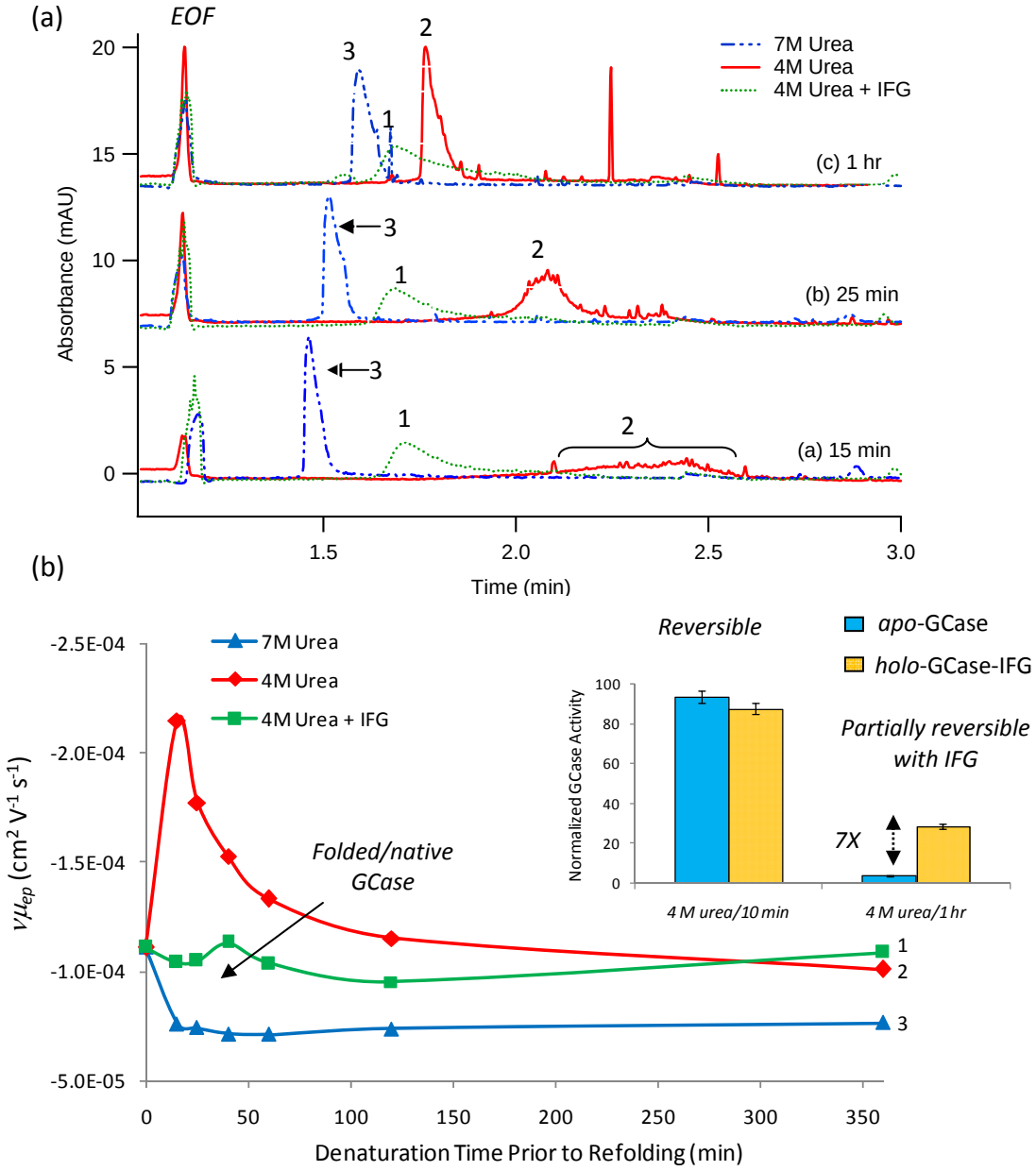

Figure 3.4 Dynamic unfolding and refolding of GCase (a) Electropherogram overlay showing dynamic unfolding of GCase as a function of denaturation time in urea. GCase exhibits slow unfolding in 4 M urea with formation of partially unfolded intermediates as resolved by CE, whereas rapid unfolding occurs in 7 M urea. Co-incubation of GCase with IFG (15 µM) stabilizes enzyme in 4 M urea similar to native GCase. (b) Overlay of viscosity-corrected electrophoretic mobilities (μ_{ep}) for GCase highlights dynamic changes in protein conformation in 4 M urea without PC unlike stable profiles measured in 7 M urea and 4 M urea with 50 nM IFG. The inset compares the reversibility of GCase folding based on GCase activity measured after denaturation in 4 M urea for 10 min or 1 hr and its subsequent dilution to 0.5 M urea with substrate incubation for 6 hrs. PC binding (50 nM IFG) restores about 30% of normalized activity for GCase after 1 hr denaturation in 4 M urea that is increased 7-fold relative to *apo*-GCase. Peak numbers refer to folded GCase (1), partially unfolded intermediates (2) and fully unfolded enzyme (3).

In contrast, diltiazam (DTZ) is a Ca^{2+} channel blocker that enhances GCase activity in cellulo for several GD variants (**Fig 3.2**).[16] Although DTZ and ABX are both mixed-type inhibitors of GCase with similar potency (IC_{50} ≈ 50-60 μM at pH 7.2),[12] DTZ has greater chaperone activity relative to ABX as reflected by its larger ΔC_M at each dosage level. For instance, 60 μM DTZ was able to restore the normalized GCase activity to about 30% in 4 M urea, which is within the critical threshold of activity under which symptoms of GD are observed.[17] In contrast, an equivalent dosage of ABX produced no significant changes in protein stability or GCase activity. Thus, inhibition type and potency alone do not reliably predict chaperone properties. GCase activity curves were also performed when using 5 nM GlcCer and 0.5 mM MNT that generate similar enzyme enhancement despite doses that vary over five orders of magnitude (**Figure S3.4**). X- ray crystal structures have shown that polyols bind to the active site of GCase, however with much lower affinity than IFG.[18] **Table. S1** summarizes three key parameters derived from READ that highlight the wide disparity in chaperone activity measured among seven model ligands, including ΔC_M, Δm and % activity at 4 M urea. Bromhexine (BHX) is a pro-drug of ABX with weaker potency (IC_{50} ≈ 86 μM), whereas fluphenazine (FLZ, IC_{50} ≈ 140 μM)[12] is an antipsychotic drug for treatment of schizophrenia, which is a thermal stabilizer of GCase yet does not enhance activity in cellulo;[8] the latter observation is likely due to the limited aqueous solubility of FLZ. In order to clearly rank chaperone potency for ligands over a wide dynamic range, Fig 3.4 compares two *log*-based READ indices derived from ΔC_M and % activity (at 4M urea) values normalized to dosage level. GlcCer was found to have the highest chaperone potency among all ligands tested, including IFG. In contrast, MNT induced the lowest stabilization to GCase, which served as a lower "cut-off" for exclusion of ligands with marginal chaperone activity, such as BHX, ABX and FLZ. The latter compounds require excessively high doses (> 200 μM) to elicit a measurable response that is similar to polyol-based osmolytes; this is undesirable as it contributes to drug toxicity with reduced selectivity in vivo.

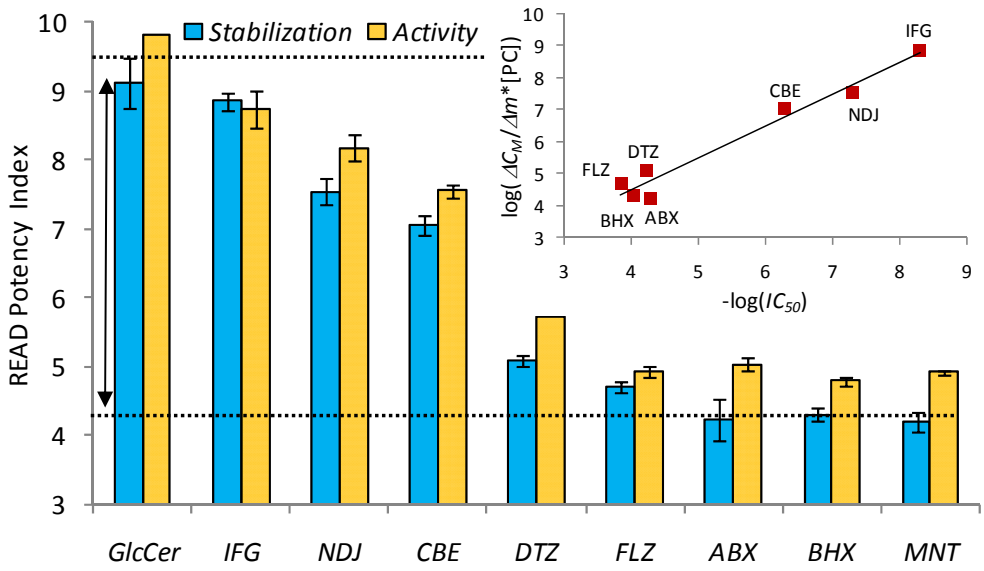

Figure 3.5 Comparison of ligand-induced stabilization with inhibition assay. Two *log*-based READ indices for assessing the chaperone potency of a ligand to enhance stability and restore the activity of denatured GCase relative to GlcCer and MNT as controls. Ligand binding that induces stabilization to GCase also increases activity at 4 M urea (a key transition point where *apo*-GCase is inactivated). Overall, there was a linear correlation (*e.g.,* slope = 0.996; R^2 = 0.961) between inhibitor potency (IC_{50}) and PC-induced stabilization (*i.e.,* ΔC_M) as shown in the inset with notable exceptions among mixed-type inhibitors.

Both covalent and competitive inhibitors of GCase, conduritol β-epoxide (CBE) and *N*-nonyldeoxynojirimycin (NDJ), possess greater chaperone activity relative to non-carbohydrate ligands, however they lack GCase specificity.[11] Thus, enzyme controls must be included in primary screens to confirm ligand selectivity with an adequate READ potency index (> 6). Overall, the inset of Figure 2 shows that there is a linear correlation between ligand-induced stabilization and IC_{50} values similar to trends for GCase melting temperature transitions.[19] However, there were several exceptions among mixed-type inhibitors that have greater chaperone potency despite their weaker inhibition properties, such as DTZ and FLZ.

3.5 Conclusion

In summary, READ directly measures the chaperone capacity of ligands that enhance enzyme activity under denaturing conditions. Although inhibitor potency is an approximate indicator of chaperone activity,[19] lead candidates are prone to false-positives that require retesting prior to cell-based assays. Moreover, screening by inhibition excludes the detection of PCs that may stabilize the native enzyme conformer without substrate displacement. Computational studies have revealed the existence of allosteric sites in GCase that may represent targets for non-active site PCs.[20] Future work will adapt READ for high-throughput screening to discover novel classes of PCs that function as stabilizers that properly refold denatured/mutant enzymes without adverse inhibition.

3.6 Funding Sources

This work was supported by Natural Science and Engineering Research (NSERC) Discovery Grant.

3.7 References

1. Meusser, B; Hirsch, C; Jarosch, E; Sommer, T. *Nat. Cell Biol.* **2005**, 7, 766-772.
2. Ong, D. S. T; Kelly, J. W. *Curr. Opin. Cell Biol.* **2011**, 23, 231-238.
3. Wei, R. R; Hughes, H; Boucher, S; Bird, J. J; Guziewicz, N. *J. Biol. Chem*. **2011**, 286, 299-308.
4. Goldblatt, J; Fletcher, J. M; McGill, J; Szer, J; Wilson, M. *Blood Cells Molecules and Diseases*, **2011**, 46, 107-110.
5. Yu, Z. Q; Sawkar, A. R; Kelly, J. W. *FEBS J.* **2007**, 274, 4944-4950.
6. Sawkar, A. R; Cheng, W. C; Beutler, E; Wong, C. H; Balch, W. E; Kelly, J. W. Proc. Nat.Acad. Sci. US. **2002**, 99, 15428-15433.
7. Benito, J. M; Fernandez, J. M. G; Mellet, C. O. *Expert Opinion Therapeutic Patents*. **2011**, 21, 885-903.

8. Maegawa, G. H. B; Tropak, M. B; Buttner, J. D; Rigat, B. A; Fuller, M. *J. Biol. Chem.* **2009**, 284, 23502-23516.
9. Motabar, O; Goldin, E; Leister, W; Liu, K; Southall, N. *Anal. Bioanal. Chem.* **2012**, 402, 731-739.
10. Tropak, M. B; Kornhaber, G. J; Rigat, B. A; Maegawa, G. H; Buttner, J. D. *ChemBioChem.* **2011**, 9, 2650-2662.
11. Sawkar, A. R; Schmitz, M; Zimmer, K. P; Reczek, D; Edmunds, T; Balch, W. E; Kelly, J. W. *ACS Chem. Biol.* **2006**, 1, 235-251.
12. Shanmuganathan, M; Britz-McKibbin, P. *Anal. Bioanal. Chem.* **2011**, 399, 2843 2853.
13. Gavina, J. M. A; White, C. E; Finan, T. M; Britz-McKibbin, P. *Electrophoresis,* **2011**, 31, 2831-2837.
14. Gavina, J. M. A; Mazhab-Jafari, M. T; Melacini, G; Britz-McKibbin, P. *Biochemistry.* **2009**, 48, 223-225.
15. Batey, S; Clarke, J. *J. Mol. Biol.* **2008**, 378, 297-301
16. Rigat, B; Mahuran. D. *Mol. Genetics Metabol.***2009**, 96, 225.
17. Kornhaber, G. J; Tropak, M. B; Maegawa, G. H; Tuske, S. J; Coales, S. J. *ChemBioChem*. **2008**, 9, 2643-2649.
18. Lieberman, R. L; Wustman, B. A; Huertas, P; Powe, A. C; Pine, C. W. *Nat. Chem.Biol.***2007**, 3, 101-107.
19. Goddard-Borger, E. D; Tropak, M. B; Yonekawa, S; Tysoe, C; Mahuran, D. J; Withers, S. G. *J. Med. Chem.* **2012**, 55, 2737-2745.
20. Landon, M. R; Lieberman, R. L; Hoang, Q. Q; Ju, S. L; Caveiro, J. M. M. *J.* Computer Aided Molec. Design. **2009**, 23, 491-500.

3.8 Supplemental Section

Table S 3.1 Characterization of ligand-induced stabilization of GCase by READ at neutral pH conditions.

Ligand (Function)	***IC_{50}[a] (μM)***	***Concentration (μM)***	***ΔC_M[b] (M)***	***Δm[b] (M^{-1})***	***%Activity[b] (at 4 M urea)***
GlcCer	*n/a*	0.005	1.68 ± 0.32	0.256 ± 0.040	34.0 ± 0.1
(*Natural substrate*)		0.050	3.33 ± 0.28	0.216 ± 0.040	69.1 ± 0.4
IFG	0.0046	0.005	0.57 ± 0.07	0.157 ± 0.040	2.8 ± 0.2
(*Active site inhibitor*)		0.050	1.99 ± 0.25	0.269 ± 0.040	51 ± 2
		0.500	4.36 ± 0.26	0.264 ± 0.026	72 ± 4
NDJ	1.0	0.050	0.20 ± 0.11	0.119 ± 0.030	7.6 ± 0.4
(*Active site inhibitor*)		50	1.27 ± 0.22	0.178 ± 0.050	28.6 ± 0.6
CBE	17	0.50	1.78 ± 0.16	0.311 ± 0.040	17.6 ± 0.5
(*Irreversible inhibitor*)		50	3.01 ± 0.46	0.227 ± 0.070	52.5 ± 0.8
ABX	50	50	0.12 ± 0.30	0.150 ± 0.040	*nd*[c]
(*Mixed-type inhibitor*)		500	2.31 ± 0.32	0.313 ± 0.050	53.2 ± 2.1
DTZ	56	60	1.33 ± 0.12	0.182 ± 0.040	30.3 ± 0.1
(*Mixed-type inhibitor*)		600	2.91 ± 0.18	0.206 ± 0.040	80.4 ± 4.0
BHX	86	90	*nd*[c]	0.029 ± 0.050	*nd*[c]
(*Mixed-type inhibitor*)		900	2.15 ± 0.21	0.119 ± 0.050	54.5 ± 1.3
FLZ[d]	140	140	0.64 ± 0.08	0.092 ± 0.010	11.8 ± 0.5
(*Mixed-type inhibitor*)					
MNT	*n/a*	500	1.74 ± 0.26	0.239 ± 0.040	41.2 ± 0.6
(*Osmolyte*)					

[a] IC_{50} measured at pH 7.2 using 25 nM GCase, 10 mM TC and 2 mM MUG as fluorogenic substrate[34] with exception of NDJ and CBE that were performed at pH 5.0 and 5.9, respectively[11]

[b] Relative changes in thermodynamic stability, where C_M is (1.62 ± 0.05) M, m is (0.415 ± 0.004)M^{-1}, whereas the *% activity* at 4 M urea is (1.5 ± 0.1)% for *apo*-GCase.

[c] Non-detectable (*nd*) change in stability and/or activity relative to *apo*-GCase.

[d] FLZ is insoluble at concentrations above 200 μM under neutral buffer conditions (pH 7.2).

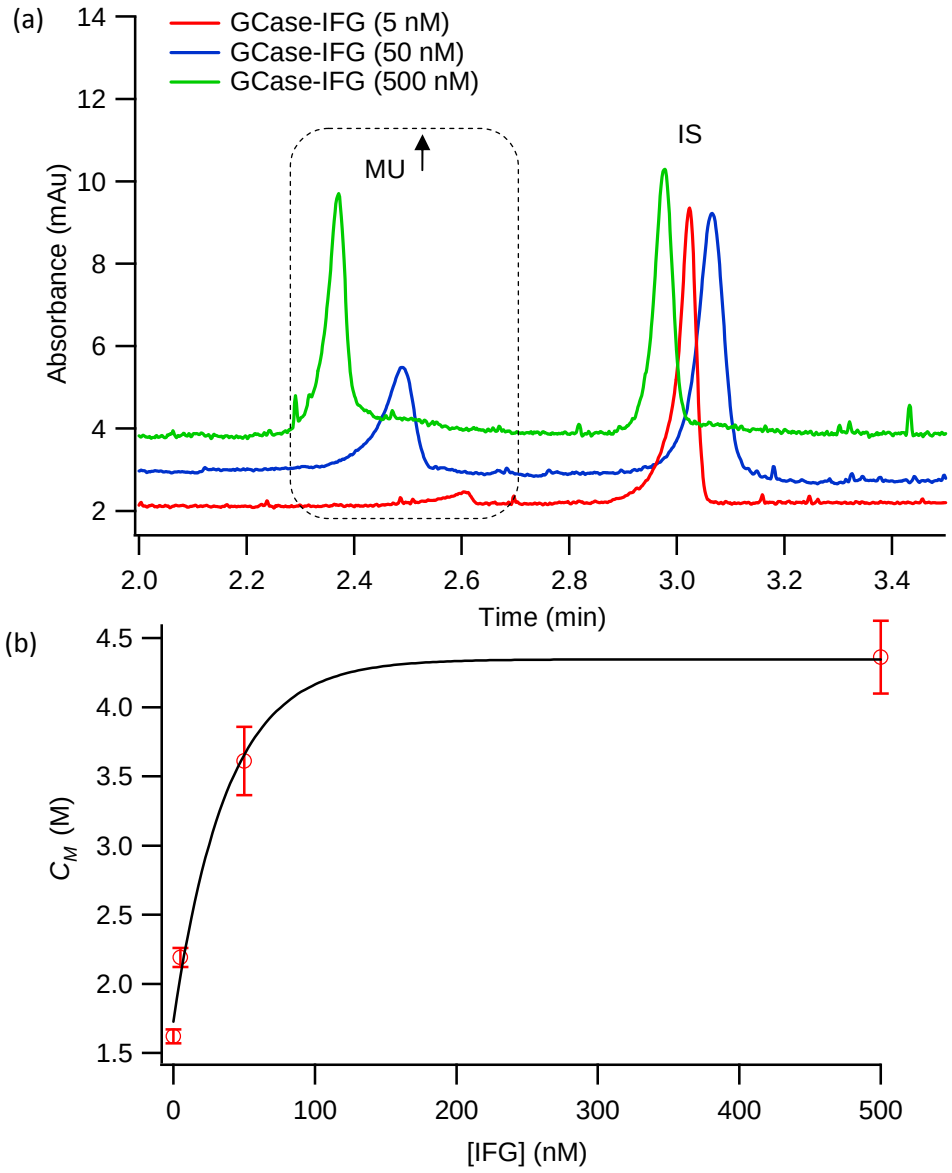

Figure S3.1 Dose-response curve of IFG for GCase (a) Electropherogram overlay that depicts the dosage-dependence of the potent active-site inhibitor IFG (IC_{50} = 4.6 nM, pH 7.2) for restoring the residual activity of GCase under denaturing conditions (at 4 M urea) as reflected by a significant increase in MU generation. (b) Dose-response curve for GCase as a function of IFG based on measurement of the mid-point urea concentration for enzyme inactivation (C_M) from activity curves (Fig 3.2), which is a key parameter associated with ligand-induced *holo*-GCase stabilization and its chaperone potency.

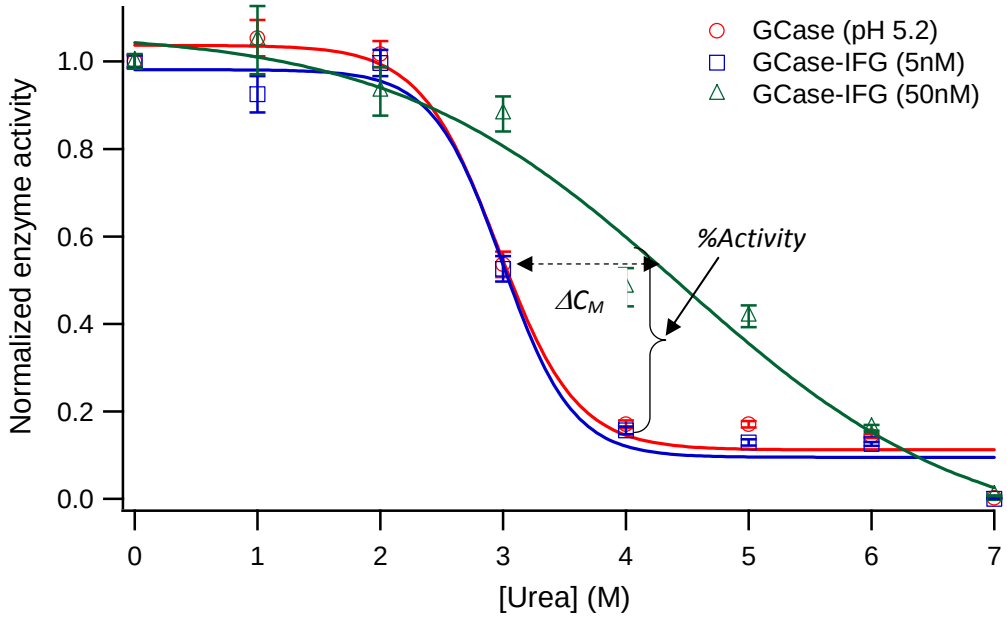

Figure S3.2 Activity curves that highlights ligand-induced stabilization of GCase under acidic conditions (pH 5.2) based on binding with 0, 5 and 50 nM IFG. Note that *apo*-GCase is intrinsically more stable under acidic relative to neutral pH conditions as reflected by an increase of C_M to (2.96 ± 0.11) M from (1.62 ± 0.05) M, respectively. Also, since the inhibitory potency of IFG is weaker under acidic conditions (IC_{50} ≈ 50 nM, pH 5.2), the addition of 5 nM IFG does not elicit any change in stabilization or cooperativity unlike neutral pH conditions (Figure 1). Moreover, the incubation of 50 nM IFG resulted in a lower increase in conformational stability to *holo*-GCase relative to *apo*-GCase as reflected by ΔC_M of 1.5 M and 2.0 M under acidic and neutral pH conditions, respectively. This data is consistent with pH-dependent changes in melting temperature for GCase of 8.7°C (pH 7.4) that is lowered to 3.7°C (pH 5.2) when using a slight molar excess of IFG [Lieberman, R. L. et al. (2009) *Biochemistry 48*, 4816-4827], which is further increased to 16°C with excess IFG under neutral pH conditions [Hill, T et al. (2011) *ChemBioChem 12*, 2151].

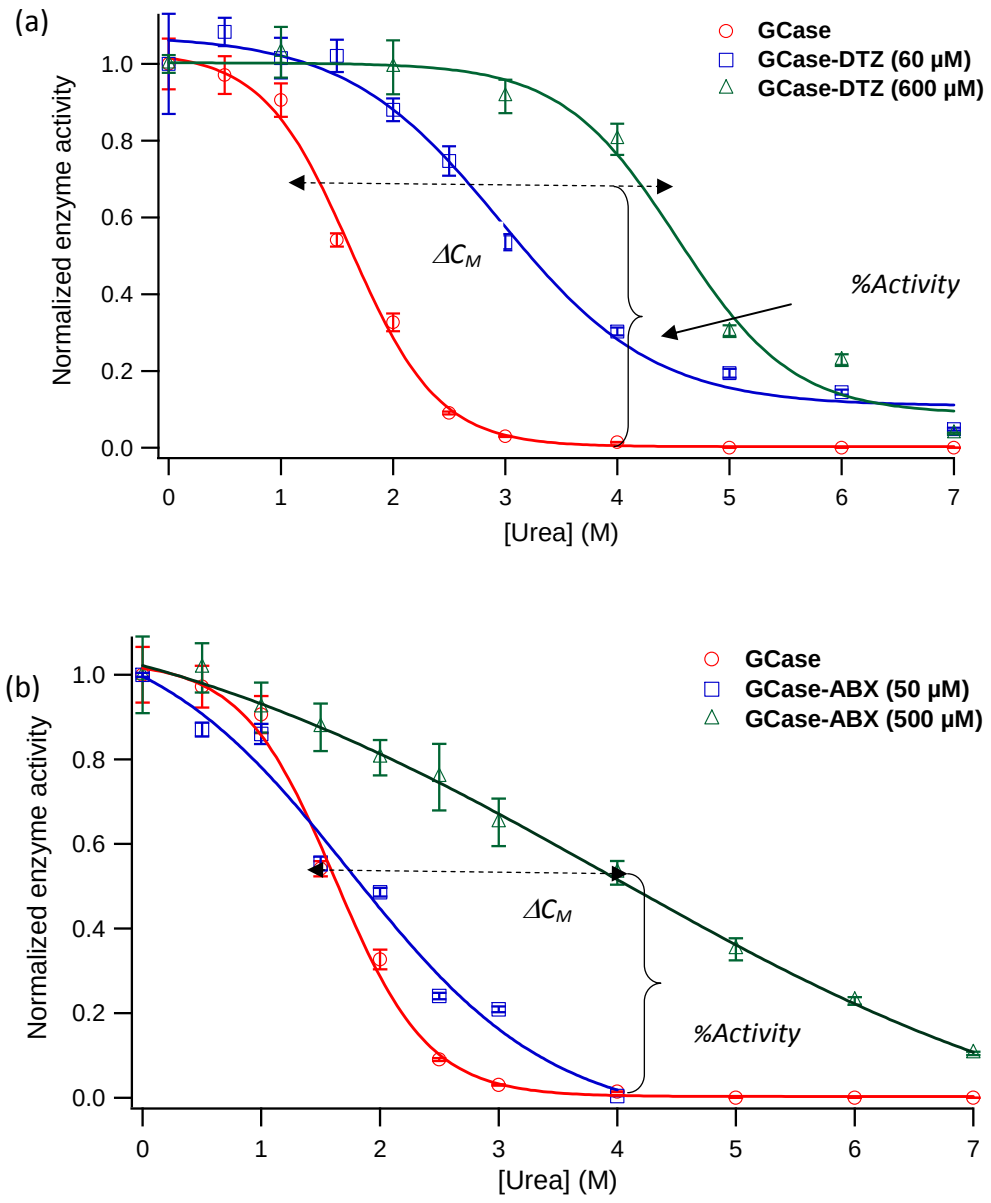

Figure S3.3 A comparison of dose-dependent activity curves for GCase under neutral pH conditions when using READ for characterization of the chaperone potency of two mixed-type inhibitors with similar potency, such as (a) diltiazem (DTZ, $IC_{50} \approx 60$ µM) and (b) ambroxol (ABX, $IC_{50} = 50$ µM). Although DTZ which is a slightly weaker mixed-type inhibitor than ABX it exhibits greater chaperone activity at a lower dosage levels reflected by increases in *holo*-GCase stabilization (ΔC_M) and enhancement in % activity (at 4 M urea) under denaturing conditions. These differences likely arise due to allosteric binding of DTZ in a region that favors global stabilization of GCase as compared to ABX, which has yet to be elucidated [Rigat, B.; Mahuran D. (2009) *Mol. Genet. Metab. 96*, 225].

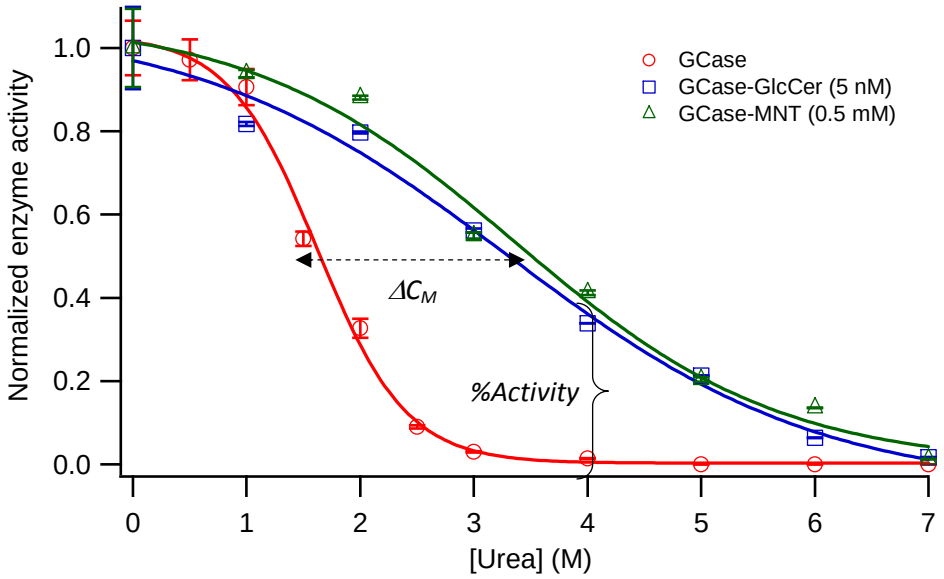

Figure S3.4. Overlay of activity curves showing the dynamic range in chaperone potency that can vary over five orders of magnitude, when comparing apo-GCase and two different holo-GCase complexes formed by addition of 5 nM GlcCer (natural glycolipid substrate for GCase) and 0.5 mM MNT (non-specific osmolyte and widely used cryoprotectant for recombinant protein) under neutral pH conditions with 25 nM GCase. These ligands can serve as useful controls for selection of promising PCs with adequate chaperone potency. Indeed, natural substrates for enzymes represent one of earliest types of PCs proposed for EET, such as galactose for treatment of β-galactosidase deficiency [Okumiya, T. *et al.* (1995) *Biochem. Biophys. Res. Comm. 214*, 1219]. However, since endogenous GlcCer accumulates in the lysosomes of macrophages in GD, intra-cellular distribution is limited for stabilizing mutant enzyme susceptible to ER-based degradation that is a key mechanism associated with the therapeutic application of PCs for treatment of genetic disorders related to protein deficiency.

Chapter IV:
A Two-tiered Functional Screen for Pharmacological Chaperones: Chaperone Activity without Inhibition for Enzyme Enhancement Therapy

Authors of this work are Meera Shanmuganathan, James McNulty, Dave McLeod, Alex Nielsen, and Philip Britz-McKibbin. I conducted most of the experiments and data analysis in this work. D. McLeod and A. Nielsen, supported with synthesizing chemically unique small molecules for a small chemical library.

4.1 Abstract

Pharmacological chaperones (PCs) are small molecules that stabilize and promote the folding of mutant protein as required for enzyme enhancement therapy of genetic diseases. Enzyme inhibition and thermal stability assays are currently used for primary screening of PCs, however, they do not accurately measure chaperone activity while probing ligand interactions with the folded/native enzyme. Herein, we introduce a high throughput fluorescence-based assay for functional screening of PCs based on restoration of enzyme activity upon chemical denaturation. A two-tiered screening approach was developed to identify new classes of PCs that activate, stabilize yet restore the activity of β-glucocerebrosidase (GCase) under denaturing conditions. This strategy was used to directly measure the chaperone activity of small molecules derived from a chemical library containing structurally unique synthetic compounds after *in silico* screening for drug-like activity. Overall, two stilbene derivatives, 4-(4-methoxystyryl)-2-methylthiazole (MSMT) and (*E*)-2,3-diphenylprop-2-en-1-ol (DPPL) were found to induce a dose-response enhancement to GCase activity up to 2.5-fold without unwanted inhibition. Moreover, these compounds were found to have better chaperone activity as compared to previously identified PCs used for treatment of Gaucher disease (GD), including isofagomine (IFG) and ambroxol (ABX). Structure-activity relationships were also explored by comparing the chaperone activity of several MSMT and DPPL analogs

for GCase under denaturing conditions. To the best of our knowledge, this is the first study that demonstrates that PCs can enhance enzyme activity without inhibition that is urgently needed for new advances in the treatment of neuronopathic forms of GD.

4.2 Introduction

Gaucher disease (GD) is the most prevalent lysosomal storage disorder (LSD) caused by a deficiency in β-glucocerebrosidase (GCase) resulting in deleterious accumulation of glucosylceramide (GlcCer) in cells of the mononuclear phagocyte system.[1] GCase catalyzes β-glycosidicbond cleavage of GlcCer to produce glucose and ceramide, a bioactive sphingolipid involved in heat stress response and apoptosis.[2] Over 200 mutations in the GCase gene can lead to aberrant folding during protein assembly that triggers endoplasmic recticulum (ER)-associated degradation pathways.[3] Defective GCases form non-native conformers with lower thermal stability under neutral pH conditions of the ER that are susceptible to proteolysis with reduced trafficking of mature enzyme to the lysosome.[4] Most clinically relevant missense mutations of GCase (*e.g.,* N370S, L444P) occur for amino acid residues distant to the active site, which retain partial catalytic activity (< 30%) under acidic conditions of the lysosome.[5,6] GD is associated with variable clinical phenotypes among patients ranging from enlarged spleen/liver, anemia, skeletal lesions and in some cases neurological impairment.[7,8] Currently, enzyme replacement therapy using recombinant enzyme is the most widely used treatment for type 1 GD.[9] However, it suffers from high costs, requires bi-weekly intravenous administration while it is not effective for disease variants of GD affecting the central nervous system. Alternatively, enzyme enhancement therapy (EET) using small molecules that function as pharmacological chaperones (PCs) offers an alternative therapeutic strategy for GD by salvaging endogenous GCase with deficient catalytic activity.[10,11] Unlike osmolytes, PCs are extrinsic small molecules that have specific yet higher binding affinity interactions to increase the cellular viability of mutant protein by stabilizing the native conformer.[12] Thus, PCs represent a novel class of drug therapy for

treatment of orphan diseases associated with protein misfolding, including phenylketonuria and cystic fibrosis.[4,13–15]

To date, PCs have largely consisted of active site inhibitors of GCase based on substrate mimics, notably natural and alkylated iminosugar analogs.[16,17,18] This has led to a counterintuitive principle that inhibitors enhance the activity of mutant enzymes by manipulating the ER folding environment.[10] This premise has guided computational and synthetic approaches for ligand design that target GCase over the past several years. To date, high-throughput screening (HTS) of chemical libraries rely on enzyme inhibition using fluorescence microarrays, where inhibitor potency and selectivity for GCase are key criteria for drug candidate selection.[17,19–22] However, primary screening by inhibition is biased towards the detection of ligands that influence the interaction of wild-type/folded GCase with a single fluorogenic substrate probe.[5,23] Moreover, not all inhibitors act as protein stabilizers as exemplified by false-positives that lack relevant chaperone activity due to ligand-induced enzyme destabilization.[24,25] For this reason, *in-vitro* thermal stability assays are required as a secondary screen to confirm chaperone activity of inhibitor candidates prior to cell-based assays to demonstrate increased enzyme activity and trafficking of mutant GCase variants in GD patient-derived fibroblasts.[26] However, orthosteric ligands may not be ideal PCs for EET since they attenuate catalytic conversion of GlcCer as highlighted by the lower apparent enhancement in GCase activity when cell lysates are not adequately prepared to wash out residual inhibitor.[27] Although selection of ligands with pH-selective binding properties that are used at sub-inhibitory concentration levels have been proposed to minimize adverse inhibitory effects, this has proven difficult to achieve for many PCs due to their poor cell permeability, bioavailability and/or metabolic stability.[28,29] Thus, there is a urgent need for alternative methods that accurately screen for chaperone activity as a way to reduce the high attrition rates of inhibitor candidates while discovering novel classes of PCs, such as allosteric ligands that stabilize the native enzyme without competing with substrate binding to the active site.[30]

Herein, a high throughput fluorescence assay based on restoration of enzyme activity upon denaturation (READ)[31] was introduced for functional screening of novel PC candidates for GCase. A two-tiered screening strategy was developed in order to directly measure chaperone activity of small molecules that enhance the catalytic activity of GCase under denaturing conditions. This functional screening method was applied on a chemical library after *in silico* screening for compounds with drug-like activity. Two stilbene derivatives namely, 4-(4-methoxystyryl)-2-methylthiazole (MSMT) and (*E*)-2,3-diphenylprop-2-en-1-ol (DPPL), were discovered to function as putative PCs based on their ability to activate, stabilize and promote the folding of GCase without unwanted inhibition. Structure-activity relationships were also explored by comparing the chaperone activity of several structural analogs of the two lead stilbene derivatives that increased enzyme activity by about 2.5-fold at 20 μM, which was superior to previously identified competitive or mixed-type inhibitors of GCase. Although our studies focus on characterization of ligand binding events that promote folding as a way to enhance the residual activity of GCase, this functional screen for PCs is envisioned to be applicable to other classes of enzymes associated with protein misfolding and orphan diseases.

4.3 Materials and Methods

4.3.1 Chemicals and Reagents

De-ionized water for buffer, stock solution and buffer preparations was obtained using a Barnstead EASYpure® II LF ultrapure water system (Dubuque, IA, USA). 4-methylumbelliferyl β-*D*-glucopyranoside (MUG, substrate of GCase) and 4-methylumbelliferone (MU, product of GCase) were purchased from Sigma-Aldrich (St. Louis, MO, USA). Citrate and phosphate were purchased from Sigma-Aldrich and used to prepare buffer solutions and 4-methylumbelliferyl-β-*D*-glucopyranoside (MUG) was used as the substrate in all enzymatic assays. Ambroxol hydrochloride (ABX), diltiazem hydrochloride (DTZ), 4-fluoro-*L*-phenylalanine hydrocholride (F-Phe), glycine (Gly), pyrimethamine (PYR), taurocholic acid (TC) were all purchased from Sigma-Aldrich,

whereas isofagomine (IFG) was obtained from Toronto Research Chemicals (North York, ON, Canada). Dimethyl sulfoxide (DMSO) was purchased from Caledon Laboratories Ltd. (Georgetown, ON, Canada), whereas Cerezyme/Imiglucerase (Genzyme Canada Inc., Mississauga, ON, Canada) was kindly provided by Dr. Michael Tropak and Dr. Don Mahuran at the Hospital for Sick Children (Toronto, ON, Canada). Cerezyme (Imiglucerase) is a recombinant modified human GCase (≈ 62 kDa) clinically approved for enzyme replacement therapy to type I GD patients, which differs from wild-type GCase by a single amino acid substitution (H495R), as well as glycosylation modifications at several amino acid residues.[32] Stock solutions of GCase were prepared in de-ionized water, aliquoted as 25 µL portions into 0.5 mL sterilized centrifuge tubes and stored at -80°C prior to use, whereas other stock reagents were prepared in DMSO and stored at +4°C. Note that only one freeze thaw cycle was permitted, and thus a new frozen aliquot was taken out and thawed in the fridge prior to daily use. Nunc®MicroWell 96 well optical bottom plates were obtained from Sigma-Aldrich.

4.3.2 Chemicals Library and Computational Screen

A customized chemical library containing six hundred structurally unique compounds was synthesized in-house and used as ligands for PC screening. One hundred compounds were selected from the library after *in silico* screening using ACD Labs PhysChem Suite 2012 software based on "Lipinski's rule of 5" comprising molecular/physicochemical parameters and their cut-off limits associated with drug-like properties,[33,34] including molecular weight (*MW* < 500 Da), octanol-water partition coefficient (*logP* < 5), hydrogen bond donors (*HBD* < 5), hydrogen bond acceptors (*HBA* < 10), rotational bonds (*RB* < 10) and total polar surface area (TPSA < 120 Å) as summarized in **Table S4.1**. Briefly, these parameters were used to select promising small molecules with adequate aqueous solubility and suitable functional groups to exploit non-covalent intermolecular interactions with protein while avoiding cytotoxicity. For instance, *logP, HBA* and *TPSA* are associated with the lipophilicity, total number of hydrogen bonding moieties and oral bioavailability of a compound, respectively.[35] All stock solutions for compounds in

chemical library were prepared in DMSO (10 mM), whereas enzyme reactions were performed with a final content of DMSO under 1% *v* in order to prevent GCase inactivation notably under native conditions without urea. In addition, screen-positive compounds identified in this work were re-synthesized *de novo* (experimental procedure stated in supplemental section) and their purity was characterized by ^{1}H-NMR and electron impact ionization-mass spectrometry (EI-MS) as shown for several lead compounds with chaperone activity for GCase in **Figure S4.1**.

4.3.3 Fluorescence-Based Screening Format

All fluorescence measurements were performed using a Tecan Infinite® 200 PRO NanoQuant Microplate Reader using Safire-XFLUOR4 (version 4.3) software. Fluorescence readings were conducted at room temperature using Nunc®MicroWell 96 clear bottom plates at gain value of 60, lag time of 0 s, integration time of 40 μs, 100 ms duration between flashes and move, shake duration of 4 s for efficient mixing of assay mixtures and bandwidth of 5 nm for excitation and emission wavelengths of 360 and 440 nm, respectively. Two complementary assays were used to measure ligand-induced stabilization effects and chaperone activity to screen a chemical library for putative PCs that enhance the residual activity of GCase under denaturing conditions. However, all compounds (20 μM) were first examined for auto-fluorescence and fluorescence quenching effects on the product MU (20 μM), in the absence of enzyme/urea to avoid false discoveries. Ten compounds due to fluorescence quenching on MU were rejected from the library prior to the two-tiered strategy for high quality screening of PCs. In addition, several control compounds previous identified with known inhibitory and/or chaperone activity for GCase were also included in the screen. All fluorescence assays were performed in duplicate and tentative hits were then confirmed with newly synthesized compounds and/or their analogs for further validation in triplicate. The reproducibility of the fluorescence assay when performing triplicate analyses of compounds over three days was found to be acceptable based on a coefficient of variance *(CV)* under 10% (n = 9).

4.3.4 Stabilization Assay for Primary Screening of PCs

Duplicate measurements were performed for each drug or control (*e.g.,* ligand-free *apo*-enzyme, GCase inhibitor, ligand from chemical library etc.) under native (0 M urea) or denaturing conditions (4.0 M urea) using a fluorescence microarray system. Enzyme reactions were performed in McIlvaine buffer consisting of 0.100 M citrate, 0.200 M phosphate, pH 7.2 with 10 mM taurocholate (TC) using recombinant GCase (10 nM). GCase and TC in McIlvaine buffer were first equilibrated at 25°C for 30 min. The reaction mixture was then pre-equilibrated with 20 μM of each ligand derived from a chemical library for 10 min. In all cases, the final DMSO content of reaction mixture did not exceed 1% *v* in order to avoid enzyme denaturation under native conditions (0 M urea). Then, the mixture was incubated for 10 min with urea (4.0 M) in order to perturb the native conformational state of the enzyme resulting in lower catalytic activity due to protein unfolding. Finally, the enzyme reaction was initiated by addition of MUG as a fluorogenic substrate using a total volume of 100 μL. The final concentrations of GCase, TC, urea and MUG in the reaction solution were 10 nM, 10 mM, 0 or 4.0 M and 2 mM, respectively. An aliquot (50 μL) was withdrawn from the bulk reaction mixture after 3 hr and placed in a fluorescence 96-microplate well containing 50 μL of quenching solution containing 0.200 M glycine, pH 12, where the final pH of solution was 10.2. These solutions were mixed effectively in a 96-microplate well using "shake" function from Safire software prior to fluorescence measurements. Preliminary enzyme kinetic studies were performed to measure optimum urea conditions (4.0 M) and pre-equilibration time (3 hr) with *apo-GCase* without ligand. Further studies demonstrated that urea did not quench fluorescence responses, whereas fluorescence signal was maximized at pH 10.2 due to the full ionization of MU (pK_a of 7.8).[36] The assay was also validated using previously reported PC candidates for GCase derived from inhibition and/or thermal stability assays, including ambroxol (ABX), diltiazem (DTZ), and isofagomine (IFG) prior to screening of ninety small molecules from a chemical library with drug-like properties (after exclusion of fluorescence quenchers) as summarized in **Table S4.1**. DTZ and ABX are previously approved FDA-approved drugs recently identified as mixed-type

inhibitors of GCase with similar potency (IC_{50} ≈ 50-60 μM at pH 7.2), whereas IFG is a competitive inhibitor with nanomolar potency that has a 10-fold higher binding affinity at neutral pH as compared acidic conditions.[36]

4.3.5 Refolding Assay for Second-tiered Testing of Chaperone Activity of PCs

Molecular chaperones are endogenous proteins that aid in protein refolding in the cell. In this context, we developed a complementary assay that is suitable for assessing the chaperone activity of small molecules that mimics the folding status of mutant GCase associated with GD. The reversibility of GCase folding was assessed by measuring its normalized catalytic activity when incubating in 4 M urea at 1 hr relative to 0.5 M urea (folded/active state) after its dilution to 0.5 M urea to trigger refolding of enzyme that was performed in the presence or absence of ligand. The buffer conditions used for protein refolding were similar to the stabilization assay used in primary screening, where GCase and TC in McIlvaine buffer were first pre-equilibrated at 25°C for 30 min and the reaction mixture was subsequently incubated for 1 hr with 4.0 M urea. The reaction mixture was then diluted to 0.5 M urea with or without ligand (20 μM unless otherwise stated) and the reaction was subsequently initiated by addition of substrate, MUG (2 mM). An aliquot (50 μL) was withdrawn from the bulk reaction mixture after a 3 hr incubation period and placed in a fluorescence 96-microplate well containing 50 μL of quenching solution. In all cases, the final concentration of GCase was 20 nM with enzyme kinetic studies performed under standardized conditions.

4.4 Results and Discussion

4.4.1 Optimization of Stabilization Assay for Primary Screening of PCs

To date, HTS of putative PC candidates for GCase has relied on *in-vitro* fluorescence-based inhibition and/or thermal stability assays followed by confirmatory testing using patient-derived cell lines.[37] Inhibition assay only focuses on the selection of potent active site competitive inhibitor using folded/native GCase that does not accurately reflect

chaperone activity for mutant enzymes. Similarly, thermal stabilization assays that evaluate the impact of ligand binding to GCase are limited to relative measurements of melting temperatures that often lead to irreversible protein aggregation and precipitation.[38,13]As a result, we recently introduced restoration of enzyme activity upon denaturation (READ) as an alternative method for functional screening of PCs for GCase when using capillary electrophoresis (CE) with UV detection.[31] Urea serves as convenient perturbant to modulate the equilibrium distribution of protein conformers while solubilizing unfolded GCase unlike thermal denaturation. Herein, we introduce a novel two-tiered fluorescence-based HTS strategy for high quality screening of PCs based on their capacity to enhance the activity of GCase under denaturing conditions. A stabilization assay (**Fig 4.2a**) was first used as a primary screen to identify novel compounds with drug-like activity from a chemical library that activate and/or stabilize GCase without inhibition. Assay conditions were first optimized when using a fluorescence 96-well plate format, including GCase concentration, pre-equilibration time, urea concentration and DMSO content. Unlike the previous CE-based assay, fluorescence takes advantage of lower enzyme concentrations (10 nM versus 15 μM) with shorter incubation times (3hr versus 6 hr) due to its higher sensitivity that also improves sample throughput when using a 96-well plate format. Our previous work demonstrated that GCase retained approximately 5% residual activity when incubated in 4.0 M for 10 mins. Herein, two different urea conditions (*i.e.,* folded/active, 0M and unfolded/inactive, 4.0 M) were used to evaluate the activation and stabilization effects of ligand binding while excluding compounds with undesirable inhibition. In addition, the primary screen also included suitable positive/negative controls and reference compounds to validate the performance of the assay. **Figure 4.1** outlines the key steps for selecting potential PCs for GCase from a library containing six hundred novel small molecules. A large fraction of primary ligand "hits" often fail at later stages of clinical trials due to cytotoxicity that is often contributed by highly water-insoluble compounds.[39] For instance, it was previously shown that fluphenazine (FlZ) functions as a strong stabilizer of GCase based on thermal denaturation assay; however, it failed to enhance mutant GCase activity in the final cell-

based assay due to poor solubility. [40] Therefore, an *in silico* filter based on Lipinski's rule of five (*MW* < 500 Da , *log P* < 5, *HBD* < 5, *HBA* < 10 and *TPSA* < 120 Å) was used to select one hundred compounds drug-like properties from a chemical library comprising six hundred unique stilbene derivatives as summarized in **Table S4.1**.[41,42] Auto-fluorescence and quenching effects of these compounds were then examined resulting in the exclusion of ten compounds due to significant quenching on MU fluorescence at 440 nm (data not shown). Next, ligand-induced activation/inhibition and stabilization effects on GCase for the remaining ninety compounds were then performed under 4.0 M and 0M urea conditions, respectively. Putative PCs that enhanced the residual activity in 4 M urea over 10% at 20 μM (*i.e.,*> 2-fold greater than ligand-free *apo*-GCase that retains only 5% residual activity) with negligible inhibition (< 10 %) in 0 M urea defined as significant "hits". Eight compounds (**Figure 4.2**) were identified as putative PCs for GCase. They were re-synthesized and repeatedly screened at three different dosage levels (0.2, 2.0 and 20 μM) using stabilization assay (4.0 M urea) and at two different dosage levels (2 and 20 μM) using conventional inhibition assay (0 M urea) as shown in **Figure 4.2b and c**. Indeed, these compounds showed negligible inhibitory activity (< 5% inhibition at 20 μM) and only in some cases modest activation properties (>10 % at 20 μM) as shown in **Figure 4.2b**. To the best of our knowledge, this is the first study that has identified moderate activators that significantly enhance GCase activity at low micromolar levels without inhibition.

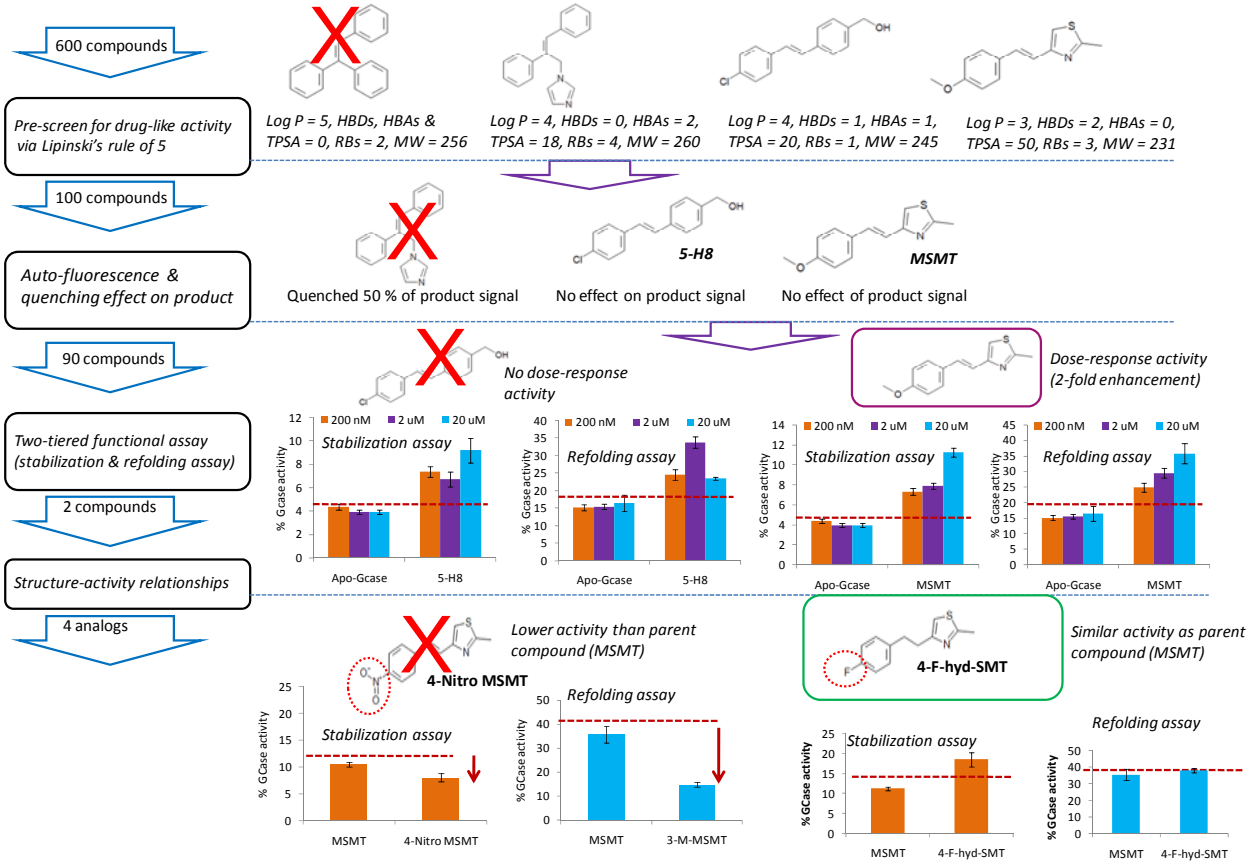

Figure 4.1 Outline of high quality screening approach for identification of novel PCs for GCase from a chemical library. One hundred drug-like compounds were selected via in silico screen based on Lipinski's rule of five. Subsequently, auto-fluorescence and quenching effects on product were monitored. After that, a "two-tiered" functional assay approach was used to select potential PCs for GCase and the compounds that induced an enhancement in GCase activity above the threshold value with a dose-response dependence were selected as hits. Structure-activity relationships were also explored for two stilebene derivatives. Cell -based assays are needed for confirmatory testing of the efficacy of putative PC candidates that do not inhibit GCase activity.

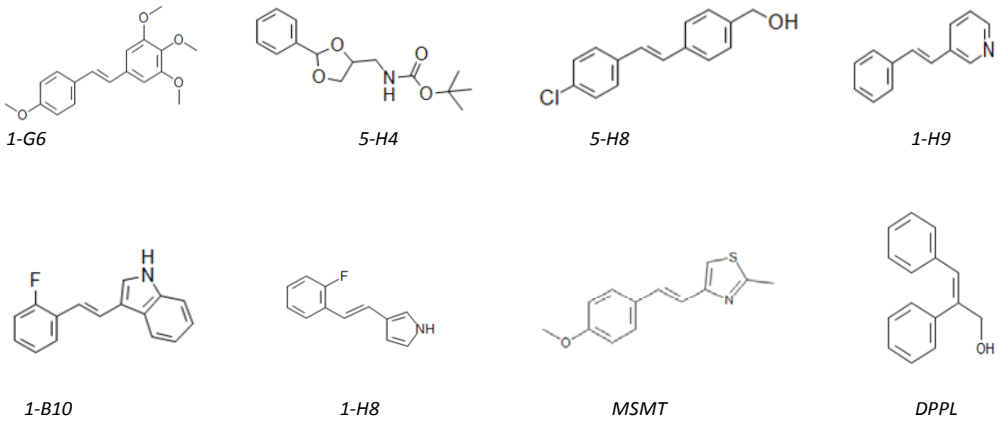

Figure 4.2. Putative PC candidates identified from a chemical library of unique stilbene derivatives with that stabilize and enhance the activity of GCase under denaturing conditions without inhibition

Ligand-free *apo*-GCase was found to retain only (5 ± 0.5) % residual activity under 4 M urea conditions, which is about 2-fold lower residual activity as compared to clinically relevant mutant, L444P (~ 10 %).[43] Overall, eight specific compounds from the chemical library were found to significantly enhance GCase activity by over 2 to 3-fold after primary screening, including 1-G6, 1-H9, 1-H8 and DPPL, as well as 1-B10, MSMT, 5-H4 and 5-H8 as shown in **Figure 4.2c**. It was previously reported that even modest enhancement in protein trafficking and enzymatic activity by PCs may be sufficient to attenuate early onset and severe clinical phenotypes of (type 2/3) GD.[13]In addition, dose-response studies are required to deduce the optimum therapeutic window required to enhance the residual activity of mutant GCase without significant cytotoxicity.[29] For instance, three compounds,1-G6, DPPL and MSMT exhibited a distinctive dose-response relationship as reflected by a steady enhancement to GCase residual activity at higher doses, whereas others showed inconsistent or ambiguous dose trends with GCase under denaturing conditions as shown in **Figure 4.2c**. For instance, compound 1-B10 showed a lower enhancement in GCase activity at higher dosage levels that may be caused by deleterious ligand interactions that result in protein aggregation.

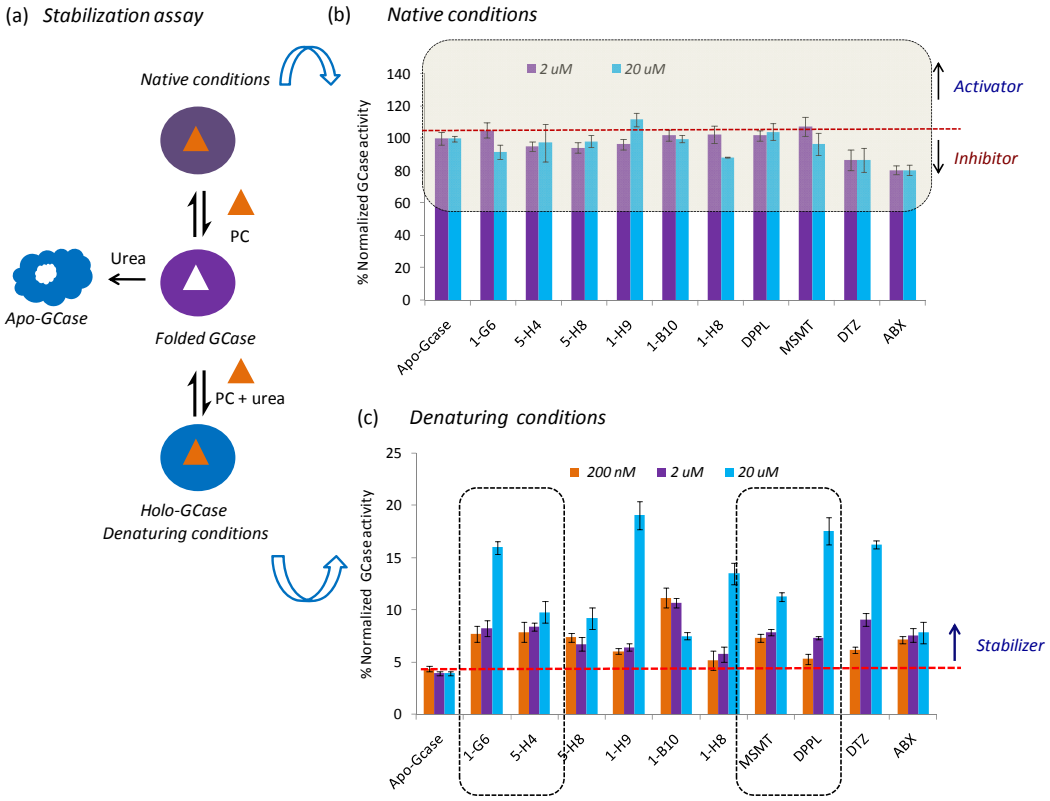

Figure 4.2 Bar graphs illustrate changes in GCase activity under denaturating and native conditions as a function of ligand type and dosage. (a) Scheme shows experimental outline of inhibition and stabilization assays when using a fluorescence microarray, where *apo* and *holo-GCase* represent ligand-free and ligand-associated enzyme complex, respectively. The inhibition assay measures GCase activity without urea under native conditions. (b) Bar graph illustrates activity of GCaseat two dosage levels (2.0 and 20 μM) under native conditions in 0 M urea.(c) Bar graph indicates the residual activity for GCase as modulated by ligand binding at three dosage levels (0.2, 2.0 and 20 μM) under denaturing conditions in 4 M urea.*Apo*-GCase retains only about 5% of its residual catalytic activity, which sets a minimum threshold value for compound selection, where error bars representing σ ± 1 (n = 3). Compounds (circled with dotted line), 1-G6, 5-H4, MSMT and DPPL showed dose-response dependent activity based on stabilization assay.

Similarly, compounds (eighty two) that did not show an enhancement to GCase activity even at maximum dosage levels (20 μM) were excluded from further testing due to concerns regarding their potential toxic effects that often contributes to false discoveries in later stages of drug discovery.[44] For instance, a recent study reported that two amino-*myo*-inositol derivatives showed GCase activity enhancement in GD patient-derived lymphoblasts expressing N370S and L444P mutants at low nanomolar levels, however inverse and/or no dose-response activity was observed at increasing concentration

levels.[45] In addition, ABX was reported to function as weak mixed-type inhibitor of GCase with favorable pH dependent binding and showed dose-response activity with 2-fold enhancement in type 1 GD (N370S) patient derived lymphoblasts.[40] Despite previous promising results of ABX, a recent pilot clinical study showed that no significant improvement in clinical outcomes under dose regime (150 mg of ABX per day).[46] Indeed, our *in-vitro* stabilization assay showed that ABX has no definitive dose response for enhancing GCase activity. In contrast, DTZ (calcium channel blocker) was not previously considered as a hit due to a 10-fold lower potency than ABX[40]; however in this work, DTZ elicited a distinct enhancement to GCase activity at higher doses based on stabilization assay.

In addition, two compounds, pyrimethamine (PYR) and 4-fluoro-*L*-phenylalanine (F-Phe) were included as negative controls in order to evaluate drug specificity during primary screening. For example, PYR is anantimalarial drug that was reported to function as a PC for the lysosomal enzyme β-hexosaminidase that is associated with Tay-Sachs disease,[45]whereas F-Phe is a weak competitive inhibitor of phenylalanine hydroxylase relevant to phenylketonuria.[47,48] As expected, PYR did not attenuate or enhance the activity of GCase under folded/denatured conditions. In contrast, F-Phe inhibited GCase activity by about (15 ± 2) % at 20 μM under native conditions. In this case, no gain in enzyme activity was measured by F-Phe association since any stabilization of GCase is offset by inhibition.

4.4.2 Refolding Assay for Confirmatory Testing of Chaperone Activity for GCase

The eight lead compounds identified as putative PCs after primary screening (**Figure 4.2)** were then further tested using a complementary assay that directly measures the chaperone activity of ligands upon GCase refolding. For instance, the primary screen is used to evaluate the potency of a ligand to stabilize low equilibrium fractions of the folded GCase state that exist under denaturing conditions (4.0 M) to boost enzyme activity, whereas the secondary screen serves as complimentary assay to assess the

potency of a ligand to assist the folding of denatured GCase into an catalytically active conformer upon dilution of chemical denaturant. Gains in residual GCase catalytic activity upon refolding was determined by measuring its normalized catalytic activity when incubating in 4.0 M urea at 1 hr relative to 0.5 M urea (folded/active state) after its dilution to 0.5 M urea as a function of ligand type/dose. Subsequently, the reaction was initiated by substrate addition, (MUG) followed by a 3 hr incubation period prior to fluorescence measurements as shown in **Figure 4.3a.** Noteworthy, urea is used as a chemical denaturant since it effectively solubilizes unfolded protein conformers, thereby allowing for partial recovery of ligand-free *apo*-GCase activity of approximately (15 ± 2) % activity as shown in **Figure 4.3b**. Furthermore, allosteric drugs are increasingly used due to fewer side effects due to their greater specificity in binding while avoiding substrate competition for active site of target enzyme.[49] In our case, three non-inhibiting compounds were found to exhibit promising chaperone activity as reflected by up to a 2.5-fold enhancement in GCase activity (20 μM) with a characteristic dose-response relationship (**Figure 4.3b**). In fact, these three lead compounds were found to display better dose-response increases to GCase activity than previously identified PCs, including IFG, ABX and DTZ. For instance, IFG is a potent competitive inhibitor of GCase, which was found to completely inhibit the residual enzyme activity at 0.20 μM under denaturant conditions (data not shown). Although IFG is safe for adult type 1 GD patients during phase II clinical trials, preliminary results indicate that the dose regimes tested did not significantly reduce GlcCer accumulation nor improve clinical symptoms of the majority of patients.[50,51] These findings likely stem from the poor bioavailability of IFG coupled with non-optimized washout periods required for balancing the stabilizing versus inhibitory mechanisms of active site inhibitors as putative enzyme enhancers. In addition, two distinct non-carbohydrate compounds, DTZ and ABX recently identified as PCs from a FDA-approved drug library, function as weak mixed-type inhibitors of GCase.[40] The latter PC is an anti-mucolytic agent used for treatment of respiratory diseases that was shown to enhance the activity and protein concentration levels of mutant GCase in GD patient- derived cell cultures.[52]

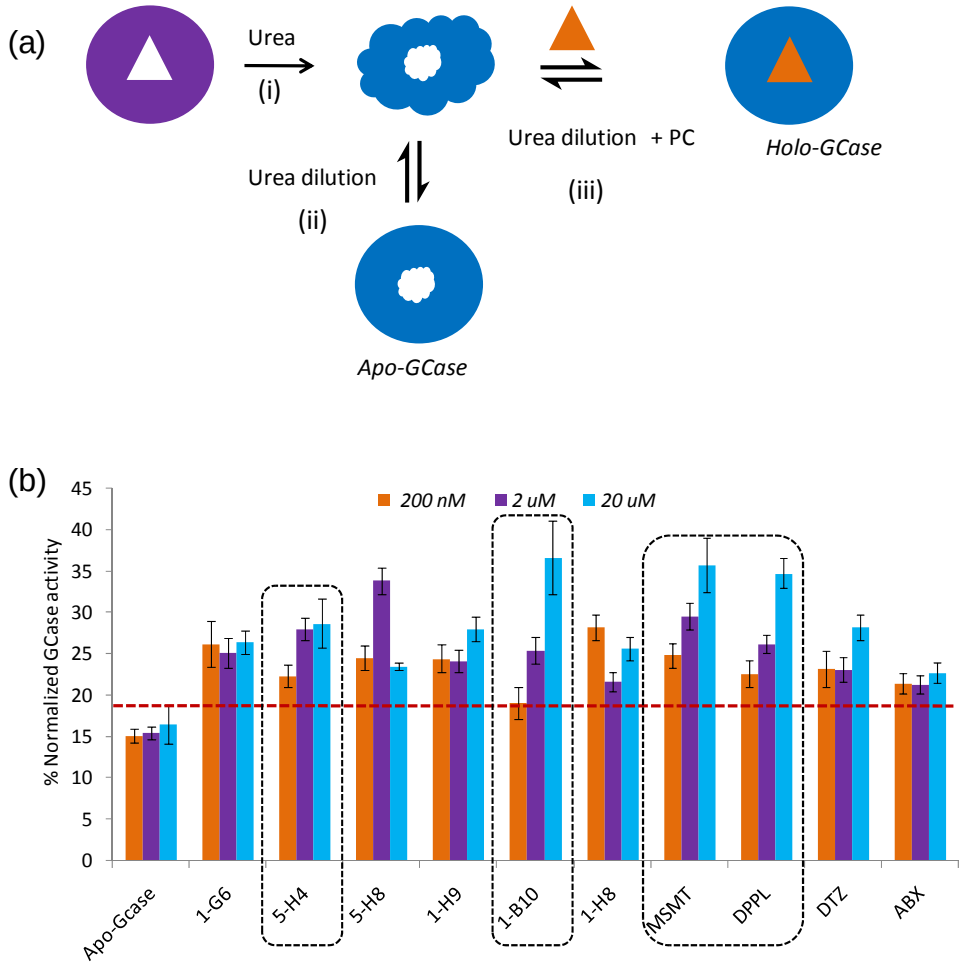

Figure 4.3 A scheme illustrating the experimental procedure of refolding assay and the potential PCs of GCase based on refolding assay. (a) Refolding assay outlines: (i) GCase incubated in 4M urea for an hour subsequently diluted urea concentration to 0.5M urea (ii) with the absence and (iii) presence of PCs prior to initiation of reaction with substrate. (b) Bar graph demonstrates percent refolding activity of *holo-GCase* at three dosage levels. *Apo-GCase* restores (15 ± 2) % of residual activity which sets as a threshold value, where error represent σ ± 1 (n = 3). Compounds (circled in dotted line), MSMT, DPPL, 1-B10 and 5-H4 showed a distinctive dose-responsive chaperone activity

Unlike IFG, ABX was shown to impart only a marginal increase in the activity of GCase in both screens without a distinct dose-response relationship as shown in **Figure 4.2 and 4.3**. Although DTZ and ABX are both mixed-type inhibitors with similar potency (IC_{50} ≈ 50-60 μM at pH 7.2), DTZ possesses greater chaperone activity relative to ABX. However, higher dosage levels of ABX may elicit significant activity enhancement in denatured GCase (**Figure 4.3b**).[36] Indeed, a recent pilot study was conducted to assess the

tolerability and efficacy of ABX as a PC for adult type 1 GD patients have demonstrated no adverse health effects, but no significant improvement in clinical outcomes were observed under the dose regime examined, such as platelet count, hemoglobin level, spleen and liver volume.[52] As a result of this major disconnect between drug discovery and clinical translation efficacy, there is growing interest in the development of alternative screening methods to identify novel PCs for oral treatment of GD. To the best of our knowledge, this is the first study demonstrating that two stilbene derivatives (MSMT and DPPL) can activate, stabilize and assist in the refolding of denatured GCase while boosting GCase activity by up to 2.5-fold without unwanted inhibition.

4.4.3 Structure-activity Relationships of Lead PC Candidates for GCase

Several structural analogs of two promising stilbene derivatives were synthesized to explore structure-activity relationships when using the two-tiered screening assay for PCs. Structural modifications of MSMT include addition of a methoxy group (3-methoxy-MSMT), replacement of methoxy group with flourine (F-SMT) and hydrogenation of the alkene bond (Hyd-MSMT), whereas structural modifications of DPPL are conversion of alcohol to either carboxylic acid (DPPA) or methyl ester (MDPA) and addition of chlorine (Cl-DPPL and Cl-MDPA) moieties as shown in **Figure 4.4**. Similar to parent compounds (MSMT and DPPL), all structural analogs were found not to exhibit inhibition for GCase at 20 μM under native conditions without urea (data not shown). Although stilbene is a distinctive chemical motifs of compounds in the library, hydrogenation of alkene bond (Hyd-MSMT) had no impact on GCase activity implying that stereochemistry of double bond is not critical to ligand binding/ chaperone activity. Furthermore, meta-methoxylation (3-Methoxy-MSMT), hydrogenation of MSMT and/or fluorination of SMT (F-SMT) and conversion of alcohol group in DPPL to methyl ester (MDPA) and para-chlorination also had no significant impact on GCase activity (data not shown). In contrast, para chlorination, nitration of MSMT and conversion of alcohol group in DPPT to carboxylic acid had induced a small decrease in residual GCase activity as the same dosage as parent compounds.

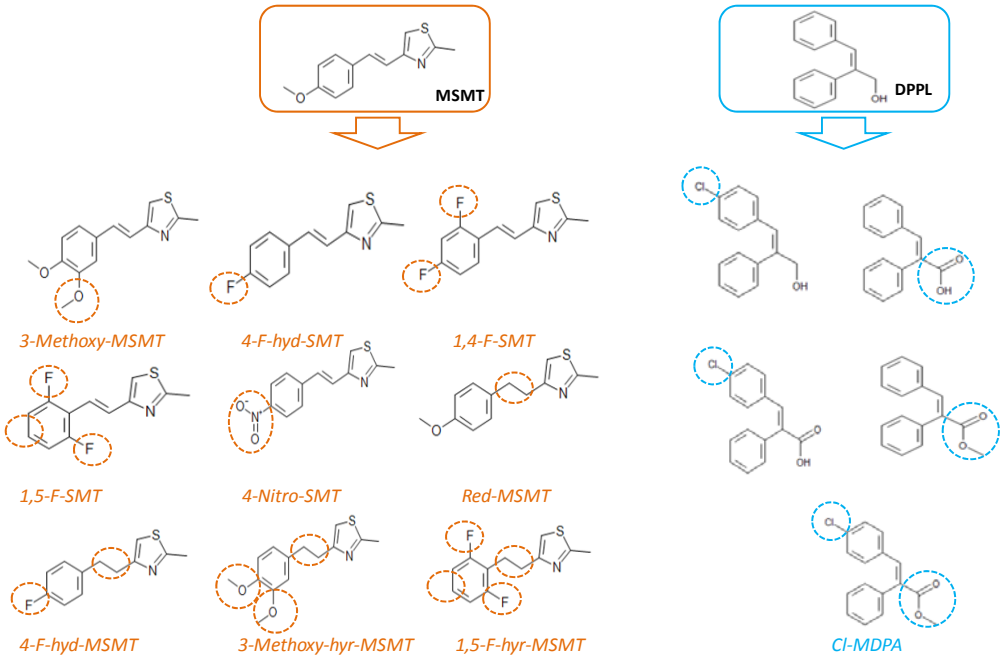

Figure 4.4. Chemical structures of two screen-positive parent compounds (MSMT and DPPL) and several structural analogs used for assessing structure-activity relationships of ligand binding to GCase. Specific structural modifications are highlighted for the two putative PCs that elicited a dose-responsive enhancement to GCase activity without inhibition after screening a chemical library with drug-like activity.

All chemical modifications of the basic stilbene structure did not generate significant changes in chaperone activity for GCase, these analogs may exhibit better bioavailability characteristics during confirmatory testing in GD patient cell lines. Cell-based assays using skin fibroblasts from individuals GD type I contain approximately 10 - 25 % residual activity (critical threshold 25- 30 %).[36] Overall, MSMT, three structural analogs (Red-MSMT, 3-Methoxy-MSMT, F-hyd-SMT), DPPL and an analog (Cl-DPPL) were able to enhance residual GCase activity between 28-32% *in-vitro* that is above the critical threshold associated with clinical symptoms in affected GD patients.[36] However, these putative PCs require further testing in cell-based and animal models of GD to confirm their overall safety and therapeutic efficacy.

4.5 Conclusions

In summary, a two-tiered fluorescence-based HTS strategy was introduced for the identification of novel PCs for GCase based on the capacity of a ligand to stabilize, refold and enhance enzyme activity under denaturing conditions. This functional screening approach was then applied to a chemical library after *in-silico* screening for drug-like activity while excluding compounds exhibiting fluorescence quenching. Eight stilbene derivatives out of eighty-two compounds were found to significantly enhance the residual activity of GCase up to 2.5-fold at 20 μM under denaturating conditions in urea without unwanted inhibition. Subsequently, these eight compounds were re-synthesized and repeatedly screened in a dose-responsive manner followed by secondary screening using a complementary dynamic refolding assay. Overall, two stilbene derivatives and four structural analogs were identified as lead compounds with putative chaperone activity. Noteworthy, these compounds were found to promote a greater enhancement in GCase activity in comparison to recently identified PCs that function as conventional competitive or mixed-type inhibitors. Additionally, these promising PC candidates enhanced greater than 30 % residual activity of GCase *in -vitro* that represents a critical threshold for clinical symptoms to be observed in affected GD patients. Future work is needed to further characterize the safety and efficacy of these putative PCs when incubated with different GCase mutants expressed in GD patient-derived cell cultures. In addition, the exact binding region of lead compounds to GCase remains to be fully elucidated. We anticipate that this two-tiered screening strategy will enable the identification of new classes of PCs that is applicable to other protein misfolding diseases, such as phenylketonuria.

4.6 Acknowledgements

Financial support was provided by the Natural Science and Engineering Council of Canada (NSERC). The authors wish to thank Dr. Michael Tropak and Dr. Don Mahuran from the Hospital for Sick Children for their generous donation of Cerezyme/Imiglucerase.

4.7 References

1. P. J. Meikle, J. J. Hopwood, A. E. Clague, and W. F. Carey, *J. Am. Med. Assoc.*, 1999, **281**, 249–254.

2. M. Fuller, *Lipids Health Dis.*, 2010, **9**, 113.

3. B. Meusser, C. Hirsch, E. Jarosch, and T. Sommer, *Nat. Cell Biol.*, 2005, **7**, 766–772.

4. Y. J. Wang, X. J. Di, and T. W. Mu, *Pharmacol. Res.*, 2014, **83**, 3–9.

5. E. Goldin, W. Zheng, O. Motabar, N. Southall, J. H. Choi, J. Marugan, C. P. Austin, and E. Sidransky, *PLoS One*, 2012, **7**, e29861–e29861.

6. H. Dvir, M. Harel, A. A. McCarthy, L. Toker, I. Silman, A. H. Futerman, and J. L. Sussman, *EMBO Rep.*, 2003, **4**, 704–709.

7. A. R. Sawkar, S. L. Adamski-Werner, W. C. Cheng, C. H. Wong, E. Beutler, K. P. Zimmer, and J. W. Kelly, *Chem. Biol.*, 2005, **12**, 1235–1244.

8. A. R. Sawkar, S. L. Adamski-Werner, W.-C. Cheng, C.-H. Wong, E. Beutler, K.-P. Zimmer, and J. W. Kelly, *Chem. Biol.*, 2005, **12**, 1235–44.

9. A. Zimran, *Blood*, 2011, **118**, 1463–1471.

10. J. Q. Fan, *Trends Pharmacol. Sci.*, 2003, **24**, 355–360.

11. B. Brumshtein, H. M. Greenblatt, T. D. Butters, Y. Shaaltiel, D. Aviezer, I. Silman, A. H. Futerman, and J. L. Sussman, *J. Biol. Chem.*, 2007, **282**, 29052–8.

12. T. Arakawa, D. Ejima, Y. Kita, and K. Tsumoto, *Biochim. Biophys. Acta - Proteins Proteomics*, 2006, **1764**, 1677–1687.

13. R. E. Boyd, G. Lee, P. Rybczynski, E. R. Benjamin, R. Khanna, B. a Wustman, and K. J. Valenzano, *J. Med. Chem.*, 2013, **56**, 2705–25.

14. N. F. Brás, N. M. Cerqueira, M. J. Ramos, and P. a Fernandes, *Expert Opin. Ther. Pat.*, 2014, **24**, 857–74.

15. T. K. Chaudhuri and S. Paul, *Febs J.*, 2006, **273**, 1331–49.

16. A. R. Sawkar, W. C. Cheng, E. Beutler, C. H. Wong, W. E. Balch, and J. W. Kelly, *Proc. Natl. Acad. Sci. U. S. A.*, 2002, **99**, 15428–15433.

17. T. Hill, M. B. Tropak, D. Mahuran, and S. G. Withers, *Chembiochem*, 2011, **12**, 2151–2154.

18. G. Schitter, A. J. Steiner, G. Pototschnig, E. Scheucher, M. Thonhofer, C. A. Tarling, S. G. Withers, K. Fantur, E. Paschke, D. J. Mahuran, B. A. Rigat, M. B. Tropak, C. Illaszewicz, R. Saf, A. E. Stütz, and T. M. Wrodnigg, *ChemBioChem*, 2010, **11**, 2026–2033.

19. R. L. Lieberman, J. A. D'Aquino, D. Ringe, and G. A. Petsko, *Biochemistry*, 2009, **48**, 4816–4827.

20. M. R. Landon, R. L. Lieberman, Q. Q. Hoang, S. Ju, J. M. M. Caaveiro, S. D. Orwig, D. Kozakov, R. Brenke, G.-Y. Chuang, D. Beglov, S. Vajda, G. a Petsko, and D. Ringe, *J. Comput. Aided. Mol. Des.*, 2009, **23**, 491–500.

21. P. Alfonso, V. Andreu, A. Pino-Angeles, A. a Moya-García, M. I. García-Moreno, J. C. Rodríguez-Rey, F. Sánchez-Jiménez, M. Pocoví, C. Ortiz Mellet, J. M. García Fernández, and P. Giraldo, *Chembiochem*, 2013, **14**, 943–9.

22. J. Castilla, D. Cruz, K. Higaki, E. Nanba, K. Ohno, Y. Suzuki, D. Yolanda, C. O. Mellet, and J. M. Garc, *J. Med. Chem.*, 2012, **55**, 6857–6865.

23. W. Zheng, J. Padia, D. J. Urban, A. Jadhav, O. Goker-Alpan, A. Simeonov, E. Goldin, D. Auld, M. E. LaMarca, J. Inglese, C. P. Austin, and E. Sidransky, *Proc. Natl. Acad. Sci. U. S. A.*, 2007, **104**, 13192–7.

24. B. Rigat and D. Mahuran, *Mol. Genet. Metab.*, 2009, **96**, 225–232.

25. A. Zimran, G. Altarescu, and D. Elstein, *Blood Cells. Mol. Dis.*, 2013, **50**, 134–7.

26. A. R. Sawkar, M. Schmitz, K. P. Zimmer, D. Reczek, T. Edmunds, W. E. Balch, and J. W. Kelly, *Acs Chem. Biol.*, 2006, **1**, 235–251.

27. Y. Sun, B. Liou, Y.-H. Xu, B. Quinn, W. Zhang, R. Hamler, K. D. R. Setchell, and G. a Grabowski, *J. Biol. Chem.*, 2012, **287**, 4275–87.

28. W. Zheng, J. Padia, D. J. Urban, A. Jadhav, O. Goker-Alpan, A. Simeonov, E. Goldin, D. Auld, M. E. LaMarca, J. Inglese, C. P. Austin, and E. Sidransky, *Proc. Natl. Acad. Sci. U. S. A.*, 2007, **104**, 13192–7.

29. G. H. B. Maegawa, M. B. Tropak, J. D. Buttner, B. A. Rigat, M. Fuller, D. Pandit, L. I. Tang, G. J. Kornhaber, Y. Hamuro, J. T. R. Clarke, and D. J. Mahuran, *J. Biol. Chem.*, 2009, **284**, 23502–23516.

30. J. M. Benito, J. M. García Fernández, and C. Ortiz Mellet, *Expert Opin. Ther. Pat.*, 2011, **21**, 885–903.

31. M. Shanmuganathan and P. Britz-Mckibbin, *Biochemistry*, 2012, **51**, 7651–7653.

32. B. Brumshtein, M. R. Wormald, I. Silman, A. H. Futerman, and J. L. Sussman, *Acta Crystallogr. D. Biol. Crystallogr.*, 2006, **62**, 1458–65.

33. C. A. Lipinski, *J. Pharmacol. Toxicol. Methods*, 2001, **44**, 235–249.

34. I. Muegge, *Med. Res. Rev.*, 2003, **23**, 302–21.

35. R. E. White, *Annu. Rev. Pharmacol. Toxicol.*, 2015, **40**, 133–157.

36. M. Shanmuganathan and P. Britz-McKibbin, *Anal. Bioanal. Chem.*, 2011, **399**, 2843–2853.

37. M. Aguilar-Moncayo, M. I. Garcia-Moreno, A. Trapero, M. Egido-Gabas, A. Llebaria, J. M. G. Fernandez, and C. O. Mellet, *Org. Biomol. Chem.*, 2011, **9**, 3698–3713.

38. R. L. Lieberman, J. A. D'Aquino, D. Ringe, and G. A. Petsko, *Biochemistry*, 2009, **48**, 4816–4827.

39. J. Harskamp, P. Britz-McKibbin, and J. Y. Wilson, *Anal. Chem.*, 2012, **84**, 862–866.

40. G. H. B. Maegawa, M. B. Tropak, J. D. Buttner, B. A. Rigat, M. Fuller, D. Pandit, L. I. Tang, G. J. Kornhaber, Y. Hamuro, J. T. R. Clarke, and D. J. Mahuran, *J. Biol. Chem.*, 2009, **284**, 23502–23516.

41. G. Horne, F. X. Wilson, J. Tinsley, D. H. Williams, and R. Storer, *Drug Discov. Today*, 2011, **16**, 107–18.

42. R. E. White, *Annu. Rev. Pharmacol. Toxicol.*, 2000, **40**, 133–157.

43. A. R. Sawkar, W. D'Haeze, and J. W. Kelly, *Cell. Mol. Life Sci.*, 2006, **63**, 1179–1192.

44. Z. Luan, K. Higaki, M. Aguilar-Moncayo, H. Ninomiya, K. Ohno, M. I. García-Moreno, C. O. Mellet, J. M. García Fernández, and Y. Suzuki, *ChemBioChem*, 2009, **10**, 2780–2792.

45. A. Trapero, P. González-Bulnes, T. D. Butters, and A. Llebaria, *J. Med. Chem.*, 2012, **55**, 4479–4488.

46. A. Zimran, G. Altarescu, and D. Elstein, *Blood Cells, Mol. Dis.*, 2013, **50**, 134–137.

47. G. H. B. Maegawa, M. Tropak, J. Buttner, T. Stockley, F. Kok, J. T. R. Clarke, and D. J. Mahuran, *J. Inherit. Metab. Dis.*, 2007, **30**, 123.

48. L. Ryan and J. A. Elliott, *Arch. Biochem. Biophys.*, 1968, **125**, 797–801.

49. R. Nussinov, C. J. Tsai, and P. Csermely, *Trends Pharmacol. Sci.*, 2011, **32**, 686–693.

50. D. Elstein, *Curr. Pharm. Biotechnol.*, 2011, **12**, 854–860.

51. D. Elstein, *Curr Pharm Biotechnol*, 2011, **12**, 854–860.

52. A. Zimran, G. Altarescu, and D. Elstein, *Blood Cells. Mol. Dis.*, 2013, **50**, 134–7.

4.8 Supplemental Section

4.8.1 Experimental Procedure of Screen-positive Compounds

Reactions were carried out under air or dry argon in oven-dried glassware unless otherwise stated. All fine chemicals were obtained from Aldrich.

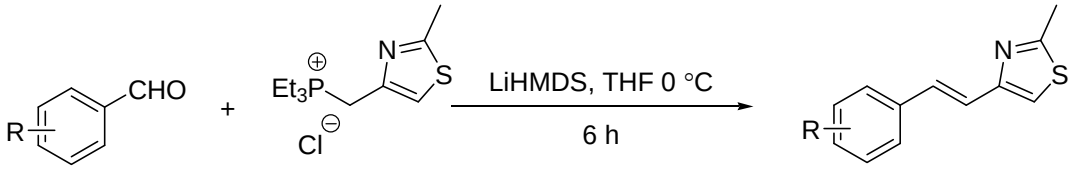

The thiazole-phosphonium salt (1 mmol) was placed in a flame-dried round-bottomed flask and THF (1 mL) added. The mixture was cooled to 0 °C prior to addition of LiHMDS (1*M* in THF, 1 mL). After stirring for 1 h at that temperature the corresponding aldehyde (0.5 mmol) was added dropwise as a neat liquid. The ice-bath was removed and the reaction mixture stirred for a further 6 h at which point TLC showed complete consumption of the starting aldehyde. A saturated aqueous solution of ammonium chloride (5 mL) was added and the mixture extracted with diethyl ether (3 x 5 mL). The combined organic extracts were dried over anhydrous $MgSO_4$ and concentrated under reduced pressure. The crude mixture was then column chromatographed over silica gel to afford the title compound.

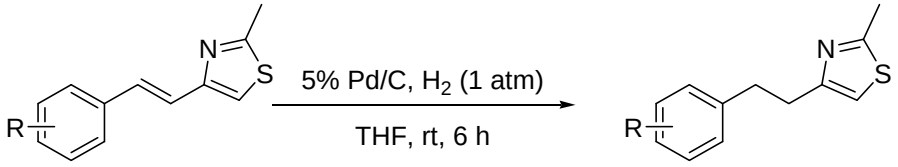

To stilbene **1a-d** (0.1 mmol)was added absolute EtOH (2 mL) and Pd/C (5% w/w, 1.1 mg, 0.01 mmol). The reaction vessel was purged with $H_{2\ (g)}$ and stirred under such an atmosphere for 6 h. Subsequent filtration of the suspension and removal of solvent afforded the reduced compound. No further purification was necessary.

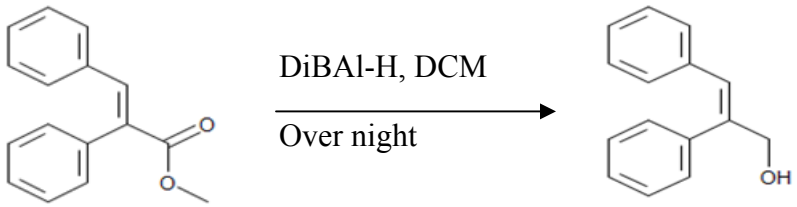

Into a round bottom flask was added 35 mg of (*E*)-methyl 2,3-diphenylacrylate (0.15 mmol, 1 Eq) in 0.15 mL DCM, and the flask was sealed under nitrogen atmosphere. The mixture was submerged in a dry ice/acetone bath and cooled for five minutes with vigorous stirring. Then, 0.31 mL of DiBAl-H (1 M in toluene, 2.1 Eq) was added drop wise to the mixture. The mixture was then placed in an ice-water bath and allowed to warm to room temperature with stirring overnight. Then, the mixture was cooled in an ice-water bath and the reaction was quenched by drop wise addition of water and then 2M HCl. The mixture was extracted with DCM, and the combined organic layers were dried over $MgSO_4$ and then evaporated to dryness under a stream of nitrogen. The resulting solid was purified via silica gel chromatography (100% DCM), and the desired fractions were combined and concentrated to give the pure product as a white solid in 84% yield. Mp (White solid from $CDCl_3$) = 70.1-7101 (Lit. 72-73[6]).Rf = 0.38 (100% DCM). 100%

Figure S 4.1 NMR and ESI data of promising PC candidates CIMS were run on a Micromass Quattro Ultima spectrometer fitted with a direct injection probe (DIP) with ionization energy set at 70 eV. HRMS (EI) were performed with a Micromass Q-Tof Ultima spectrometer. ^{1}H, ^{13}C and ^{31}P spectra were recorded on Bruker 200, AV 600 spectrometers in $CDCl_3$ or MeOD-d_4 with TMS as internal standard, chemical shifts (δ) are reported in ppm downfield of TMS and coupling constants (*J*) are expressed in Hz; ^{31}P spectra were calibrated using an external reference of 85% H_3PO_4. Signal assignments were accomplished *via* analysis of HMBC, HMQC, COSY, NOESY experiments where necessary. The (*E*) to (*Z*) ratios were determined from the relative integration of the ^{1}H spectra for the olefinic protons. All melting points are corrected.

4-(4-methoxystyryl)-2-methylthiazole (MSMT)

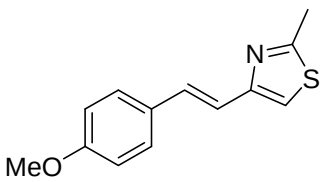

Yield 76%, Beige solid; TLC (EtOAc:hexanes, 1:4 v/v): R_f = 0.33; ^{1}H-NMR [$CDCl_3$, 600 MHz] δ: 5.24 (td, *J* = 5.6, 2.3 Hz, 1H), 2.68 (dd, *J* = 13.1, 5.6 Hz, 2H), 2.46 – 2.38 (m, 6H), 1.57 (dt, *J* = 11.3, 7.6 Hz, 6H), 1.12 (s, 6H), 1.09 (s, 6H), 1.03 (td, *J* = 7.2, 1.5 Hz, 9H);; ^{13}C-NMR [$CDCl_3$, 150 MHz] δ: 165.98, 159.44, 154.15, 130.52, 129.84, 127.87, 119.35, 114.15, 114.00, 55.27, 19.37; HREI MS $(M)^+$ calcd. for $C_{13}H_{33}NOS$ 231.0718; found 231.0710.

3-Methoxy-(4-methoxystyryl)-2-methylthiazole (3-Methoxy-MSMT)

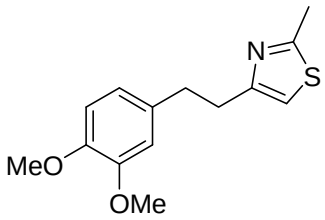

Yield 90%, Colourless oil; TLC (EtOAc:hexanes, 1:4 v/v): R_f = 0.21; ^{1}H-NMR [$CDCl_3$, 600 MHz] δ: 6.72 (d, *J* = 8.1 Hz, 1H), 6.67 (dd, *J* = 8.1, 1.9 Hz, 1H), 6.63 – 6.62 (m, 1H), 6.59 (s, 1H), 3.79 (s, 3H), 3.77 (s, 3H), 2.98 – 2.91 (m, 2H), 2.91 – 2.85 (m, 2H), 2.64 (s, 3H); ^{13}C-NMR [$CDCl_3$, 150 MHz] δ: 165.46, 156.15, 148.74, 147.25, 134.19, 120.22, 112.80, 111.80, 111.19, 55.91, 55.78, 35.24, 33.71, 19.17; HRES MS $(M+1)^+$ calcd. for $C_{14}H_{18}NO_2S$ 264.1058; found 264.1049.

hyd-4-(4-methoxystyryl)-2-methylthiazole (Red-MSMT)

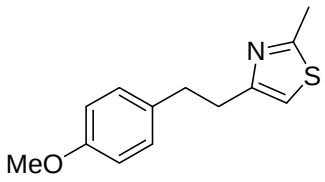

Yield 93%, Colourless oil; TLC (EtOAc:hexanes, 1:4 v/v): R_f = 0.33; ^{1}H-NMR [$CDCl_3$, 600 MHz] δ: 7.03 (d, *J* = 8.6 Hz, 2H), 6.75 (d, *J* = 8.6 Hz, 2H), 6.57 (s, 1H), 3.71 (s, 3H), 2.95 – 2.90 (m, 2H), 2.90 – 2.86 (m, 2H), 2.63 (s, 3H); ^{13}C-NMR [$CDCl_3$, 150 MHz] δ: 165.41, 157.86, 156.24, 133.63, 129.34, 113.76, 112.71, 55.25, 34.67, 33.66, 19.17; HRES MS $(M+1)^+$ calcd. for $C_{13}H_{16}NOS$ 234.0953; found 234.0948.

3-Methoxy-hydrogenated-(4-methoxystyryl)-2-methylthiazole (3-Methoxy-hyd-MSMT)

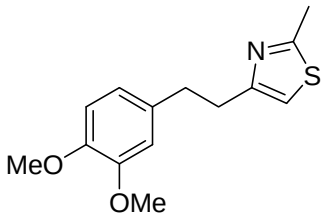

Yield 90%, Colourless oil; TLC (EtOAc:hexanes, 1:4 v/v): R_f = 0.21; ^{1}H-NMR [$CDCl_3$, 600 MHz] δ: 6.72 (d, *J* = 8.1 Hz, 1H), 6.67 (dd, *J* = 8.1, 1.9 Hz, 1H), 6.63 – 6.62 (m, 1H), 6.59 (s, 1H), 3.79 (s, 3H), 3.77 (s, 3H), 2.98 – 2.91 (m, 2H), 2.91 – 2.85 (m, 2H), 2.64 (s, 3H); ^{13}C-NMR [$CDCl_3$, 150 MHz] δ: 165.46, 156.15, 148.74, 147.25, 134.19, 120.22, 112.80, 111.80, 111.19, 55.91, 55.78, 35.24, 33.71, 19.17; HRES MS $(M+1)^+$ calcd. for $C_{14}H_{18}NO_2S$ 264.1058; found 264.1049.

4- Fluoro-hydrogenated-2-methylthiazole (F-hyd-SMT)

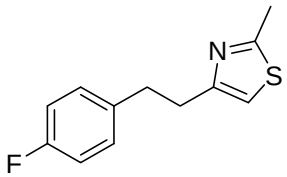

Yield 95%, yellow oil; TLC (EtOAc:hexanes, 1:4 v/v): R_f = 0.58; ^{1}H-NMR [$CDCl_3$, 600 MHz] δ: 7.14 – 7.01 (m, 2H), 6.95 – 6.83 (m, 2H), 6.71 – 6.57 (m, 1H), 3.10 – 2.91 (m, 4H), 2.79 (s, 3H); ^{13}C-NMR [$CDCl_3$, 150 MHz] δ: ; HRES MS $(M+1)^+$ calcd. for $C_{12}H_{13}NFS$ 222.0753; found 222.0753

(E)-2,3, diphenylprop-2-en-1-ol (DPPL)

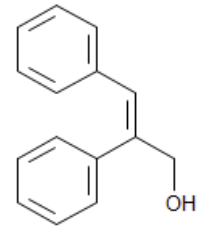

100% (*E*) by ^{1}H NMR.^{1}H NMR (600 MHz, $CDCl_3$) δ 7.34 (m, 2H), 7.30 (m, 1H), 7.25 – 7.22 (m, 2H), 7.15 – 7.08 (m, 3H), 7.01 (dd, *J* = 7.4, 2.0 Hz, 2H), 6.70 (s, 1H), 4.47 (d, *J* = 1.4 Hz, 2H), 1.70 (s, 1H).^{13}C NMR (151 MHz, $CDCl_3$) δ 141.6, 138.7, 136.6, 129.4, 129.0, 128.9, 128.1, 127.7, 127.0, 126.6, 68.7. EI-HRMS calculated for $C_{15}H_{14}O$ $(M)^+$: 210.1045 found 210.1035

(*E*)-methyl 2,3-diphenylacrylate (MDPA)

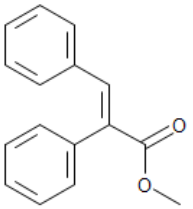

100% (*E*) by ^{1}H NMR.^{1}H NMR (600 MHz, $CDCl_3$) δ 7.86 (s, 1H), 7.40 – 7.34 (m, 3H), 7.25 – 7.19 (m, 3H), 7.16 (t, *J* = 7.5 Hz, 2H), 7.05 (d, *J* = 7.6 Hz, 2H), 3.80 (s, 3H). ^{13}C NMR (151 MHz, $CDCl_3$) δ 168.5, 140.7, 136.0, 134.7, 132.6, 130.7, 129.9, 129.2, 128.8, 128.3, 128.0, 52.5. EI-HRMS calculated for $C_{16}H_{14}O_2$ $(M)^+$: 238.0994 found 238.0993.

(*E*)-methyl 3-(4-chlorophenyl)-2-phenylacrylate (Cl-MDPA)

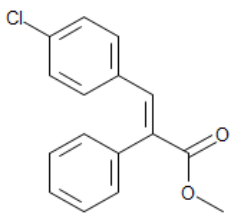

100% (*E*) by ^{1}H NMR.^{1}H NMR (600 MHz, $CDCl_3$) δ 7.79 (s, 1H), 7.40 – 7.34 (m, 3H), 7.22 – 7.17 (m, 2H), 7.12 (d, *J* = 8.6 Hz, 2H), 6.95 (d, *J* = 8.6 Hz, 2H), 3.79 (s, 3H).^{13}C NMR (151 MHz, $CDCl_3$) δ 168.3, 139.3, 135.6, 135.1, 133.2, 133.2, 131.9, 129.8, 128.9, 128.6, 128.2, 52.6. EI-HRMS calculated for $C_{16}H_{13}O_2Cl$ $(M)^+$: 272.0604 found 272.0606.

(*E*)-3-(4-chlorophenyl)-2-phenylprop-2-en-1-ol (Cl-DPPL)

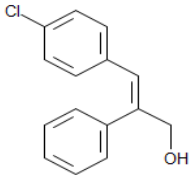

100% (*E*) by ^{1}H NMR.^{1}H NMR (600 MHz, $CDCl_3$) δ 7.37 – 7.28 (m, 3H), 7.22 – 7.18 (m, 2H), 7.08 (d, *J* = 8.5 Hz, 2H), 6.91 (d, *J* = 8.6 Hz, 2H), 6.65 (s, 1H), 4.46 (d, *J* = 1.3 Hz, 2H), 1.67 (s, 1H). ^{13}C NMR (151 MHz, $CDCl_3$) δ 142.4, 138.3, 135.1, 132.6, 130.6, 129.1, 128.8, 128.3, 127.9, 125.2, 68.4. EI-HRMS calculated for $C_{15}H_{13}OCl$ $(M)^+$: 244.0655 found 244.0665.

Supplemental Table 4.1 In silico screen of hundred drug-like compounds based on"Lipinski's rule of five.Compounds that showed MW < 500, HBDs and Log P < 5, HBAsand RDs < 10 and TPSA < 120 were considered as potential molecules for initial screen. Eight promising candidates are highlighted below

Name	Log D (pH 7.2)	Log P (<5)	MW (<500)	HBDs (<5)	HBAs (<10)	TPSA (<120)	RDs (<10)
3-G11	2.1	2.3	152.1	1	3	46.5	2
3-E6	3.1	3.1	164.2	0	2	26.3	3
3-A7	3.1	3.1	164.2	0	2	26.3	3
4-H9	-1.1	2.0	167.1	1	5	86.1	2
4-A10	-1.4	1.8	167.1	1	5	86.1	2
1-C8	3.1	2.9	169.2	1	1	15.8	2
5-C8	-4.1	-1.6	174.2	4	5	98.0	1
3-C7	3.6	3.6	178.2	0	2	26.3	3
3-D7	3.6	3.6	178.2	0	2	26.3	3
3-F6	2.6	2.5	180.2	0	3	35.5	4
1-H9	3.0	2.7	181.2	0	1	12.9	2
1-B9	3.5	3.1	183.2	1	1	15.8	3
4-F8	4.0	4.0	184.2	0	1	9.2	2
3-G6	3.0	2.9	184.6	0	2	26.3	3
1-H8	3.0	2.8	187.2	1	1	15.8	2
3-F7	3.1	3.1	194.2	0	3	35.5	4
3-H6	2.2	2.2	195.2	0	5	75.1	4
5-B8	3.1	3.2	196.6	0	2	26.3	3
1-C4	2.7	2.7	197.2	1	2	32.9	3
1-F3	2.8	2.7	198.2	0	2	30.2	3
6-B8	3.9	3.7	198.3	0	1	9.2	2
3-G7	3.4	3.3	198.6	0	2	26.3	3
1-G11	3.2	3.1	199.2	0	1	12.9	2
1-C9	3.2	3.2	199.2	1	2	25.0	2
5-A8	0.1	3.0	201.0	1	2	37.3	1
1-E8	3.3	3.2	207.3	0	1	69.4	2
3-C6	2.2	2.0	208.2	0	4	44.8	4
1-G10	3.9	3.7	209.2	1	2	28.9	1
2-D2	3.2	3.0	210.3	1	1	20.2	3
5-D8	3.5	3.4	210.3	1	1	20.2	3
1-D4	2.9	3.2	213.2	2	3	53.1	3
1-H3	3.2	3.2	214.2	1	3	50.4	3
4-D8	3.5	3.4	214.3	0	2	18.5	3
1-G3	3.5	3.4	214.3	0	1	45.3	3
1-G7	3.3	3.1	219.3	0	1	41.1	2
3-D6	2.4	2.2	222.2	0	4	44.8	4
1-A2	3.6	3.5	224.3	1	2	37.3	3
1-B4	3.5	3.4	224.3	0	2	26.3	1

1-D2	3.1	3.0	224.3	1	2	37.3	3
5-G8	4.0	3.9	224.3	1	1	20.2	3
3-H2	2.2	2.1	225.3	0	3	45.8	2
4-H7	3.3	3.3	226.3	0	2	26.3	3
4-C8	3.3	3.3	226.3	0	2	26.3	3
5-E8	3.4	3.3	228.3	1	1	20.2	3
1-A4	3.6	3.6	230.3	1	2	65.5	3
1-A8	3.3	3.0	231.3	0	2	50.4	3
3-H11	1.7	1.5	235.2	1	5	64.6	6
1-B10	3.9	3.2	237.3	1	1	15.8	3
1-E2	3.5	3.4	238.3	0	2	26.3	4
3-F2	2.9	2.9	239.3	0	3	45.8	2
1-H2	3.0	3.0	240.3	2	3	57.5	3
1-C3	3.5	3.4	240.3	1	2	56.9	2
3-G2	1.7	1.8	241.3	0	4	55.0	2
1-C3	4.0	3.7	242.7	0	1	17.1	3
5-H8	3.9	3.7	244.7	1	1	20.2	3
1-F8	3.1	3.0	246.3	0	4	90.0	3
1-A9	4.4	4.5	248.1	1	1	15.8	2
5-H5	-0.7	1.4	250.3	3	6	90.7	5
2-A4	3.0	2.6	254.3	1	3	38.7	3
2-A2	2.8	2.8	256.3	1	3	46.5	5
1-H11	4.0	3.7	260.1	0	1	12.9	2
2-C3	3.8	4.0	260.3	0	2	17.8	4
3-A2	3.5	3.5	261.3	1	3	54.6	3
1-A3	3.9	3.7	268.3	0	3	35.5	5
3-E2	1.7	1.8	268.4	0	4	49.0	3
1-H5	3.6	3.2	270.3	0	3	27.7	5
5-H6	2.7	2.5	277.3	0	4	47.8	5
3-B2	3.1	3.2	277.3	1	4	63.8	4
3-C2	3.3	3.2	277.3	1	4	63.8	4
3-D2	3.1	3.1	277.3	1	4	63.8	4
5-H4	2.7	2.5	279.3	1	5	56.8	5
5-H2	2.8	2.8	279.3	1	4	50.9	5
2-H3	3.8	3.2	282.3	0	4	44.8	4
1-F6	3.7	3.0	284.3	0	4	36.9	4
2-D6	0.9	1.7	287.3	2	5	62.2	0
2-C6	0.3	1.6	289.3	3	5	73.2	1
3-F5	2.3	2.3	293.3	1	7	90.9	7
3-B6	1.8	1.5	295.3	1	7	83.1	8
5-C3	2.5	3.1	297.4	1	3	32.7	5
2-E3	2.3	2.1	300.3	1	5	65.0	5

1-E6	3.4	2.9	300.3	0	4	36.9	6
1-G6	3.5	2.9	300.3	0	4	36.9	6
1-H6	4.2	3.8	304.8	0	3	27.7	5
5-G4	2.9	2.1	307.3	1	6	73.9	5
3-C9	3.3	3.1	312.2	1	3	54.6	3
1-E7	3.3	3.0	314.3	0	5	46.2	5
1-A7	3.5	3.2	315.3	0	6	76.5	6
2-E5	1.3	3.3	315.4	0	5	48.0	2
3-E5	1.9	2.3	320.3	1	7	77.1	6
3-B9	3.6	3.6	326.2	1	3	54.6	3
2-H4	3.2	3.0	328.4	1	5	65.0	6
1-C7	3.0	2.8	330.4	0	5	46.2	7
2-F5	1.2	1.3	331.4	1	6	60.4	1
5-A5	3.9	3.6	358.2	1	5	64.6	8
2-F10	2.8	2.2	364.4	1	7	83.5	6
2-H10	3.3	2.7	366.4	1	7	75.6	8
3-A6	-1.9	-1.8	379.4	1	8	86.6	7
3-C5	-2.1	-2.1	379.8	1	8	86.3	9
2-A11	2.5	2.5	396.4	1	8	92.7	8
3-D5	-2.3	-2.3	410.2	1	8	86.3	8
2-E7	2.4	2.2	429.5	3	8	106.5	7

Chapter V:
Shikimic Acid Restores Activity of Mutant Phenylalanine Hydroxylase: A Natural Product Exhibiting Chaperone Potency Without Inhibition

Authors of this work are Meera Shanmuganathan, Bryanna Tibensky, James McNulty, Dave McLeod, Aurora Martinez, Oscar Aubi and Philip Britz-McKibbin. I conducted most of the experiments and data analysis in this work, B. Tibensky (undergraduate thesis student) helped me with pre-selection of PC candidates. Dr. J. McNulty and his group members, D. McLeod supported with synthesizing chemically unique small molecules for a customized small chemical library. Dr. A. Martinez and O. Aubi provided with human recombinant WT-PAH and clinically relevant two PKU-mutants.

5.1. Abstract

Pharmacological chaperones (PCs) represent a promising strategy for the treatment of genetic disorders based on enzyme enhancement therapy, such as phenylketonuria (PKU). Enzyme inhibition and thermal stabilization assays are widely used in drug discovery of PC candidates, however these methods do not accurately measure chaperone activity. We introduce a new strategy for the screening of PCs that target phenylalanine hydroxylase (PAH) when using capillary electrophoresis (CE) with UV detection, which enables label-free characterization of enzymatic activity via *L*-tyrosine (Tyr) formation kinetics. This functional assay directly measures PAH activity with short analysis times (< 3 min), low detection limits (S/N≈ 3, 1.0 μM) and good inter-day precision (CV < 10%) without spectral interferences. A two-tiered approach was applied to screen a chemical library comprising structurally unique small molecules after *in -silico* assessment for drug-like properties. Compounds that activate, stabilize and refold wild-type (WT)-PAH under denaturating conditions were selected as lead candidates for subsequent testing *in-vitro* using two distinct PAH mutants impacting the regulatory and catalytic domain. Overall,

two lead compounds, 1,2,3-trimethoxy-5-[2-(4-methoxyphenyl)ethenyl] benzene (MMP) and shikimic acid (SA), were found to function as PCs for WT-PAH in a dose-dependent manner resulting in a 3-and 5-fold (at 20 μM) enhancement in enzyme activity unlike screen negative controls. Both MMP and SA also induced about a 2-fold enhancement in PAH activity for the I65Tmutant, as well as a significant 3 to 5-fold enhancement in the activity of the R261Q mutant that is associated with atypical or classical PKU. Structure-activity relationships were also examined for several different SA analogs for WT and/or mutant. PAH, including 3-dehydro-SA, *D*-quinic acid and gallic acid. We demonstrate for the first time that natural products represent novel PCs for restoring the activity of mutant enzymes without undesirable inhibitory effects. This work is urgently needed for improved treatment of variable or severe PKU phenotypes that do not respond to tetrahydrobiopterin supplementation and/or lifelong phenylalanine-dietary restriction.

5.2 Introduction

Phenylalanine hydroxylase (PAH) is a multimeric hepatic enzyme that catalyzes the hydroxylation of *L*-phenylalanine (Phe) to *L*-tyrosine (Tyr) in the presence of iron, molecular oxygen and a redox-active cofactor, tetrahydrobiopterin (BH4).[1–3] Phenylketonuria (PKU) is a heterogeneous group of disorders that can lead to intellectual disability, seizures, and impaired growth and development in affected children if left untreated with an average reported incidence rate of 1:12,000 in North America.[4] PKU is a common in-born error of amino acid metabolism that is related to more than 500 disease-causing mutations of PAH or by a defect in the synthesis or regeneration of BH4.[5] Due to the great allelic variation and large number of pathogenic mutations, universal newborn screening (NBS) for PKU relies on tandem mass spectrometry to detect hyperphenylalaninaemia in the population from dried blood spot extracts with follow-up diagnostic testing by quantitative analysis of plasma Phe and Tyr.[6] Several PAH mutations have been shown to affect protein folding in the endoplasmic reticulum resulting in accelerated degradation and/or aggregation due to missense mutations (63%)

and small deletions (13%) in protein structure that attenuates or largely abolishes enzyme catalytic activity. In general, three major phenotypic groups are classified in PKU based on Phe levels measured at diagnosis, dietary tolerance to Phe and potential responsiveness to BH4 therapy, including classical PKU (Phe > 1200 μM), atypical or mild PKU (Phe 600 - 1200 μM) and permanent mild hyperphenylalaninaemia (HPA, Phe < 600 μM).[5,7,8] Currently, lifelong dietary restriction of Phe and BH4 supplementation are the only two available treatment options for PKU, where early therapeutic intervention is critical to ensure optimal clinical outcomes in affected infants.[9] However, costly medication and special low-protein foods imposes a burden on patients that can lead to malnutrition, psychosocial or neurocognitive complications notably when these products are not fully covered by private health insurance.[10] Moreover, BH4 therapy is primarily effective for treatment of mild hyperphenylalaninaemia as related to defects in BH4 biosynthesis,[11–13]whereas only 20-30% of patients with mild or classical PKU are responsive.[12,14] Thus, there is urgent need for new treatment modalities for PKU as an alternative to burdensome Phe-restriction diets[6],[15] including large neutral amino acid formulations[16] and enzyme replacement therapy using PEGylated recombinant phenylalanine ammonia lyase.[17]

Pharmacological chaperones (PC) offer a novel strategy for treatment of orphan diseases based on extrinsic small molecules that correct the folding of PAH mutants associated with PKU.[11,18] PC therapy was first proposed to stabilize and increase trafficking of mutant enzymes associated with lysosomal storage disorders, such as Fabry and Gaucher disease.[19–22] However, endogenous ligands or cofactors can also function as natural chaperones for specific enzymes such as BH4, which has been shown to promote the thermodynamic and kinetic stability of certain PAH mutants.[23] Drug discovery of new classes of PCs has expanded to target other protein misfolding diseases, including cystic fibrosis and Alzheimer's disease.[24,25] To date, high throughput screening (HTS) methods for PCs use fluorescence-based inhibition assays for lead candidate selection from large chemical libraries with confirmatory testing based on thermal stability, patient-derived

cell-based assays and/or animal models.[26–30] However, inhibitors are paradoxical agents for PC therapy since they attenuate substrate turn-over in the cell without alleviating toxic substrate accumulation, such as Phe-induced neuronal apoptosis.[31] As a result, a HTS fluorescence-based thermal stability assay was used to identify two putative PCs for treatment of PKU that increase the stability and activity of misfolded PAH.[11] Recently, two novel PCs were also reported to correct PKU in mice models after lead compounds were characterized using surface plasmon resonance after virtual screening from a National Cancer Institute (NCI) compound database.[32] In this case, benzyl hydantoin was found to be two-fold more effective than BH4 while binding to the same cofactor-binding region of PAH. However, ligand binding affinity is often mutation-specific with greater stabilization for BH4-responsive PAH deficiency[33] involving site mutations in the regulatory domain as opposed to the catalytic domain with low residual enzyme activity (< 4 %).[34]

Herein, we introduce a selective yet sensitive capillary electrophoresis (CE)-based assay that directly measures PAH activity based on *L*-tyrosine (Tyr) formation. CE offers a versatile platform for drug screening due to its short analysis times, minimal sample volume requirements, and high separation efficiency that reduces spectral interferences in complex sample mixtures, including stereoisomers and natural product extracts.[35] In this work, a two-tiered screening approach was developed for selection of lead PC candidates based on restoration of enzyme activity upon denaturation (READ),[36] which measures ligand-induced stabilization in terms of dose-responsive changes to enzyme catalytic activity. This strategy was first applied on a chemical library after *in-silico* screening for compounds with drug-like activity based on Lipinski's rule of five[37] when using wild-type (WT)-PAH with two different chemical denaturants to elicit protein unfolding and loss in enzyme function mimicking a severe mutation. Shikimic acid (SA) and 1,2,3-trimethoxy-5-[2-(4-methoxyphenyl)ethenyl]benzene (MMP) were discovered as novel PCs based on their ability to significantly enhance and restore the activity of WT-PAH under denaturing conditions, as well as two PAH mutants with partial (I65T) and low

(R261Q) residual catalytic activity. Structure-activity relationships were also explored by comparing the chaperone activity of several SA analogs, including *D*-quinic acid. Interestingly, SA is a key intermediate for biosynthesis of lignin, alkaloids and aromatic amino acids by plants and microbes,[38] as well as important chiral precursor for production of the neuroaminidase inhibitor, oseltamivirphosphate or Tamiflu®.[39] To the best of our knowledge, we report the first example of a safe and well tolerated natural product that can induce up to a five-fold enhancement in mutant PAH activity without unwanted inhibition or catalytic uncoupling.

5.3 Materials and Methods

5.3.1 Chemicals and Reagents

De-ionized water for buffer, stock, and sample preparations was obtained using a Barnstead EASYpure® II LF ultrapure water system (Dubuque, IA, USA). Boric acid, 4-(2-Hydroxyethyl) piperazine-1-ethanesulfonic acid (HEPES),sodium chloride (NaCl), and sodium hydroxide (NaOH) were obtained from Sigma-Aldrich (St. Louis, MO, USA) which were used in buffer preparation and 1 M NaOH was used to adjust the pH of the assay and separation buffer. *L*-phenylalanine (Phe), L-tyrosine (Tyr), 3-fluoro-L-phenylalanine (F-Phe),the internal standard (IS) 3-O-methyl-L-tyrosine (Me-Tyr), shikimic acid (SA), *D*-quinic acid (QA), gallic acid and 3-deoxyshikimic acid (3-DSA) were all purchased from Sigma-Aldrich. Stock solutions were prepared in HEPES buffer (20 mM HEPES pH 7.0, 0.2 M NaCl) and stored refrigerated at +4°C. Chemical denaturants, urea was purchased from Bioshop (Burlington, ON, Canada), whereas guandium hydrochloride (GndCl)was obtained from Sigma-Aldrich. Stock solutions of chemical denaturants (20M urea, 20 M GndCl) were freshly prepared each day in HEPES buffer with gentle heating. Catalase, (6R)-*L*-erythro-5,6,7,8-tetrahydro-L-erythro-biopterin sulfate (BH4), *DL*-dithiothreitol (DTT) and ammonium iron (II) sulfatehexahydrate (Fe^{2+}) were all purchased from Sigma-Aldrich. BH4 and DTT stock solutions were prepared in 0.1 M HCl and$FeSO_4$ stocks were prepared in de-ionized

water. Dimethyl sulfoxide (DMSO) was purchased from Caledon Laboratories Ltd. (Georgetown, ON, Canada) and used for preparation of primary stock solutions for ligands in chemical library, as well as lead compound analogs purchased commercially. 3-amino-2-benzyl-7-nitro-4-(2-quinolyl)-1,2-dihydroisoquinolin-1-one (compound III) and (5,6-dimethyl-3-(4-methyl-2-pyridinyl)-2-thioxo-2,3-dihydrothieno[2,3-d] pyrimidin-4(1H)-one (compound IV) were donated by Dr. Martinez laboratory for validation of chaperone activity using our two-tiered screening method for identification of novel PCs from a chemical library.[11]

5.3.2 Chemical Library and Computational Screen for Drug-like Activity

A customized chemical library containing 600 unique small molecules were synthesized in the laboratory of Dr. McNulty at McMaster University. All compounds were stored refrigerated (+4°C) in DMSO (10 mM) after spectral characterization by ^{1}H-NMR and electron impact ionization (EI)-MS to confirm their purity. Lead compounds identified after primary screening were also re-synthesized to confirm their chaperone activity with WT and mutant PAHs notably for ligands stored in DMSO over several years. *In-silico* screen was performed using ACD Labs PhysChem Suite 2012 software for predicting drug-like properties of compounds based on Lipinski's rules of five[37] (molecular weight (*MW*) < 500, *Log P* < 5, hydrogen bond donors (*HBDs*) < 5, hydrogen bond acceptors (*HBAs*) < 10, rotational bonds (RBs) < 10)) and total polar surface area (*TPSA*) < 120 Å, resulting in 100 candidates (**Table S4.1**) for screening in order to avoid false positives due to insolubility, aggregation and/or cell toxicity. To note, this *in-silico* screen is different from virtual screening which focuses on the structural similarity of ligand binding environment in PAH.[18]

5.3.3 Recombinant Expression of PAH in Escherichia Coli

Expression of recombinant human WT-PAH and two PAH mutants (I65T and R269Q) as fusion protein with maltose-binding protein in eukaryotic cell cultures using pMAL expression vector was performed by the Martinez laboratory at the University of Bergen

as described elsewhere.[40] Briefly, purification of the fusion proteins expressed in the pMAL vector system was performed using affinity chromatography followed by size-exclusion chromatography to remove low molecular weight components. Subsequently, the fusion proteins were cleaved by the restriction protease factor Xa and then phosphorylated by cyclic adenosine monophosphate (cAMP)-dependent protein kinase. The two clinically relevant PAH mutants, I65T and R261Q comprise single-point mutations in the regulatory and catalytic domain, respectively [23] which are associated with highly variable phenotypes ranging from mild to classical PKU.[11,41] For instance, patients with R261Q genotypes are reported to have inconsistent responses to BH4 therapy.[12,11] In this work, I65T and R261Q PAH mutants were measured to have residual catalytic activities of (35 ± 1)% and (5 ± 0.5)% relative to WT PAH under standardized conditions (*i.e.,* enzyme concentrations, assay buffer etc.), respectively. Stock solutions of WT-PAH and PAH mutants were prepared in enzyme reaction buffer (20 mM HEPES pH 7.0, 200 mM NaCl), and divided into separate 10 μL aliquots in 0.5 mL sterilized centrifuge tubes prior to storage at -80°C. Note that all enzyme assays were performed on aliquots of frozen enzymes thawed slowly in the fridge prior to daily use. Multiple freeze-thaw cycles of PAH were found to contribute to lower enzymatic activity, whereas all final solutions for enzyme reactions were prepared containing < 1% *v* DMSO to prevent enzyme inactivation.

5.3.4 Capillary Electrophoresis Separations

All CE separations for measuring PAH activity were performed on a Hewlett Packard 3D CE system (Agilent Technologies Inc., Waldbronn, Germany) equipped with UV photodiode array (PDA) detection. Uncoated open tubular fused-silica capillaries (Polymicro Technologies Inc., Phoenix, AZ, USA) with dimensions of 25 μm inner diameter, 360 μm outer diameter and total capillary length of 35 cm were used for this study. New capillaries were conditioned by rinsing with methanol for 30 min, de-ionized water for 30 min, 1 M NaOH for 30 min and background electrolyte (BGE) for 60 min. The BGE used in CE separations for measuring PAH-catalyzed Tyr formation was 200

mM borate, pH 10.3. At the beginning of each day, the capillary was rinsed with 1.0 M NaOH for 10 min and BGE for 15 min. Each separation started with a pre-rinsing of the capillary with 1.0 M NaOH for 3 min and BGE for 3 min followed by hydrodynamic injection of the sample at 50 mbar for 75 s. For enzymatic assays, resolution of Phe (substrate), Tyr (product), Me-Tyr (internal standard), and reduced/oxidized cofactors, tetrahydrobiopterin (BH4) and dihydrobiopterin (BH2),were performed under an applied voltage of 30 kV using a positive gradient pressure of 20 mbar over 5.0 min with UV absorbance monitored at 200 nm. Due to the narrow optical path length (25 μm) and small sample volumes typically injected on-column in CE, an on-line sample pre-concentration technique based on dynamic pH junction[42]was developed that is compatible with buffer conditions used in the enzyme reaction. In this case, weakly acidic metabolites within a long sample plug (75 sec) are electrokinetically focused at the boundary of a discontinuous electrolyte system comprising HEPES (pH 7.0) and borate (pH 10.3) as sample and BGE segments, respectively. The CE system stability was monitored daily by performing quality control runs of a standard sample mixture prior to enzymatic reactions.

5.3.5 External Calibration Curve for Measurement of Enzyme Activity.

PAH catalytic activity was measured directly by CE with UV detection based on the rate of formation of Tyr that is resolved from excess Phe and other components in the enzyme reaction. In this case, stock solution of Tyr was diluted to twelve different concentrations ranging from 2.5 to 1000 μM in the enzyme reaction buffer (20 mM HEPES and 200 mM NaCl, pH 7.0), whereas Me-Tyr was used as internal standard (IS) at a final concentration of 100 μM. The calibration curve was generated using an average of nine replicates performed over three days (n = 9) with good precision as reflected by a coefficient of variance (*CV*) under 5%. Overall, excellent linearity over a 400-fold concentration range was realized for calibration curves as reflected by a correlation of determination (R^2) of 0.9995. The limit of quantification (*LOQ*) and limit of detection (*LOD*) for Tyr when

using CE with UV detection was 2.5 μM and 1μM, respectively based on capillary dimensions and sample injection conditions used in this work.

5.3.6 Enzyme Kinetics of WT and Mutant PAH

Tetrameric human phenylalanine hydroxylase (PAH) enzyme kinetic assays were performed off-line under standardized conditions prior to quantification of Tyr formation by CE with UV detection. Enzyme assays were performed by first mixing together Phe (1 mM), catalase (100 nM) and PAH (0.25 μM/subunit)in a reaction buffer (20 mM HEPES and 200 mM NaCl, pH 7.0) that were equilibrated at 25°C for 4 min. Then, ferrous (Fe^{2+}) ammonium sulfate (100 μM) was added to the solution for 1 min and the reaction was subsequently initiated by addition of BH4 (100 nM) with DTT (5 mM) using a total volume of 100 μL. The reaction mixture was then vortexed for 60 s followed by sonication for 2 min prior to centrifugation for 10 s at 4 *g* and storage in a refrigerator (+4°C). An aliquot (20 μL) was withdrawn from the quenched enzyme reaction and placed in a micro vial containing Me-Tyr as IS (100 μM) prior to CE analysis. The stability of the quenched enzyme reaction was confirmed by intermittent analysis of PAH activity over 6 h at room temperature, and no significant changes in the Tyr/IS or Phe/Tyr response ratio were measured. Enzymatic reactions were performed for both WT-PAH and two PAH mutants by pre-equilibrating each ligand for 10 min prior to addition of ferrous ion and BH4/DDT as described in enzyme reaction protocol in order to assess for ligand-induced PAH inhibition or activation. Overall, PAH activity was measured in triplicate (n = 3) by CE based on the average relative peak area ratio of Tyr to IS, whereas the reproducibility of three biological replicates performed over three days was found to be acceptable with an overall *CV* under 10% (n=9).

5.3.7 Primary Assay for PC Screening Based on Resistance to Urea Denaturation and Enzyme Deactivation

Unlike thermal stability assays that can induce protein aggregation, chemical denaturants are more suitable as perturbants to promote unfolding and enzyme inactivation while solubilizing multimeric proteins.[34] In this context, restoration of enzyme activity upon

denaturation (READ) was first introduced to characterize PCs that stabilize yet enhance the activity of a lysosomal enzyme, β-glucocerebrosidase (GCase).[36] Herein, READ was modified, further optimized and validated for primary screening of PCs for a cytosolic enzyme (PAH) using a chemical library containing structurally unique compounds with drug-like activity. For instance, the primary screen was used to measure ligand-induced stabilization of PAH by extrinsic small molecules that impart greater resistance to urea unfolding as compared to ligand-free *apo*-enzyme condition. PAH activity was first examined as a function of urea concentration (0 to 8 M) and pre-equilibration time (10 min to 2 hr) in order to determine optimum conditions where residual enzyme activity was largely attenuated below 10% due to protein unfolding. Protein unfolding was performed in triplicate *off-line* with the enzyme reaction buffer (20 mM HEPES and 200 mM NaCl, pH 7.0) using tetrameric human PAH (1 μM and/or 0.1 μM) or mutant PAH (1 μM and/or 0.1 μM) incubated 10 min in 0 M or 8 M urea in the presence or absence of ligand (20 μM).Dose-response studies (0, 2.0 and 20 μM) were subsequently performed in triplicate on screen-positive compounds using re-synthesized ligands in order to further validate initial screen results. In all cases, quenched enzyme reactions were processed as described previously prior to CE analysis. PAH activity measurements based on Tyr formation at 8M urea with the presence or absence of PC were normalized to 0 M urea for each aliquot enzyme reaction to minimize long-term variation, which also enables direct comparison of the ligand-induced stabilization activity under denaturing conditions (8M urea) while confirming inhibition and activation effects for ligands under native conditions (0 M urea).

5.3.8 Secondary Assay for Confirmation of PCs with Chaperone Activity upon Enzyme Refolding

A secondary assay was developed to directly measure chaperone activity of screen-positive compounds in terms of ligand interactions that enhance recovery of PAH activity after protein unfolding. A stronger chemical denaturant than urea, GndCl, was required in this case in order to perturb PAH structure and conformation to a greater extent as a way to significantly attenuate enzyme activity upon refolding. For instance, a recovery of 50%

of residual enzyme activity was achieved without ligand when PAH was incubated in 8.0 M urea after its dilution to 0.5 M urea to trigger protein refolding. In order to further reduce enzyme reversibility, the recovery of PAH activity was subsequently assessed when it was incubated using 6.0 M GndCl for 10 min and subsequently diluted to 0.5 M GndCl in the presence or absence of screen-positive ligands (20 μM) in enzyme reaction buffer with PAH activity measurements performed by CE as described previously. In this case, WT-PAH was found to regain approximately (7 ± 0.5) % residual activity (three biological replicates , CV < 10 %) when it was initially incubated at 6 M GndCl for 10 min then subsequently diluted to 0.5 M GndCl as compared to PAH activity measured at 0.5 M GndCl, where enzyme exists in a folded and active state. Two lead compounds and several analogs of SA were subsequently tested using two different mutants of PAH (I65T and R261Q) without chemical denaturants after the two-tiered screening

5.4 Results and Discussion

5.4.1 Optimization of Separation Conditions for Tyr Quantification

Due to the weak native fluorescence properties of Tyr that contributes to poor sensitivity and spectral interferences when using deep UV excitation without separation,[43] HTS screening of PCs for PAH has relied on differential scanning fluorometry[18] using extrinsic fluorescent probes to evaluate ligand-induced changes in protein thermodynamic stability as reflected by increases in mid-point denaturation melting temperature.[44] Alternatively, SPR offers a label-free approach to probe the thermodynamics and kinetics of reversible ligand binding to immobilized PAH.[18] However, both primary screening methods do not directly measure changes in enzyme activity, modes of ligand binding or chaperone activity with a selection bias towards active-site competitive inhibitors that are undesirable ligands for enzyme enhancement therapy.[18] In this work, an enzyme kinetic assay for functional screening of PCs[36] was developed for accurate quantification of PAH-catalyzed Tyr formation using CE with UV detection. Full resolution of all components of the quenched enzyme reaction is achieved by CE as shown in **Figure. 5.1,**

including excess substrate (Phe, 1 mM), product (Tyr), oxidized/reduced forms of cofactor (BH4/BH2), buffer (HEPES) and IS (Me-Tyr). Tyr formation was measured in a reaction containing both Phe and BH4, whereas no product formation is detected in a negative control without BH4 as required for enzyme activity. On-line sample preconcentration was used in CE to enhance concentration sensitivity notably when using narrow internal diameter fused-silica capillaries (25 μm) to improve separation efficiency under high voltages with fast analysis times (< 4 min). **Table 5.1** summarizes the major analytical merits of the CE assay for enzyme kinetic studies of PAH, which was found to have excellent linearity, reproducibility and adequate sensitivity while using low amounts (1 pmol) of recombinant enzyme. Moreover, greater selectivity and lower detection limits ($LOD \approx 1.0$ μM) are achieved by CE with conventional UV absorbance as compared to nitrosonaphtol derivatization of Tyr with fluorimetric detection.[45] Indeed, a 30-fold lower detection limit can also be achieved for Tyr when using CE with laser-induced native fluorescence detection.[43]

Table 5.1. Summary of CE assay for assessment of PAH activity

Figures of merit	***L-Tyr***
Linearity (R^2)	0.9995
Linear Range	2.5 - 1000 μM
Intra-day assay precision *(% CV)*	3.0
Inter-day assay precision *(% CV)*	5.7
Sensitivity (μM^{-1})	0.0068 (± 0.0001)
Limit of detection ($S/N \approx 3$)	1.0 μM
Limit of quantification ($S/N \approx 10$)	2.5 μM

5.4.2 Optimization of a Functional Two-tiered PC Screening Method for PAH

Since inhibitor potency or ligand binding affinity is not always directly associated with increases to protein conformational stability[46], we developed a label-free CE assay for characterization of changes in PAH catalytic activity upon ligand association. Primary screening methods also rely on WT enzymes for PC candidate selection under native conditions, which contributes to potential bias during follow-up testing on various PAH

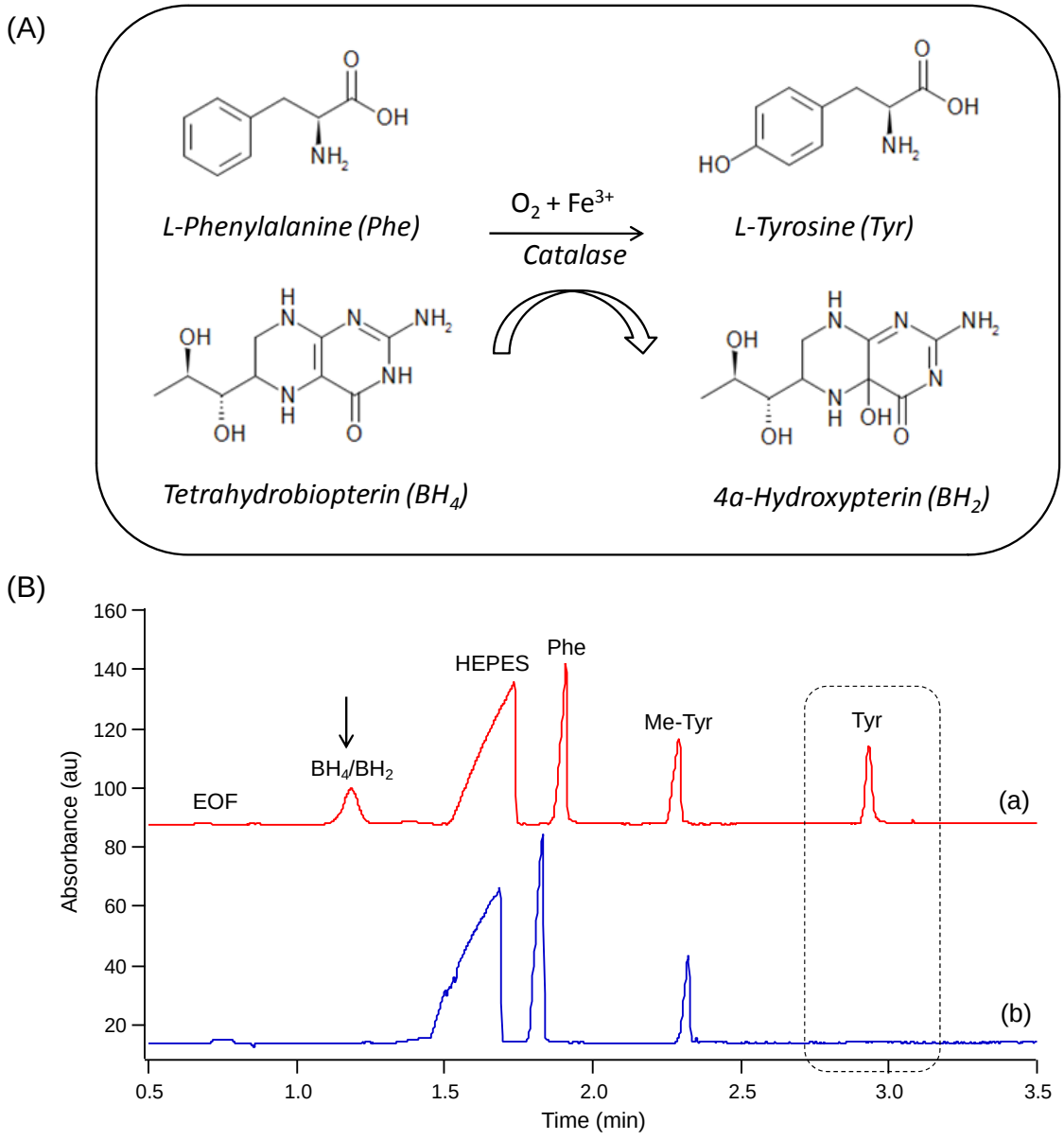

Figure 5.1 Optimization of PAH kinetic assay components on CE (A) Schematic of the PAH enzymatic reaction and (B) electropherogram overlay depicting (a) resolution of major components in a PAH-catalyzed enzymatic reaction relative to (b) a negative control without addition of BH_4 and DTT, where no product (Tyr) is detected. All separations were performed using a BGE of 200 mM borate, pH 10.3 using a voltage of 30 kV with UV detection at 200 nm, whereas enzyme reactions were performed off-line in 20 mM HEPES, 200 mM NaCl, pH 7.0.

mutations associated with the PKU disease spectrum with loss in function pathogenesis due to reduced stability.[47] In this context, we recently introduced READ as high-quality screening method for PCs[36] that measures enzyme activity enhancement due to ligand-induced stabilization under denaturing conditions with chemical denaturants. Herein, READ was further modified and optimized for better selection of PCs for PAH from a small library containing structurally novel synthetic compounds. PAH activity was initially monitored as a function of urea concentrations (0 to 8 M) with pre-equilibration times ranging from 10 min to 2 hr prior to initiation of enzyme reaction. **Figure 5.2** demonstrates that Tyr formation by WT-PAH was significantly attenuated when pre-equilibrated using 8 M urea with rapid protein unfolding within 10 min that did not change over 1 hr. In this case, CE also resolves excess urea that co-migrates with the electroosmotic flow (EOF) as a neutral solute without spectral interferences impacting Tyr quantification. Overall, the normalized activity of WT-PAH was reduced to only (7.0 ± 0.5) % (under these conditions (8 M urea/10 min) relative to the native/folded enzyme without urea. Since WT-PAH was found to regain about half of its catalytic activity upon dilution of urea without extrinsic ligands, protein refolding was performed using a stronger denaturant, GndCl in order to perturb PAH structure to a greater extent in order to mimic a severe mutation associated with a significant loss in catalytic activity. As a result, the reversibility of WT-PAH activity was monitored when pre-equilibrated with various concentrations of GndCl (4-8 M) for 10 min and subsequently diluted to 0.5 M GndCl (data not shown). In this case, WT-PAH was found to retain only about (7 ± 0.5) % when using 6.0 M GndCl for 10 min followed by dilution to 0.5 M GndCl where the activity is normalized to enzyme at 0.5 M GndCl concentration (data not shown). Unlike thermal denaturation techniques (*e.g.,* isothermal calorimetry) that often induce irreversible precipitation of multimeric protein, solubilizing chemical denaturants enables direct characterization of the chaperone potential of ligand binding that assists in the refolding of denatured/mutant enzyme in order to significantly enhance the residual activity of PAH.

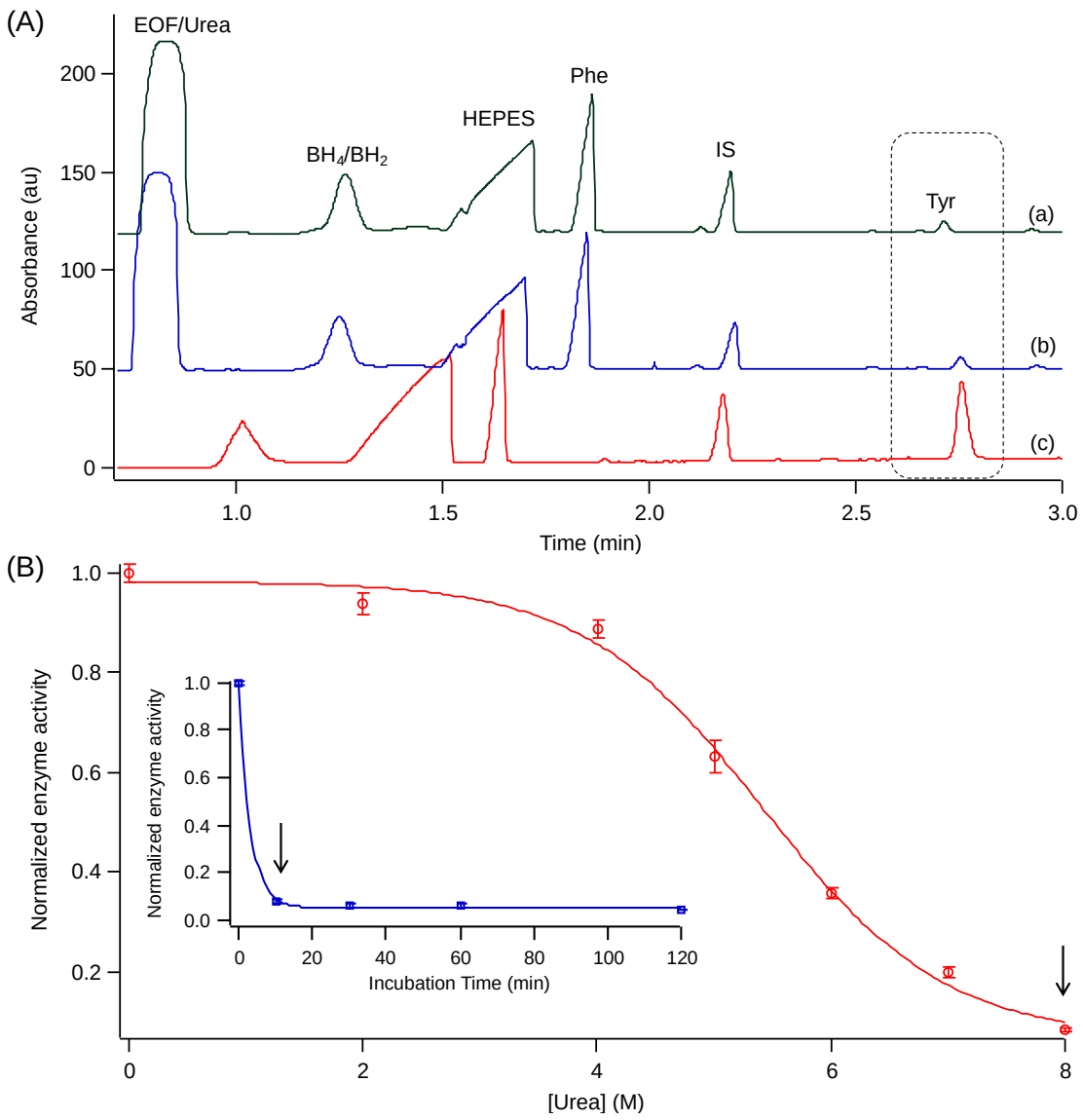

Figure 5.2 Optimization conditions of stabilization assay (A) Series of electropherograms depicting the loss in enzymatic activity of PAH upon denaturation in urea. Tyr formation was significantly attenuated in 8 M urea after (a) 10 min or (b) 60 min incubation relative to (c) 0 M urea conditions for the wild-type/folded enzyme. (B) PAH activity curve as a function of urea concentration highlights that only about 7% of residual activity remains at 8 M urea with rapid unfolding occurring within 10 min of equilibration.

5.4.3 Discovery of Novel PCs for PAH from a Chemical Library

A hundred drug-like compounds were pre-selected via *in-silico* screen from an in-house chemical library comprising six hundred structurally unique synthetic compounds based on Lipinski's rule of five, including *MW* < 500 Da, *log P* < 4, *HBDs* <5, *HBA* < 10 and *TSPA* < 120 Å. *In-silico* screen minimizes false discoveries during primary screening by eliminating compounds that have undesirable properties such as insolubility and cytotoxicity.[37] A primary screen using CE was first performed based on ligand-induced stabilization of WT-PAH activity under denaturing conditions for identification of putative PC candidates at a 20 μM dosage level. Screen-positive compounds were selected if they induced a significant enhancement in PAH activity exceeding a 8 % cut-off since ligand-free enzyme was found to retain only (7 ± 0.5) % residual activity at 8 M urea. In addition, PC candidates were selected provided they did not induce significant WT-PAH inhibition (< 20%) under native conditions without urea, such as the competitive inhibitor F-Phe[48] that was used as a screen-negative control in our work. **Figure 5.3(a)** depicts a plot that compares the measured activity of WT-PAH under native and denaturing conditions for a sub-group of 7 lead candidates with putative PC activity. In most cases, these compounds did not display any measurable enzyme inhibition at 20 μM with two ligands (*e.g.,* 5-H4 and SA) having weak activation effects on WT-PAH. Moreover, three compounds (*e.g.,* MMP, 2-E7 and 5-H4) were found to enhance WT-PAH residual activity by over 3-fold (> 21%) under denaturing conditions. PC selectivity was evaluated by including competitive and mixed-type inhibitors to β-glucocerebrosidase that is associated with Gaucher disease[49] such as isofagomine, ambroxol, diltiazem and fluphenazine, which showed no enhancement effect on PAH activity (data not shown). In addition, two recently reported PCs for PAH, 3-amino-2-benzyl-7-nitro-4-(2-quinolyl)-1,2-dihydroisoquinolin-1-one (compound III) and (5,6-dimethyl-3-(4-methyl-2-pyridinyl)-2-thioxo-2,3-dihydrothieno [2,3-d] pyrimidin-4(1H)-one (compound IV) were included as positive controls in our work since they were reported to stabilize PAH by shifting denaturation temperatures greater than 14°C and 7°C at 100 μM relative to ligand-free enzyme, respectively.[11,18]

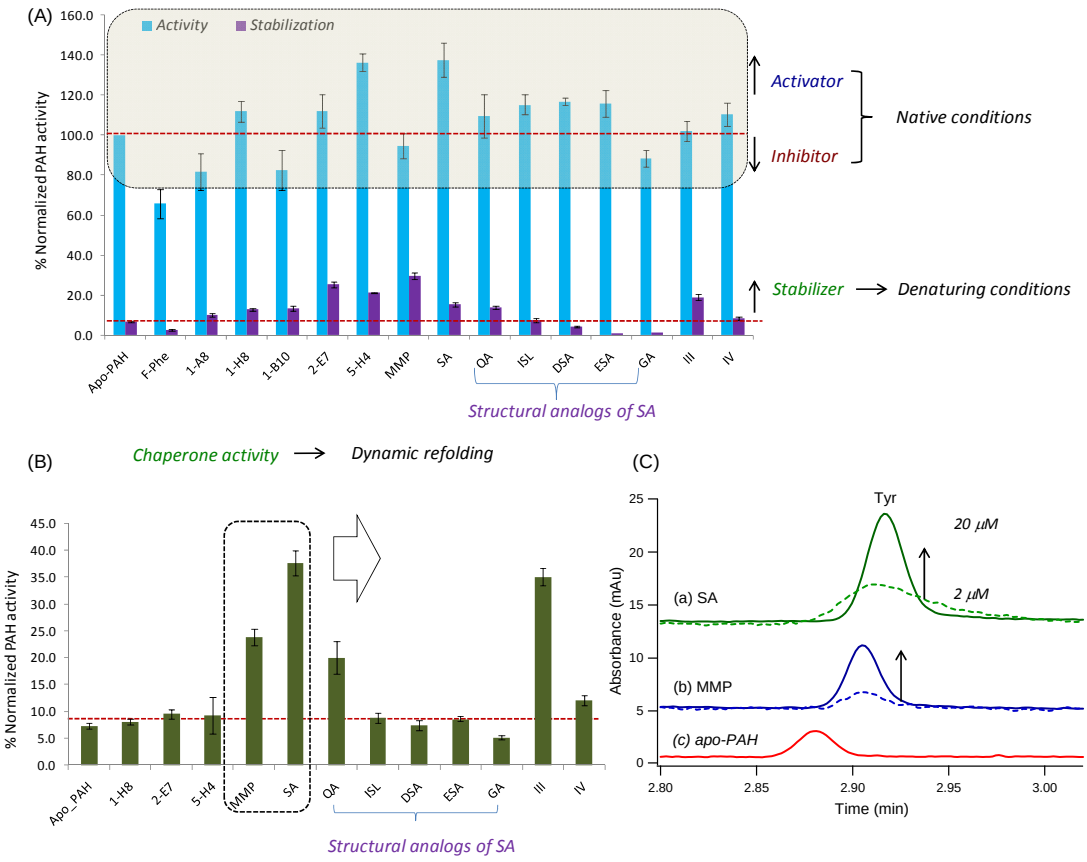

Figure 5.3 Identification of PC candidates for PAH based on two-tiered functional assay (A) Primary screening of representative PCs derived from a chemical library with drug-like properties (100 compounds, 20 μM) under native/folded (0 M urea, activity) relative to denaturing/unfolded conditions (8 M urea) (B) Chaperone activity by dynamic refolding studies of PAH after dilution from 6.0 M to 0.5 M GdnCl with the presence of PCs, lead compounds (MMP, SA and QA) significantly restored Compounds III and V are screen-positive controls previously determined to have PC activity for PAH (C) Chaperone potency is indicated by a dose-dependent enhancement in residual PAH activity that is restored in presence of 20 μM of SA or MMP by three and five-fold relative to *apo-PAH*, respectively, where error represents ± 1σ with precision (n = 6) under 10%.

In our case, compounds III and IV at 20 μM increased PAH residual activity to 19 % and 9 % of WT-PAH in comparison to lead candidates identified from our chemical library, including SA, 5-H4, 2-E7 and MMP which increased enzyme activity to 16, 21, 25 and 35% residual activity of WT-PAH, respectively as shown in **Figure 5.3a**. Five lead compounds that function as significant stabilizers of PAH without undesirable inhibition from the primary screen were subsequently tested for chaperone activity by measuring changes in enzyme activity upon ligand association after dynamic protein refolding upon

dilution from 6.0 M to 0.5 M GdmCl. In this case, **Figure 5.3b** demonstrates that two compounds (MMP, SA) were found to induce a 3 and 5-fold increase in WT-PAH activity relative to ligand-free *apo*-PAH enzyme, respectively. Differences in ligand ranking as measured by our two-tiered screening strategy for PCs highlights that they probe distinct binding interactions associated with ligand-induced stabilization of the native state enzyme (*i.e.,* primary screen) as compared to stabilization of the PAH tetramerization process and/or partially unfolded intermediates during protein refolding (*i.e.,* secondary screen).[50] **Figure 5.3c** highlights the dose-response effect on measured Tyr formation by CE with UV detection as related to increases WT-PAH activity when comparing equimolar doses (2 and 20 μM) of MMP and SA relative to ligand-free *apo*-enzyme. Similarly, compounds III and IV were found to increase the residual activity of WT-PAH after refolding by about 5- and 1.5-fold, respectively. The latter two molecules were previously shown to enhance the thermal stability and activity of PAH in vitro, as well as the steady-state levels of PAH *in-vivo*.[11] Compound IV acts as a weak competitive inhibitor to PAH (K_i = 200 μM) unlike other related tyrosine and tryptophan hydroxylase enzymes[51] while enhancing the folding of the PAH tetramer similar to BH4.[50] Although three compounds, 1-H8, 2-E7 and 5-H4 were weak activators or stabilizers of WT-PAH under native or denaturing conditions (**Figure 5.3a**), they did not display any significant chaperone activity when using the refolding assay (**Figure 5.3b**). Thus, the optimum PC candidates for subsequent testing with PKU-mutants activate, stabilize and assist refolding of WT-PAH in a dose-response dependent manner, such as SA.

5.4.4 Structure-activity Relationships for Shikimic Acid Analogs

Due to the remarkable properties of SA that assists in protein refolding to enhance the residual activity of WT-PAH from (7 ± 0.5) % to about (38 ± 2) %, several other SA analogs were also explored to identify structural motifs associated with its unique chaperone activity. Indeed, SA is a key intermediate in the biosynthesis of aromatic amino acids (**Figure 5.4**) that also serves as a precursor to lignin and numerous bioactive secondary metabolites in plants and microbes.[52] Due to the absence of the shikimate pathway in mammals, it also represents a key target in medicinal chemistry.[53,54]

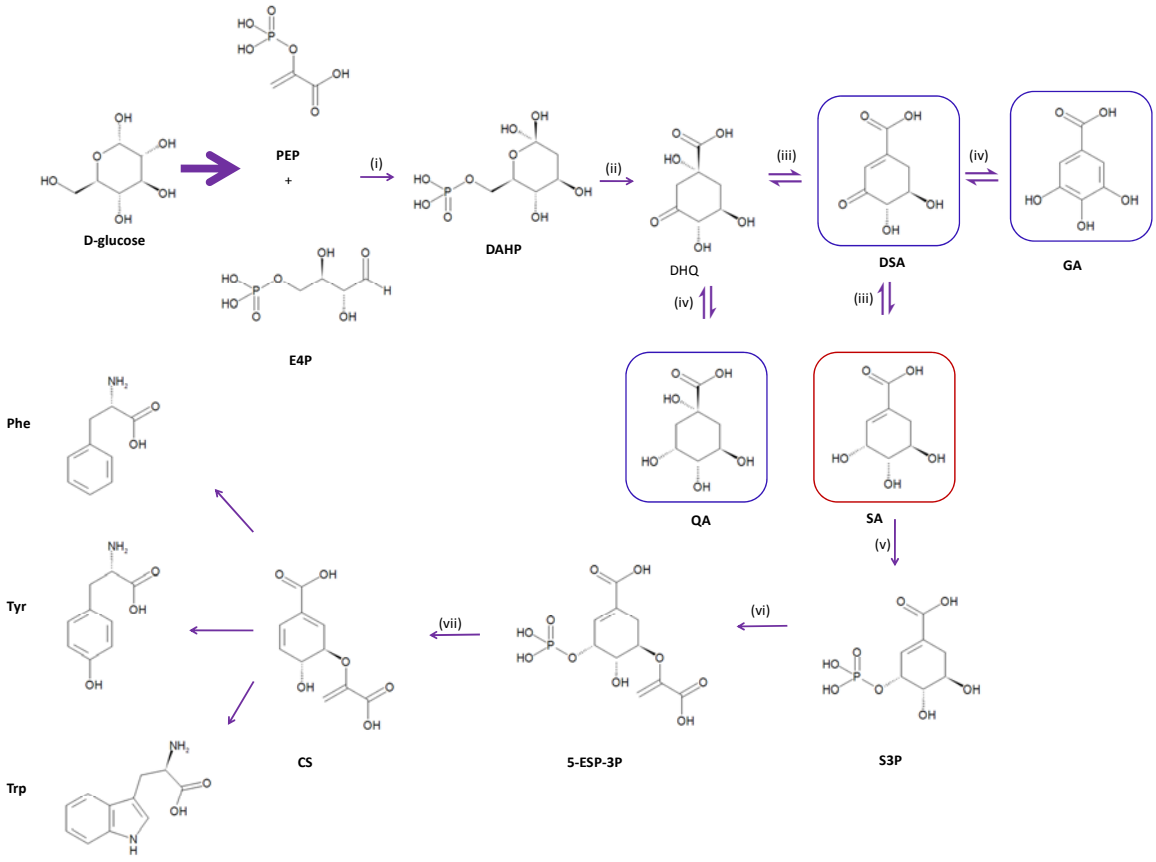

Figure 5.4 Biosynthesis of the aromatic amino acids in plants and microbes via shikimic acid (SA) pathway. Enzymes that involve in synthesizing intermediates as follows: (i) 3-deoxy-*D*-arabino-heptulosonic acid 7-phophate synthase, (ii) 3-dehydroquinate synthase, (iii) 3-dehydroquniate dehydratase, (iv) shikimate dehydrogenase, (v) shikimate kinase, (vi) 5-enolpyruvylshikimate-3-phosphate synthase (vii) chrosmate synthase. Intermediates from each steps are: Phosphoenolpyruvate (PEP), D-erythrose-4-phosphate (E4P), 3-deoxy-D-arabino-heptulosonic acid-7-phosphate (DAHP), 3-dehydroquinate (DHQ), 3-dehydroshikimic acid (DSA), quinic acid (QA), shikimic acid (SA), shikimate-3-phosphate (S3P), 5-enolpyruvylshikimate-3-phosphate (5-EPS-3-P), chorismate (CS), phenylalanine (Phe), tyrosine (Tyr), tryptophan (Trp).[39,53,61] SA and structural analogs of SA that were used in structural-activity relationship studies for WT or mutant PAH are highlighted as key intermediate in this metabolic pathway.

For instance, 6-fluoro-shikimate, is a synthetic SA analog used as an antimicrobial agent that acts as a competitive inhibitor (IC_{50} = 15 µM) of *Plasmodium falciparum*.[55–58] Also, the aromatic polyphenol analog of SA, gallic acid (GA) which is synthesized via shikimate dehydrogenase from 3-dehydroshikimic acid (DSA) has shown to inhibit oligomerization of beta-amyloid peptide.[59] **Figure 5.5** depicts the chemical structures of five different SA analogs that were examined for their ability to stabilize the native enzyme

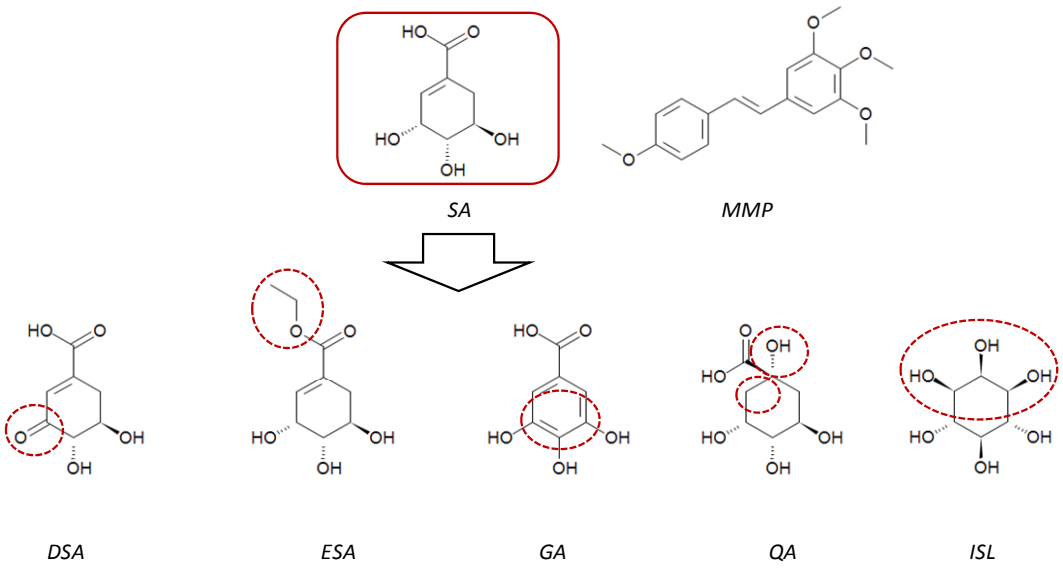

Figure 5.5 Structure of shikimic structural analogs. Structures of two promising PCs (MMP & SA) based on "two-tiered" functional assay approach using WT-PAH. Structural analogs of SA, 3-dehydroshikimic acid (DSA), ethoxyshikimate (ESA), gallic acid (GA), , D-(-)-quinic acid (QA), myo-inositol (ISL). Modification of functional group moiety from parent compounds SA is highlighted in dotted circle.

and/or enhance residual PAH activity upon refolding. **Figure 5.3** demonstrates that *D*-quinic acid (QA) was the only structural analog to partially retain the stabilization effect and chaperone activity as SA. This suggests that the reduction of the double bond and hydroylation at C-1 does not significantly alter reversible ligand binding interactions with WT-PAH.QA is a major plant-derived component in human diet recently shown to induce biosynthesis of tryptophan and nicotinamide by microflora in the gastrointestinal tract.[60] In contrast, oxidation of the 3-hydroxyl moiety (DSA) and esterification of the carboxylic acid (ethoxyshikimate, ESA) abolishes the chaperone activity as measured for SA, whereas GA in fact destabilizes and reduces the activity of WT-PAH upon refolding. Similarly, *myo*-inositol (IST) is a cyclic polyol analog of SA and major renal osmolyte[62] shows no significant activity at 20 μM for stabilizing WT-PAH. These observations indicate that the stereochemistry of the three polyol moieties and the weak acidity of the carboxylic group are critical motifs to preserve favourable interactions with WT-PAH without unwanted inhibition. Although the specific binding region involving SA for WT-PAH remains unclear in this work, the lack of even weak inhibitory effects suggests

allosteric binding to WT-PAH unlike the majority of PCs reported to date. Moreover, the wide distribution of SA and QA in nature suggests that these well-tolerated plant-derived metabolites are safe for human consumption since they are aromatized by gut microflora and excreted as hippuric acid in urine.[63]

5.4.5 Confirmatory Testing of Lead PC Candidates with PKU-mutants

MMP, SA and QA and two reference compounds (III and IV) were further tested with two PKU mutants due to their significant ligand-induced stabilization and activity enhancement effects on WT-PAH. This is critical to validate whether the two-tiered *in-vitro* screen relying on unfolded/inactive WT-PAH under denaturing conditions display activity towards clinically relevant mutant enzymes associated with the PKU disease spectrum. Herein, we selected two clinically relevant PAH mutants, I65T and R261Q without chemical denaturants by measuring changes in Tyr formation by CE after ligand association. For instance, I65T mutation is proposed to distort the hydrophobic packing in the regulatory domain core and is associated with mild to moderate PKU phenotypes, whereas R261Q mutation affects the structure of PAH and exhibits highly variable PKU from mild-moderate-severe form.[11] It was previously reported that a modest increase in PAH activity with BH4 oral supplementation induces a 2.5-fold higher rate in Phe oxidation in certain patients with mild PKU[11] despite conflicting data caused by large between-subject differences in responsiveness.[64] Herein, QA, MMP and SA at 20 μM enhanced the activity of I65T PAH mutant from 1.2- to 2-fold, whereas a 3- to5-fold enhancement in R261Q PAH mutant was measured in this work as shown in **Figure 5.6**. Also, 2-E7 was included as a screen-negative control, which showed no measurable activity enhancement for either PAH mutant at 20 μM (data not shown).In comparison, compounds III and IV were found to include a 1.6 to 2.0-fold enhancement in both PKU-mutants at the same dosage level.

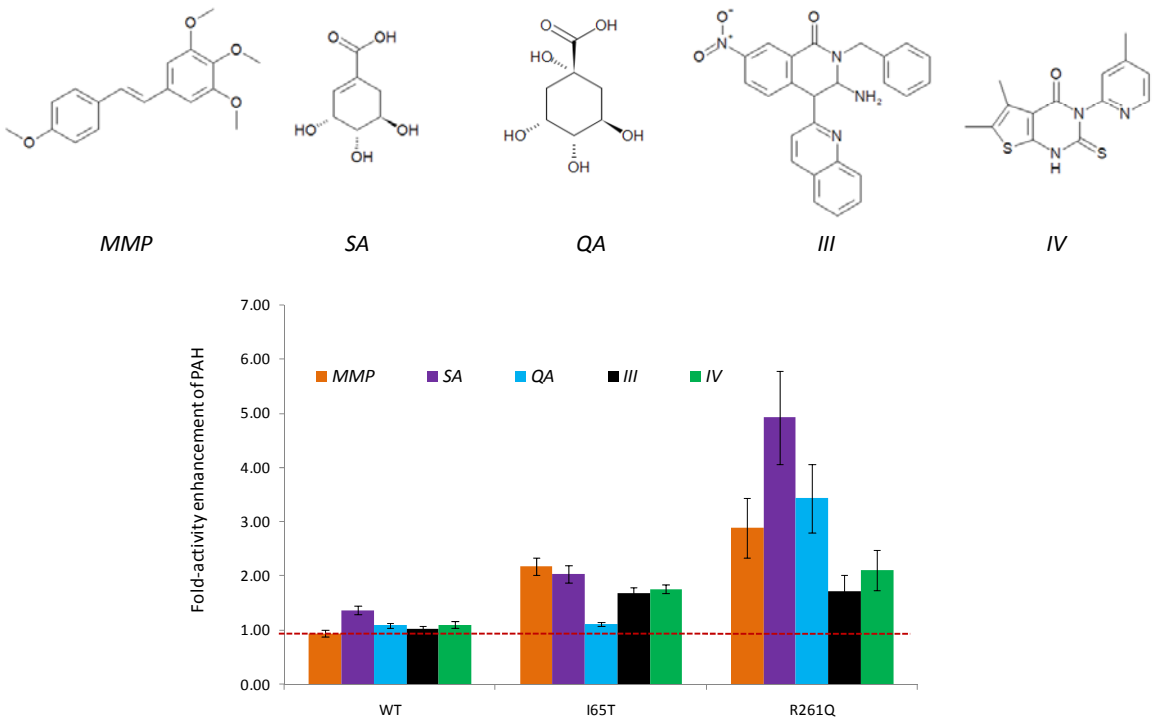

Figure 5.6 Validation of promising PCs with PKU-mutants Stabilization effect of two hits (MMP & HCH) and two reference compounds was tested with WT and two PKU-mutants (I65T and R261Q) of PAH. MMP showed 2-fold activity enhancement with I65T mutant form whereas HCH showed 5-fold increased activity with R269Q mutant form. The two reference compounds (III and IV) showed approximately 1.5-fold activity enhancement with the both mutant forms of PAH that is consistent with previously results based on cell-based assays. Error represents σ ± 1 (*n=3*).

Despite using a new CE-based functional assay to measure ligand-induced increases to PAH activity *in-vitro*, this data is consistent since compounds III and IV were recently reported to induce a 1.2 to 2.0-fold enhancement in activity of PKU-mutants (I65T and R261Q) in A293 cells while inducing a 2-fold enhancement in PAH activity in WT mouse liver.[11] Overall, SA displayed the greatest chaperone activity notably for the more severe mutant (R261Q) retaining only 5% residual PAH activity, which is well above the therapeutic threshold reported for the efficacy of BH4 supplementation.[11] Unlike BH4, SA offers a cost-effective option for PC therapy for treatment of PKU since it is a widely sought after natural product in the food, cosmetic and pharmaceutical industry that can be manufactured by large-scale microbial fermentation processes.[54] Although our *in-vitro* results for two reference compounds (III and IV) are consistent with previously reported

data from cell-based and animal models, further validation studies are required to evaluate the efficacy of our three lead candidates (SA, MMP and QA) as putative PCs for treatment of PKU, especially moderate to severe disease phenotypes that are not responsive to BH4 therapy or dietary Phe restriction. Further studies will use time-resolved electrospray ionization-mass spectrometry with hydrogen-deuterium exchange to elucidate the binding mechanism of SA to PAH that impacts protein conformational stability and folding dynamics.[65]

5.5 Conclusion

In summary, PAH activity was determined by accurate quantification of Tyr formation using a selective, sensitive yet label-free CE-based assay with UV detection. A functional two-tiered screening strategy was developed and validated for discovery of novel PCs for PAH from a chemical library comprising structurally unique compounds with drug-like activity. Overall, three new compounds were found to activate, stabilize and assist with refolding of denaturated WT-PAH, which was demonstrated to have significant chaperone activity for two PKU-mutants relative to two reference compounds with known activity *in-vivo*. Noteworthy, SA was found to induce an unprecedented 3 - 5 fold enhancement in WT-PAH activity, as well as two PKU-mutants. To the best of our knowledge, this is the first example of a natural product that functions as a weak activator and PC for WT and mutant enzymes without unwanted inhibition. Further work is needed to validate its overall efficacy in cell-based assays and animal models of PKU while identifying the binding specificity to PAH in comparison to related enzymes. Ultimately, SA or combination therapy with BH4 may provide better overall efficacy for treatment of mild to severe PKU phenotypes that overcomes quality of life, costs and compliance issues of lifelong Phe-restriction diets.

5.6 Acknowledgements

Financial support was provided by the Natural Science and Engineering Council Discovery Grant of Canada (NSERC) and Ontario Graduate Student scholarship (OGS).

5.7 References

1. F. Fusetti, *J. Biol. Chem.*, 1998, **273**, 16962–16967.

2. M. I. Flydal and A. Martinez, *IUBMB Life*, 2013, **65**, 341–9.

3. E. K. Jaffe, L. Stith, S. H. Lawrence, M. Andrake, and R. L. Dunbrack, *Arch. Biochem. Biophys.*, 2013, **530**, 73–82.

4. C. A. Seymour, R. A. Chalmers, G. M. Addison, and M. Roland, *Health Technol. Assess. (Rockv).*, 1997, **1**, 1–95.

5. J. Underhaug, O. Aubi, and A. Martinez, *Curr. Top. Med. Chem.*, 2012, **12**, 2534–45.

6. C. I. Kaye, F. Accurso, S. La Franchi, P. a Lane, N. Hope, P. Sonya, S. G Bradley, and L.-P. Michele A, *Pediatrics*, 2006, **118**, e934–63.

7. L. . Ogier de Baulny, H, Abadie, V, Feillet, F, Parscau, *J. Nutr.*, 2007, **137**, 1561S–1563S.

8. C. Heintz, R. G. H. Cotton, and N. Blau, *Hum. Mutat.*, 2013, **34**, 927–36.

9. G. M. Enns, R. Koch, V. Brumm, E. Blakely, R. Suter, and E. Jurecki, *Mol. Genet. Metab.*, 2010, **101**, 99–109.

10. S. a Berry, C. Brown, M. Grant, C. L. Greene, E. Jurecki, J. Koch, K. Moseley, R. Suter, S. C. van Calcar, J. Wiles, and S. Cederbaum, *Genet. Med.*, 2013, **15**, 591–9.

11. A. L. Pey, M. Ying, N. Cremades, A. Velazquez-Campoy, T. Scherer, B. Thöny, J. Sancho, and A. Martinez, *J. Clin. Invest.*, 2008, **118**, 2858–2867.

12. C. Heintz, R. G. H. Cotton, and N. Blau, *Hum. Mutat.*, 2013, **34**, 927–36.

13. J. B. Hennermann, C. Bührer, N. Blau, B. Vetter, and E. Mönch, *Mol. Genet. Metab.*, 2005, **86 Suppl 1**, S86–90.

14. J. Zschocke, *Hum. Mutat.*, 2003, **21**, 345–56.

15. *Pediatrics*, 2000, **4**, 972–998.

16. F. J. van Spronsen, M. J. de Groot, M. Hoeksma, D.-J. Reijngoud, and M. van Rijn, *J. Inherit. Metab. Dis.*, 2010, **33**, 671–6.

17. L. Wang, M. Charbonneau, P. Fitzpatrick, J. F. Lemontt, C. N. Sarkissian, A. Ga, B. Zhao, M. Vellard, S. M. Bell, C. Henschell, A. Lambert, L. Tsuruda, R. C. Stevens, and C. R. Scriver, *Proc. Natl. Acad. Sci. U. S. A.*, 2008, **105**, 20894–20899.

18. J. Underhaug, O. Aubi, and A. Martinez, *Curr. Top. Med. Chem.*, 2012, **12**, 2534–45.

19. J. M. Benito, J. M. García Fernández, and C. Ortiz Mellet, *Expert Opin. Ther. Pat.*, 2011, **21**, 885–903.

20. G. Home, F. X. Wilson, J. Tinsley, D. H. Williams, and R. Storer, *Drug Discov. Today*, **16**, 107–118.

21. J. Q. Fan, *Trends Pharmacol. Sci.*, 2003, **24**, 355–360.

22. O. Motabar, E. Sidransky, E. Goldin, and W. Zheng, *Curr. Chem. Genomics*, 2010, **4**, 50–56.

23. H. Erlandsen, A. L. Pey, A. Gámez, B. Pérez, L. R. Desviat, C. Aguado, R. Koch, S. Surendran, S. Tyring, R. Matalon, R. Scriver, M. Ugarte, A. Martínez, R. C. Stevens, E. Beutler, H. Erlandsen, A. L. Pey, A. Gamez, B. Perez, L. R. Desviat, C. Aguado, and R. C. Stevens, *Proc. Natl. Acad. Sci. U. S. A.*, 2014, **101**, 16903–16908.

24. T. K. Chaudhuri and S. Paul, *Febs J.*, 2006, **273**, 1331–49.

25. V. Bellotti and M. Stoppini, *Open Biol. J.*, 2009, **2**, 228–234.

26. M. R. Landon, R. L. Lieberman, Q. Q. Hoang, S. Ju, J. M. M. Caaveiro, S. D. Orwig, D. Kozakov, R. Brenke, G.-Y. Chuang, D. Beglov, S. Vajda, G. a Petsko, and D. Ringe, *J. Comput. Aided. Mol. Des.*, 2009, **23**, 491–500.

27. A. Trapero, I. Alfonso, T. D. Butters, and A. Llebaria, *J. Am. Chem. Soc.*, 2011, **133**, 5474–5484.

28. G. Babajani, M. B. Tropak, D. J. Mahuran, and A. R. Kermode, *Mol. Genet. Metab.*, 2012, **106**, 323–329.

29. T. Hill, M. B. Tropak, D. Mahuran, and S. G. Withers, *Chembiochem*, 2011, **12**, 2151–2154.

30. M. Shanmuganathan and P. Britz-McKibbin, *Anal. Bioanal. Chem.*, 2011, **399**, 2843–2853.

31. Y. Zhang, J. Zhao, J. Wang, and X. Jiao, *Neurochem. Res.*, 2010, **35**, 480–6.

32. S. Santos-Sierra, J. Kirchmair, A. M. Perna, D. Reiss, K. Kemter, W. Röschinger, H. Glossmann, S. W. Gersting, A. C. Muntau, G. Wolber, and F. B. Lagler, *Hum. Mol. Genet.*, 2012, **21**, 1877–87.

33. S. Kure, D. Hou, T. Ohura, H. Iwamoto, S. Suzuki, N. Sugiyama, O. Sakamoto, K. Fujii, Y. Matsubara, and K. Narisawa, *J. Pediatr.*, 1999, **135**, 375–378.

34. S. W. Gersting, K. F. Kemter, M. Staudigl, D. D. Messing, M. K. Danecka, F. B. Lagler, C. P. Sommerhoff, A. a Roscher, and A. C. Muntau, *Am. J. Hum. Genet.*, 2008, **83**, 5–17.

35. M. Shanmuganathan and P. Britz-McKibbin, *Anal. Chim. Acta*, 2013, **773**, 24–36.

36. M. Shanmuganathan and P. Britz-Mckibbin, *Biochemistry*, 2012, **51**, 7651–7653.

37. A. P. Li, *Drug Discov. Today. Technol.*, 2005, **2**, 179–85.

38. D. V Bochkov, S. V Sysolyatin, A. I. Kalashnikov, and I. a Surmacheva, *J. Chem. Biol.*, 2012, **5**, 5–17.

39. K. M. Draths, D. R. Knop, and J. W. Frost, *J. Am. Chem. Soc.*, 1999, **121**, 1603–1604.

40. R. M. Svebak, M. Bozzini, J. Apoldt, and T. Flatmark, *Biochem. J.*, 1995, **306**, 589–597.

41. R. M. Svebak, M. Bozzini, J. Apoldt, and T. Flatmark, *Biochem. J.*, 1995, **306**, 589–597.

42. A. S. Ptolemy and P. Britz-McKibbin, *Analyst*, 2008, **133**, 1643–8.

43. C. Dailey A, N. Garnier, S. Rubakhin S, and J. Sweedler A, *Anal. Bioanal. Chem.*, 2014, **405**, 2451–2459.

44. J. M. Sanchez-Ruiz, *Biophys. Chem.*, 2007, **126**, 43–9.

45. J. A. Ambrose and E. Blake, *Clin. Chem.*, 1974, **20**, 505–510.

46. D. Ringe and G. A. Petsko, *J. Biol.*, 2009, **8**, 80.

47. A. L. Pey, F. Stricher, L. Serrano, and A. Martinez, *Am. J. Hum. Genet.*, 2007, **81**, 1006–1024.

48. S. Gillam, S. Woo, and L. Woolf, *Biochem. J.*, 1974, **139**, 731–739.

49. M. Shanmuganathan and P. Britz-McKibbin, *Anal. Bioanal. Chem.*, 2011, **399**, 2843–2853.

50. R. Torreblanca, E. Lira-Navarrete, J. Sancho, and R. Hurtado-Guerrero, *Chembiochem*, 2012, **13**, 1266–9.

51. A. C. Calvo, T. Scherer, A. L. Pey, M. Ying, I. Winge, J. McKinney, J. Haavik, B. Thöny, and A. Martinez, *J. Neurochem.*, 2010, **114**, 853–63.

52. M. Na cha, H. Jeong Kim, B. Gyu Kim, and J.-H. Ahn, *J.Microbiol.Biotechnol*, 2014, **24**, 1109–1117.

53. D. J. Wilson, S. Patton, G. Florova, V. Hale, and K. A. Reynolds, *J. Ind. Microbiol. Biotechnol.*, 1998, **20**, 299–303.

54. G. Rawat, P. Tripathi, and R. K. Saxena, *Appl. Microbiol. Biotechnol.*, 2013, **97**, 4277–87.

55. J. Zucko, W. C. Dunlap, J. M. Shick, J. Cullum, F. Cercelet, B. Amin, L. Hammen, T. Lau, J. Williams, D. Hranueli, and P. F. Long, *BMC Genomics*, 2010, **11**, 628.

56. K. E. L. E. Dmisten and R. A. W. Ells, *J. Agric. Food Chem.*, 2002, **50**, 506–512.

57. U. Kingdom, *Antimicrob. Agents Chemother.*, 1999, **43**, 175–177.

58. B. I. R. K. Amara, D. J. A. B. Rand, E. V. I. B. Randt, and E. L. J. Oubert, *J. Agric. Food Chem.*, 2004, **52**, 5391–5395.

59. Y. Liu, T. L. Pukala, I. F. Musgrave, D. M. Williams, F. C. Dehle, and J. a Carver, *Bioorg. Med. Chem. Lett.*, 2013, **23**, 6336–40.

60. R. W. Pero, H. Lund, and T. Leanderson, *Phyther. Res.*, 2009, **346**, 335–346.

61. S. Jiang and S. Gurdial, *Tetrahedron*, 1998, **54**, 4697–4753.

62. R. Jackson-Atogi, P. K. Sinha, and J. Rösgen, *Biophys. J.*, 2013, **105**, 2166–74.

63. R. Pero, *Curr. Clin. Pharmacol.*, 2010, **5**, 67–73.

64. A. Ponzone, F. Porta, A. Mussa, A. Alluto, S. Ferraris, and M. Spada, *Metabolism.*, 2010, **59**, 645–52.

65. D. Resetca and D. J. Wilson, *Febs J.*, 2013, **280**, 5616–25.

Chapter VI:
Future Directions for High Quality Screening of Pharmacological Chaperones for Genetic Diseases.

6.1 Overview of Thesis Contributions

The work presented in this thesis has contributed new bio-analytical tools for improved characterization of pharmacological chaperone (PCs)in drug discovery that is relevant to orphan diseases, including Gaucher disease and phenylketonuria (PKU). For instance, this research has developed, optimized and implemented a high throughput and a high quality platform for drug screening as required for enzyme enhancement therapy. In this context, capillary electrophoresis (CE) was used as a versatile micro-separation platform for studying enzyme kinetics, ligand-induced protein stabilization and protein unfolding/refolding dynamics in free solution. The motivation of this work stems from an urgent need for developing safe, effective yet low-cost therapies for treatment of rare genetic disorders in support of universal newborn screening programs. However, current high throughput screening (HTS) strategies continue to rely on conventional inhibition or thermal stabilization assays for identification of putative PC candidates from large chemical libraries.[1] Thus, the majority of PC candidates to date often fail during later stages of drug development due to unfavorable inhibition activity and/or cytotoxicity. As a result, this thesis has introduced a new two-tiered approach for functional screening of compounds based on ligand-induced stabilization and refolding of a target enzyme that ultimately enhances its catalytic activity under denaturing conditions. This assay not only reveals compounds that function as activators and/or stabilizers of protein, but also identifies ligands with definitive chaperone activity using solubilizing chemical denaturants. One of the major goals of this thesis was to identify novel PC candidates that do not exhibit undesirable inhibitory effects, as well as further validate this screening approach using clinically relevant enzyme mutants and compounds previously identified as PCs by independent analytical methods, such as differential scanning fluorimetry.

Chapter I provided an in-depth overview of pharmacological chaperone therapy (PCT) as a novel approach for treatment of genetic disorders caused by protein misfolding while identifying the key limitations of current PC screening protocols.[1] Chapter II introduced a simple yet selective CE-based inhibition assay for better understanding of pH-dependent ligand binding interactions, mode of binding and potency of previously identified FDA drugs that function as PCs for β-glucocerebrosidase (GCase), the lysosomal enzyme associated with Gaucher disease.[2] The advantage of screening a previously approved "off-patent" drug library for chaperone activity is based on the long-established safety record that is needed to accelerate clinical translation for oral treatment of rare genetic disorder.[3]However, this premise assumes that most drugs do not bind to their original protein target selectively, which can be useful provided that their chaperone activity for a new enzyme target is adequately established within an appropriate therapeutic dosage window. This work introduced the first CE-based inhibition assay that rigorously analyzed the mode of drug binding, pH-dependent binding and potency of PCs when using non-linear regression of enzyme inhibition curves. CE was also used as a novel biophysical tool to quantify product formation from off-line enzymatic/inhibition assays, as well as measure relevant physicochemical properties of lead drug candidates, such as weak acid dissociation constant (pK_a). However, PC candidates selected by conventional enzyme inhibition assay do not accurately reflect chaperone activity since they ultimately attenuate product turn-over rates by competing with substrate binding to active site. Indeed, severe clinical symptoms in patients with genetic diseases are caused by deleterious substrate accumulation due to protein misfolding and enzyme deficiency. Chapter III introduced a CE assay based on restoration of enzyme activity via denaturation (READ) as a novel approach for characterization of PC candidates for GCase based on their capacity to restore enzyme activity under denaturing conditions.[4] Unlike conventional inhibition assays that rely on inhibition potency when using folded wild-type (WT) enzyme, and thermal stabilization assays that provide information as related to the conformational stability of an enzyme, READ is a functional screening tool for assessing the impact of ligand binding that ultimately enhances the catalytic activity

of a denatured/inactivated WT enzyme. In addition, dynamic unfolding studies of GCase was developed using CE to provide deeper insight into structural changes associated with apparent loss of catalytic activity with urea denaturation that can be partially restored with PC binding. Although all characterization of protein unfolding/enzyme kinetics and determination of physicochemical properties of small molecules were performed using CE, this is not suitable to HTS of large chemical libraries (> 1,000 compounds) as required for drug discovery of novel PCs that bind allosterically to an enzyme target without inhibition effects. Chapter IV focused on further modification and adaptation of the original CE-based assay for READ to a fluorescence-based microplate platform suitable for HTS drug screening. Additionally, a complimentary refolding assay was developed for characterization chaperone activity of promising PCs. A large fraction of primary ligand "hits" often fail at later stages of clinical trials when rigorous characterization is not performed to exclude unlikely drug candidates from a chemical library using computational approaches for virtual screening. Thus, an orthogonal two-tiered approach was introduced to screen a small chemical library consisting of 600 structurally unique small molecules after *in silico* assessment for drug-like properties based on Lipiniski's rule of five.[5] The latter approach was used to improve drug screening efficacy by excluding compounds with poor aqueous solubility, low permeability and high cytotoxicity at the initial stage of drug screening. In addition, compounds with auto-fluorescence properties and quenching effects with fluorogenic product were also rejected to avoid any false discoveries. Dose-response dependent activity and structure-activity relationship were also explored when using denatured WT-enzyme when using READ. Dose-response studies are generally established to identify the optimum range of concentrations for a PC to enhance the residual activity of mutant enzyme in a patient derived cell-line without noticeable cytotoxicity.[6] Therefore, putative PCs that do not elicit an enhancement in enzyme activity in a dose-responsive manner when using *in-vitro* assays should be rejected prior to cell-based or animal studies. In addition, structure-activity relationships were also explored in this thesis by comparing the chaperone activity of several structural analogs with defined structural modifications among the lead

drug candidates. Although two parent compounds and six structural analogs of stilbene derivatives showed promising chaperone activity based on *in-vitro* assay, activity of these PCs at a cellular level needs to be explored when using cell-based assays expressing clinically relevant mutants of GCase. Chapter V further modified and adapted the two-tiered functional screening approach for the discovery of novel PCs using the same chemical library for a different enzyme target, namely phenylalanine hydroxylase (PAH) that is associated with mild to severe PKU. Unlike GCase, which is membrane-bound monomeric lysosomal enzyme, PAH is a cytosolic oxireductase protein that requires a cofactor, molecular oxygen and iron for catalytic function while forming a homotetramer in free solution. Therefore, assay conditions for READ, such as chemical denaturant type, concentration and pre-equilibration time were optimized to obtain a residual activity of WT-PAH that was comparable to severe PKU-mutants. For instance, GCase required lower urea (4.0 M) concentration for both stabilization and refolding assays (Chapter III & IV). In contrast, PAH required higher urea concentration (8.0 M) for the stabilization assay, whereas a stronger denaturant, GdnCl (6.0 M) concentration was needed for chaperone activity assay based on enzyme refolding. In addition, conventional fluorescence-based HTS approaches are not ideal for PAH enzyme kinetic studies when relying on the weak native fluorescence properties of *L*-tyrosine (Tyr) with deep UV excitation. Therefore, a selective yet sensitive label-free CE-based assay was introduced to directly measure residual PAH activity under denaturing conditions based on Tyr formation without chemical derivatization. A two-tiered screening approach was applied using the CE assay to identify compounds with promising chaperone activity to WT-PAH. Overall, two lead compound, ,2,3-trimethoxy-5-[2-(4-methoxyphenyl)ethenyl] benzene (MMP) and shikimic acid (SA) were found to function as promising PCs for WT-PAH in a dose-dependent manner while also enhancing the activity of clinically relevant PAH mutants. Furthermore, structure-activity relationships were established by comparing the chaperone activity of several different SA analogs to WT-PAH, which revealed that the stereochemistry the three polyol moieties and the weak acidity of the carboxylic acid group were critical features to PC function. Overall, *D*-quinic acid (QA)

and especially SA showed better chaperone activity in terms of enhancement to the activity of two PKU mutants relative to two positive controls, which were previously identified as promising PCs for PAH based on a cell-based assay and WT-mouse model.[7] SA is widely used in various food products, as well as important chiral precursor for production of the neuroaminidase inhibitor, oseltamivir phosphateor Tamiflu®.[8] This work demonstrates for the first time that plant-derived natural products can function as novel PCs for restoring the activity of mutant enzymes without inhibition. However, the efficacy of these PCs on stabilizing and enhancing PAH activity will be further examined using cell-based and animal models in order to evaluate their efficacy for treatment of mild to severe PKU phenotypes that are not responsive to tetrahydrobiopterin (BH4) supplementation. Overall, this work offers a safe, low cost yet effective modality for treatment of rare genetic disorders that is advantageous relative to enzyme replacement therapy (*i.e.,* recombinant GCase) and restrictive lifelong dietary management (*i.e.,* Phe-restricted diet) for better clinical outcomes in patients and improved quality of life.

6.2 Expansion of Two-tiered Screening Method to a Previously FDA-approved Drug Library

Chapter II introduced the benefits of identifying PC candidates from a previously FDA-approved drug chemical library that are safe and yet no longer under patent protection as a way to fast-track clinical translation of new therapies for rare genetic disorders. However, previous studies used conventional inhibition assay and secondary thermal stabilization assay for the identification of lead candidates from a large National Institute of Neurological Disorders and Strokes (NINDs) library that can lead to high attrition rates during drug development as a result of false-positive (*e.g.,* enzyme destabilizers) and false negative(*e.g.,* allosteric ligands that stabilize enzyme without inhibition) screen results.[3] In other words, the specificity, sensitivity and functional relevance of the primary screening method for PC candidate selection is critical to later stages of drug development. Chapter IV introduced a new two-tiered functional assay for better selection of PC candidates, which will be applied to the same NINDS library to reveal any

promising PC candidates that were previously identified as false negatives. For instance, previous study identified ambroxol (ABX) as the most promising PCs for GCase based on primary HST format inhibition assay subsequently by thermal stabilization assay and then followed by cell-based assay and animal model.[6] However, a recent pilot clinical trials with seventy type I GD patients showed no significant improvement in clinical outcomes with the treatment of ABX.[9] Therefore, application of our improved "two-tiered" functional assay to the same NINDS library may reveal drug compounds that have chaperone like properties which was failed to identify by previous methods.

6.3 Identification of PC Binding Region and Ligand-induced Protein Folding Dynamics

Recently, the conformational stability of GCase upon binding of PCs (IFG, DTZ and ABX) was examined using three different techniques including differential scanning fluorimetry (DSF) and stability of unpurified proteins from rates of hydrogen-deuterium exchange (SUPREX) method.[3,10,11] DSF focused on the impact of thermal denaturaion on protein-PC complex stability based on the measured red shift using intrinsic tryptophan fluorescence properties or fluorescence enhancement of an extrinsic fluorescent probe. The thermal stability of protein in the absence (*apo*-state) and presence (*holo*-state) of increasing concentrations of a ligand is determined using DSF, where ligand-induced stabilization of protein results in an increase in the denaturation midpoint temperature. In addition, hydrogen/deuterium exchange-electrospray ionization-mass spectrometry (HDX-ESI-MS) is used to identify regions within protein that undergo stabilization upon ligand binding since less ordered/solvent-exposed domains undergo changes in their measured mass-to-charge ratio (*m/z*) as a result of higher rates of deuterium exchange.[6] The binding of a competitive inhibitor not only restricts the local protein dynamics of the active site, but also propagates this effect into surrounding regions. Alternatively, SUPREX method is a HDX technique based on matrix-assisted laser desorption ionization (MALDI) for characterizing the equilibrium unfolding/refolding properties of proteins and protein−ligand complexes. A recent study demonstrated that the change in

the stability of GCase upon binding of ambroxol (ABX) or isofagamine (IFG) with increasing the concentration of GndCl (strong denaturant) based on increasing average rates of deuteration measured by MALDI-MS. However, these studies fail to address how conformational stability impact on GCase activity and refolding kinetics. For instance, conventional structural biology techniques including, X-ray crystallography and NMR spectroscopy have been used to identify PC interaction regions on GCase[12] and PAH [13] However, these techniques are limited to performing dynamic kinetic experiments which provide crucial structural and mechanistic insights associated with ligand binding.[14] Recently, an integrated lab-on-a-chip method was introduced by combining time-resolved ESI-MS with pulsed HDX labelling followed by rapid digestion for investigating the protein dynamics in real-time.[15] Future work will apply this approach to characterize the global impacts of ligand binding on protein structure and folding dynamics using lead PC candidates identified in Chapter IV and V.

6.4 Further Confirmation of Promising PCs from In-vitro Assay with Cell-based Assays

Although few non-inhibitor/activator PCs showed promising chaperone activity for WT and mutant enzymes when using *in-vitro* assays in Chapter IV and V, impact of these PCs at cellular level needs to be evaluated using cell-based assays. Cell-based assays are not only assess the effect of PCs at the cellular level but also evaluate their efficacy to treat different enzyme mutations and clinically relevant patient genotypes.[1] However, cell-based assays do not provide information whether mutant enzymes has trafficked to the final destination and is able to hydrolyse endogenous substrate. Thus, two analytical methods based on Western blotting and fluorescence-based inhibition are used to assess increases in both local protein abundance and enzyme activity, respectively. Since the efficacy of PCT is based on enzyme enhancement in order to alleviate deleterious substrate accumulation in the target organelles, kinetic assays are needed to quantify enzyme activity in cell lysates. To date, all PCs have been competitive inhibitors, a washout procedure of drug from cells is necessary prior to cell lysis as carryover of

residual PC may lead to bias with a lower apparent enzyme activity. At the same time, performing a washout may also decrease the apparent activity of non-inhibiting PCs, such as allosteric site binders and/or activators. Therefore, a washout procedure can be eliminated when quantifying activity in cell lysates that is incubated with non-inhibitor or allosteric PCs. In addition to characterizing the efficacy and safety (*i.e.,* toxicity) of lead PCs using cell-based assays, the ability of a PC to restore enzymatic activity in the disease relevant tissues also needs to be evaluated *in-vivo* using appropriate animal models.

6.5 Expansion of PCT to other Protein Misfolding Disorders such as Cystic Fibrosis

Accelerated cellular degradation of misfolded protein results in protein deficiency, loss in function and deleterious aggregation effects, which is associated in the pathogenesis of a wide range of human diseases, including cystic fibrosis (CF). CF is an autosomal recessive disorder caused by mutations in the cystic fibrosis transmembrane conductance regulator (CFTR),where ΔF508 is the most common mutation relevant to homozygote patients with classical CF.[16]CFTR is a membrane-bound protein that regulates chloride transport that plays critical roles in the function of exocrine glands/tissues, including lungs, liver, pancreas and intestine. Indeed, CF is the most common genetic disorder affecting Canadian children and young adults with an average incidence of 1:3600.[17]The current NBS protocol for early detection of CF involves multiple stages. The usefulness of a screening test depends on the existence of a validated yet effective treatment option for infants at an early-stage who often express a spectrum of different phenotypes for a specific IEM.[18]. CF is now part of a panel of genetic diseases included in NBS that require better treatment options but the current treatments include vitamin and pancreatic enzyme supplementation to avoid malnutrition due to pancreas insufficiency, antibiotic treatment to prevent recurrent lung infections, as well as exercise and drug therapy used to treat symptoms of disease.[19] Despite the improvements and benefits of these therapeutic options, some patients are not still receiving appropriate therapies.

Alternatively, PCT therapy was recently introduced a promising avenue where PC specifically binds and overcomes folding defects of CFTR intermediate during folding process in the ER. In the past few years, HTS of chemical libraries has been use to identify potential PCs or corrector of CFTR, mutation ΔF508 folding. Although PCs such as a bisaminometylbithiazole derivative (corr-4a) and a pyrazol derivative (VRT-532) can promote maturation of ΔF508 CFTR with some specificity, the level of correction is still inadequate.[20] Therefore, application of newly developed "two-tiered" functional primary approach to large chemical libraries will enable to identify potential PCs that could further increase the efficiency of maturation and/or increase channel activity.

In summary, an integrated two-tiered strategy for high quality screening of PCs has been developed in this thesis as required for the development of new drug candidates for treatment of orphan diseases based on enzyme enhancement therapy. To the best of our knowledge, this is first report that adopts a relevant functional assay for primary screening of a chemical library that directly measures the chaperone activity of novel PC candidates that activate, stabilize and ultimately refold denatured enzymes and clinically relevant protein mutants. Dose-response and structure-activity relationships established that several unique synthetic compounds and plant-derived natural products function as promising PCs that significantly enhance the activity of enzymes associated with Gaucher disease and PKU without inhibition as compared to previously identified drug candidates.

6.6 References

1. K. J. Valenzano, R. Khanna, A. C. Powe, R. Boyd, G. Lee, J. J. Flanagan, and E. R. Benjamin, *Assay Drug Dev. Technol.*, 2011, **9**, 213–235.

2. M. Shanmuganathan and P. Britz-McKibbin, *Anal. Bioanal. Chem.*, 2011, **399**, 2843–2853.

3. G. H. B. Maegawa, M. B. Tropak, J. D. Buttner, B. A. Rigat, M. Fuller, D. Pandit, L. I. Tang, G. J. Kornhaber, Y. Hamuro, J. T. R. Clarke, and D. J. Mahuran, *J. Biol. Chem.*, 2009, **284**, 23502–23516.

4. M. Shanmuganathan and P. Britz-Mckibbin, *Biochemistry*, 2012, **51**, 7651–7653.

5. C. A. Lipinski, *J. Pharmacol. Toxicol. Methods*, 2001, **44**, 235–249.

6. G. H. B. Maegawa, M. B. Tropak, J. D. Buttner, B. a Rigat, M. Fuller, D. Pandit, L. Tang, G. J. Kornhaber, Y. Hamuro, J. T. R. Clarke, and D. J. Mahuran, *J. Biol. Chem.*, 2009, **284**, 23502–16.

7. N. F. Brás, N. M. Cerqueira, M. J. Ramos, and P. a Fernandes, *Expert Opin. Ther. Pat.*, 2014, **24**, 857–74.

8. D. J. Wilson, S. Patton, G. Florova, V. Hale, and K. A. Reynolds, *J. Ind. Microbiol. Biotechnol.*, 1998, **20**, 299–303.

9. A. Zimran, G. Altarescu, and D. Elstein, *Blood Cells. Mol. Dis.*, 2013, **50**, 134–7.

10. Z. Luan, K. Higaki, M. Aguilar-Moncayo, H. Ninomiya, K. Ohno, M. I. García-Moreno, C. O. Mellet, J. M. García Fernández, and Y. Suzuki, *ChemBioChem*, 2009, **10**, 2780–2792.

11. K. Yu,Z, Sawkar, A.R, Whalen, L.J, Wong, C, R. A. Steet, S. Chung, B. Wustman, A. Powe, H. Do, S. A. Kornfeld, H. H. Chang, N. Asano, S. Ishii, Y. Ichikawa, and J. Q. Fan, *Febs J.*, 2006, **273**, 4082–4092.

12. M. R. Landon, R. L. Lieberman, Q. Q. Hoang, S. Ju, J. M. M. Caaveiro, S. D. Orwig, D. Kozakov, R. Brenke, G.-Y. Chuang, D. Beglov, S. Vajda, G. a Petsko, and D. Ringe, *J. Comput. Aided. Mol. Des.*, 2009, **23**, 491–500.

13. J. Underhaug, O. Aubi, and A. Martinez, *Curr. Top. Med. Chem.*, 2012, **12**, 2534–45.

14. J. Underhaug, O. Aubi, and A. Martinez, *Curr. Top. Med. Chem.*, 2012, **12**, 2534–45.

15. D. Resetca and D. J. Wilson, *Febs J.*, 2013, **280**, 5616–25.

16. Y. Wang, T. W. Loo, M. C. Bartlett, and D. M. Clarke, *Mol. Pharmacol.*, 2007, **71**, 751–758.

17. J. S. Elborn, D. J. Shale, and J. R. Britton, *Respir. Med.*, 1994, **88**, 135–138.

18. J. S. Elborn, D. J. Shale, and J. R. Britton, *Thorax*, 1991, **46**, 881–885.

19. M. D. Amaral, *J. Inherit. Metab. Dis.*, 2006, **29**, 477–487.

20. T. W. Loo and D. M. Clarke, *Expert Rev. Mol. Med.*, 2007, **9**, 1–18.